ANL-ARC-226 Rev.1

Benchmark Specifications and Data Requirements for EBR-II Shutdown Heat Removal Tests SHRT-17 and SHRT-45R

Nuclear Engineering Division

About Argonne National Laboratory
Argonne is a U.S. Department of Energy laboratory managed by UChicago Argonne, LLC under contract DE-AC02-06CH11357. The Laboratory's main facility is outside Chicago, at 9700 South Cass Avenue, Argonne, Illinois 60439. For information about Argonne and its pioneering science and technology programs, see www.anl.gov.

ANL-ARC-226 Rev.1

Benchmark Specifications and Data Requirements for EBR-II Shutdown Heat Removal Tests SHRT-17 and SHRT-45R

prepared by
T. Sumner and T.Y.C. Wei
Nuclear Engineering Division, Argonne National Laboratory

May 31, 2012

SUMMARY

Argonne National Laboratory's (ANL) Experimental Breeder Reactor II (EBR-II) was a liquid metal reactor (LMR) with a sodium-bonded metallic fuel core that contributed very favorably to the reactor's negative reactivity feedback. On June 20, 1984, a severe loss-of-flow test in the Shutdown Heat Removal Test (SHRT) series demonstrated the effectiveness of natural circulation in the EBR-II reactor. This test was SHRT-17 and at the beginning of the test the primary pumps were tripped at the same time as a full control rod insertion.

On April 3, 1986, a severe unprotected loss-of-flow test demonstrated the effectiveness of passive feedback in the EBR-II reactor. This test, SHRT-45R, was very similar to SHRT-17 except that during the test the plant protection system (PPS) was disabled to prevent it from initiating a control rod scram. Both tests began from full reactor power and were initiated when both primary coolant pumps and the intermediate loop pump were simultaneously tripped to simulate a loss-of-flow accident (LOF).

In the case of SHRT-45R, the loss of forced coolant flow caused reactor temperatures to rise temporarily to a high, but acceptable, level as the reactor safely shut itself down due to total negative reactivity feedback. The SHRT-45R test demonstrated that an EBR-II type Sodium-Cooled Fast Reactor (SFR) plant could be designed such that natural phenomena (e.g., thermal expansion of reactor materials), in addition to electromechanical systems (e.g., control rod drives), are effective in protecting the reactor against the potentially adverse consequences of unprotected accidents.

Argonne National Laboratory has prepared a detailed benchmark specification for the analysis of the SHRT-17 and SHRT-45R tests. This specification will provide the necessary benchmark data for collaborative efforts within international partnerships under the auspices of the International Atomic Energy Agency as a Coordinated Research Project (CRP) in support of validation of simulation tools and models for the safety analysis of SFR. Validated tools and models are needed both to evaluate SFR passive safety phenomena and to evaluate reactor designs incorporating passive features into the system response to accident initiators.

This report provides comprehensive details on the following aspects of the SHRT-17 and SHRT-45R tests:

- EBR-II reactor plant overview,
- Detailed initial and transient benchmark boundary conditions,
- Detailed reactor core description with subassembly dimensions,
- Detailed primary cooling system description with component dimensions,
- Material properties and heat transfer coefficients,
- Necessary data for the calculation of reactivity feedback coefficients,
- Detailed decay heat parameters, and
- Detailed measurements and descriptions of the instrumentation used to measure that data.

An overview of the EBR-II reactor is given in Chapter 2 followed by a description of the SHRT-17 and SHRT-45R tests and the benchmark boundary conditions in Chapter 3. Chapters 4 and 5 provide detailed descriptions of the reactor core and coolant system in EBR-II, respectively. Chapter 6 provides suggested data that benchmark participants should calculate for measured test data and direct code-to-code comparisons.

TABLE OF CONTENTS

LIST OF TABLES

LIST OF FIGURES

ACRONYMS

14TC – Above core Thermocouple

ANL – Argonne National Laboratory

ATC – Annulus Thimble Thermocouple

BOP – Balance of Plant

CRP – Coordinated Research Project

DAS – Data Acquisition System

EBR-II – Experimental Breeder Reactor II

gpm – United States gallons per minute

HFD – High-Flow Driver

HWCR – High Worth Control Rod

IB – Inner Blanket

IHX – Intermediate Heat Exchanger

INCOT – In-Core instrument Test facility

INSAT – instrumented subassembly

LMR – Liquid Metal Reactor

M-G – Motor-Generator set

MTC – Midplane Thermocouple

OB – Outer Blanket

OTC – Outlet-coolant Thermocouple

PPS – Plant Protection System

SFR – Sodium Fast Reactor

SHRT – Shutdown Heat Removal Test

TTC – Top-of-core Thermocouple

ULOF – Unprotected Loss-of-Flow

ACKNOWLEDGEMENTS

We wish to acknowledge and thank the following people for their contribution to this work:

Laural Briggs

Tom Fanning

Chris Grandy

Amr Mohamed

Anton Moisseytsev

Tanju Sofu

Rick Vilim

Art Wright

We also wish to give a special thank you to the following people for their significant contributions:

Floyd Dunn

Earl Feldman

Karl Grimm

Hubert Ley

Richard McKnight

Doug Porter

1 Introduction

Argonne began power operations of the Experimental Breeder Reactor II (EBR-II) in 1964 and continued until the reactor was shut down in 1994. EBR-II was operated initially to demonstrate the feasibility of a closed fuel cycle that required the addition of only uranium-238 to fuel the breeding process and allow for sustained operation. To achieve the intended fuel utilization, the initial EBR-II operating period was closely tied to research into pyrometallurgical reprocessing for irradiated nuclear fuel. This period lasted five years. Following the fuel cycle demonstration phase, the focus of EBR-II shifted for much of the next ten years towards irradiation experiments of advanced binary and ternary metal fuels and also advanced oxide fuels. During the last 15 years, EBR-II was used for experiments designed to demonstrate the importance of passive safety in liquid metal reactors (LMR).

The Shutdown Heat Removal Test (SHRT) program was carried out in EBR-II between 1984 and 1986. The objectives of this program were to support U.S. LMR plant design, provide test data for validation of computer codes for design, licensing and operation of LMRs, and demonstrate passive reactor shutdown and decay heat removal in response to protected and unprotected transients. The protected and unprotected transients tested include loss of flow in the primary and/or intermediate sodium loops as well as a loss of heat sink from the balance of plant. Additional tests were performed to examine the response of the system to balance of plant changes and others were performed to characterize reactivity feedbacks.

Passive safety response in sodium fast reactors is the result of reactor design features that will shut down the reactor, remove residual heat, and keep the core cooled during accidents. In addition to the Doppler effect, negative reactivity feedback mechanisms based on thermal expansion and contraction of structural materials, which affect neutron leakage in the fast spectrum core, can be used to passively shut down the fission process. Radial and axial core expansion, subassembly bending, and control rod driveline expansion are examples of these passive reactivity feedbacks. To keep the core cooled when forced circulation is lost, coolant density changes in sodium can be utilized in the design to produce natural circulation flow. Passive heat removal can be accomplished through use of natural convection, conduction and vessel wall radiation.

On June 20, 1984, the SHRT-17 loss of flow test, was conducted where a loss of electrical power to all the plant sodium coolant pumps was used to demonstrate the effectiveness of natural circulation cooling characteristics. Starting from full power and flow, both the primary and intermediate-loop coolant pumps were simultaneously tripped and the reactor was scrammed to simulate a protected loss-of-flow accident. In addition, the primary system auxiliary coolant pump that normally had an emergency battery power supply was turned off. Temperatures in the reactor quickly rose to high, but acceptable levels as the natural circulation characteristics cooled the reactor down safely at decay heat levels. SHRT-17 demonstrated that natural phenomena such as thermal expansion of the sodium coolant and thermal inertia of the primary pool sodium, as opposed to electromechanical systems such as electrically driven pumps, can be effective in protecting the reactor against potentially adverse consequences from protected loss-of-flow and loss-of-heat-sink accidents.

On April 3, 1986, the SHRT-45R unprotected loss of flow test was conducted to demonstrate the effectiveness of EBR-II's passive feedbacks. During the test, the plant protection system (PPS) was disabled to prevented initiation of a scram. Starting from full power and flow, both the primary and intermediate-loop coolant pumps were simultaneously tripped to simulate an unprotected loss-of-flow accident. Temperatures in the reactor quickly rose to high, but acceptable levels as the inherent reactivity feedbacks terminated the fission process. SHRT-45R demonstrated that natural phenomena such as thermal expansion of reactor materials can be effective in protecting the reactor against potentially adverse consequences from unprotected loss-of-flow and loss-of-heat-sink accidents.

EBR-II's response to off-normal conditions in the primary and intermediate systems during the SHRT-17 and SHRT-45R tests included a variety of physical phenomena that combined to form a system of natural feedback effects. These feedbacks could either exacerbate or mitigate transient conditions depending upon the reactor's design and operating conditions. The tight coupling of thermal-hydraulic phenomena in the core and the primary loop that were exhibited in the SHRT-17 test creates conditions for a challenging benchmark project. The tight coupling of neutronic phenomena to the thermal-hydraulic and structural mechanic phenomena for the SHRT-45R test further increases the challenge of the benchmark.

The benchmark specification of SHRT-17 and SHRT-45R provided in this report addresses the requirements for collaborative efforts within international partnerships on the validation of simulation tools and models in the area of sodium fast reactor (SFR) passive safety. Validated tools and models are needed both to evaluate SFR passive safety phenomena and to assess reactor designs that incorporate these passive features into the system's response to accident initiators. Comparisons with experimental data and other safety codes create unique opportunities to improve SFR computational codes and methods.

An overview of the EBR-II reactor is given in Chapter 2 followed by a description of the SHRT-17 and SHRT-45R tests and the benchmark boundary conditions in Chapter 3. Chapters 4 and 5 provide detailed descriptions of the reactor core and coolant system in EBR-II, respectively. Chapter 6 provides suggested data that benchmark participants should calculate for measured test data and direct code-to-code comparisons.

2 EBR-II Plant Overview

The EBR-II plant is located in Idaho and was designed and operated by Argonne National Laboratory for the U.S. Department of Energy. Operation began in 1964 and continued until 1994. EBR-II was rated for a thermal power of 62.5 MW with an electric output of approximately 20 MW. Mass flow rates in the three cooling loops were rated as:

- Primary sodium at 485 kg/s,
- Intermediate sodium at 315 kg/s, and
- Secondary steam at 32 kg/s.

The primary tank in EBR-II is illustrated in Figure 2.1 below. All major primary system components were submerged in the primary tank, which contained approximately 340 m^3 of liquid sodium at 371°C. Two primary pumps drew sodium from this pool and provided sodium to the two inlet plena for the core. Subassemblies in the inner core and extended core regions received sodium from the high-pressure inlet plenum, accounting for approximately 85% of the total primary flow. The blanket and reflector subassemblies in the outer blanket region received sodium from the low-pressure inlet plenum.

Hot sodium exited the subassemblies into a common upper plenum where it mixed before passing through the outlet pipe into the intermediate heat exchanger (IHX). The pipe feeding sodium to the IHX is referred to as the ‘Z-pipe’ and will be described in greater detail in Chapter 5. Sodium then exited the IHX back into the primary sodium tank before entering the primary sodium pumps again. The shutdown coolers shown in Figure 2.1 are not included in the benchmark model.

Sodium in the intermediate loop traveled from the IHX to the steam generator where its heat was transferred to the balance-of-plant (BOP). The colder sodium in the intermediate loop then traveled through a similar length of piping back to the IHX. The steam generator consisted of two parallel superheaters and seven parallel evaporators. Figure 2.2 shows a simple schematic of the primary, intermediate and steam systems. Note that the power, flow and temperature conditions described earlier are for typical EBR-II operation. These conditions differ slightly from initial conditions for the SHRT-17 and SHRT-45R tests, which are discussed in Chapter 3.

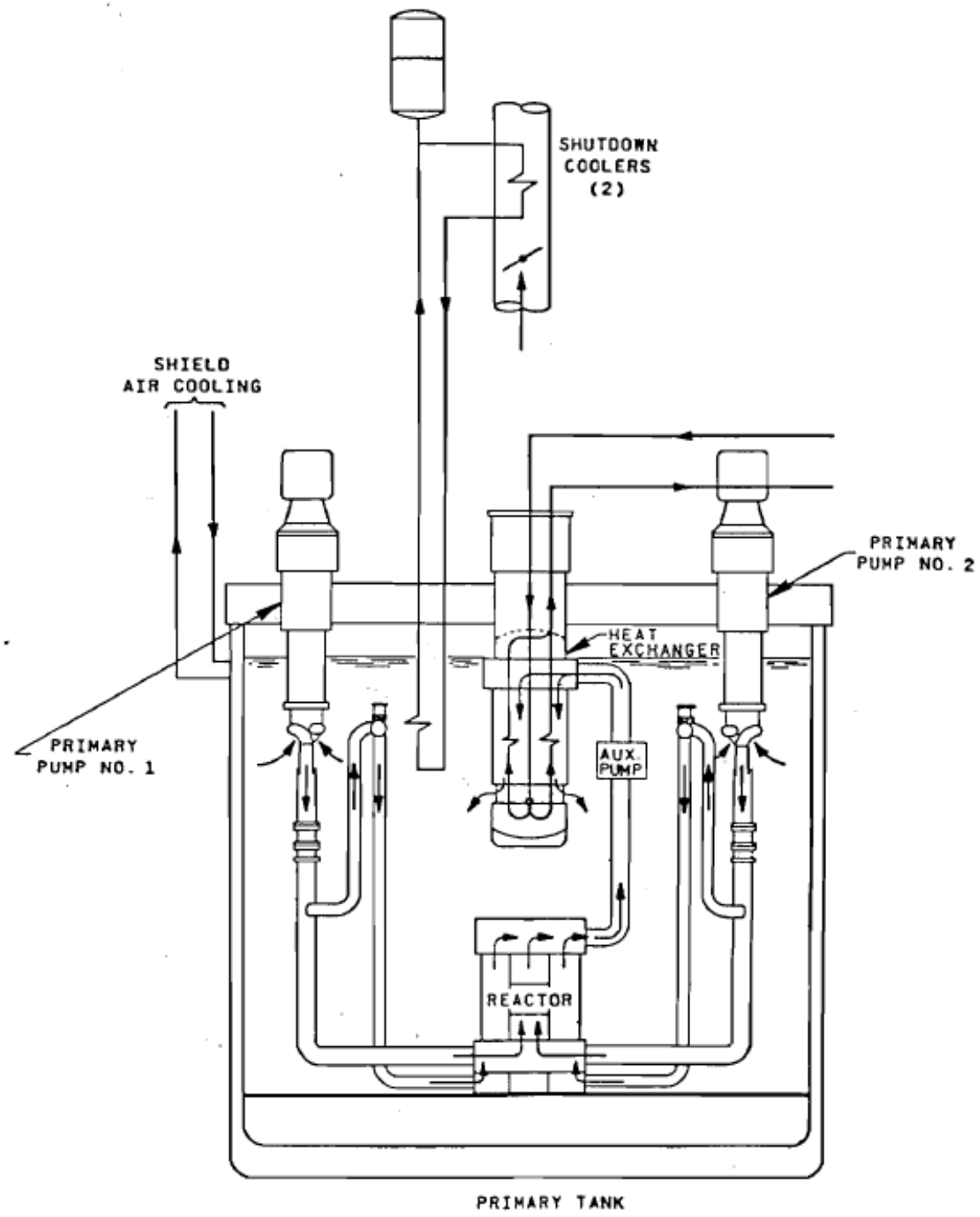

Figure 2.1. EBR-II Primary Tank Sodium Flow Paths

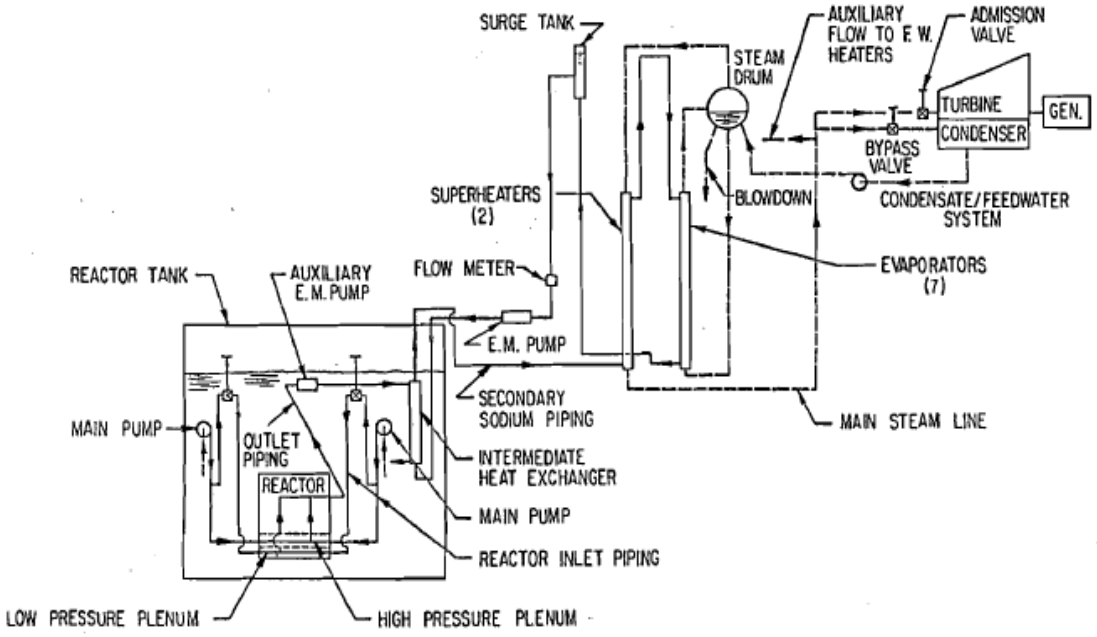

Figure 2.2. EBR-II Plant Schematic

The reactor-vessel grid-plenum assembly accommodated 637 hexagonal subassemblies. The subassemblies were segregated into three regions: core, inner blanket (IB) and outer blanket (OB). Figure 2.3 illustrates the subassembly arrangement of the reactor and the subassembly identification convention. Each subassembly position was identified by a unique combination of three parameters: row, sector and position within the sector. Subassembly row identification begins at Row 1 for the subassembly in the core-center and moves outward to Row 16. Row 1 had one subassembly. Row 2 had six subassemblies. From Row 2 outward to Row 14, each row had 6 more subassemblies than the last. Rows 15 and 16 were not complete rows and had 66 and 24 subassemblies, respectively.

Each row was broken up into six sectors A through F. As each row approximated a hexagon, each side of the row was assigned to one of the six sectors. The final parameter needed to identify a subassembly location is the position within the sector. The line of subassemblies dividing sectors A and F were defined as the subassemblies in position 1 of their respective rows within sector A. The line of subassemblies that divide sectors A and B are therefore defined as the subassemblies in position 1 of their respective rows within sector B. This pattern continues for the remaining four sides of the core layout. As an example, the subassembly labeled as CR #10 in Figure 2.3 is positioned in subassembly location 4B3, where 4 is the row, B is the sector and 3 is the position within the sector.

The central core comprised the 61 subassemblies in the first five rows. Two positions in row 3 contained safety-rod subassemblies, and eight positions in Row 5 contained control-rod subassemblies. Two positions in Row 5 contained the instrumented subassemblies (INSAT) XX09 and XX10, and one position in Row 5 contained the in-core instrument test facility (INCOT) XY16. The remainder of the central core region contained driver fuel or experimental-irradiation subassemblies.

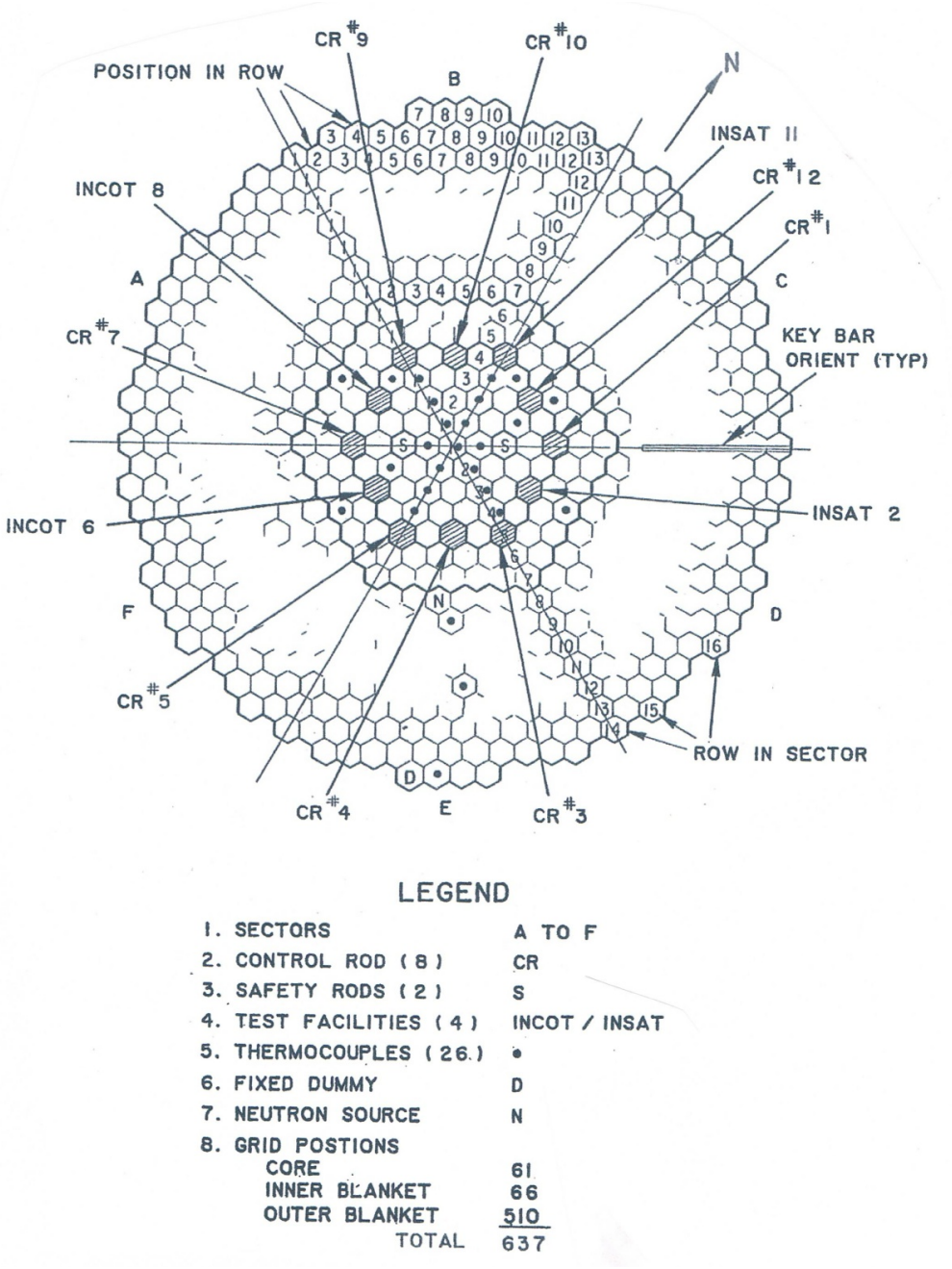

Figure 2.3. EBR-II Core Layout

The inner blanket region was composed of Rows 6 and 7. Originally these rows were loaded with blanket subassemblies. But for SHRT-17 and SHRT-45R, no blanket subassemblies were loaded in this region. Instead, Row 6 contained the driver-fuel and irradiation subassemblies of the expanded core and Row 7 contained reflector subassemblies. The outer blanket region comprised the 510 subassemblies in Rows 8-16, which were either blanket or reflector subassemblies.

EBR-II was heavily instrumented to measure mass flow rates, temperatures and pressures throughout the system. While several instruments failed prior to the shutdown heat removal tests, a large number of measurements are available throughout the system to compare benchmark simulation results against experimental data. Measurements are also available for the fission power during the transient. However, because these measurements only cover fission power, decay heat production is estimated for the transients to produce the total transient power. The appropriate measurements for comparison with benchmark simulation results are discussed in Chapter 6.

3 Description of the Tests

On June 20, 1984 a full power loss-of-flow test in the SHRT series demonstrated the effectiveness of natural circulation in the EBR-II reactor. During this test the plant protection system (PPS) was used to simultaneously scram the reactor. To initiate the SHRT-17 test, both primary coolant pumps and the intermediate-loop pump were tripped to simulate a protected loss-of-flow accident beginning from full power and flow conditions. In addition, the primary system auxiliary coolant pump that normally had an emergency battery power supply was also turned off. The reduction in coolant flow rate caused reactor temperatures to rise temporarily to high, but acceptable levels as the reactor safely cooled itself down by natural circulation.

On April 3, 1986 a full power loss-of-flow test in the SHRT series demonstrated the effectiveness of passive reactivity feedback in the EBR-II reactor to bring the reactor to decay heat power. During this test the plant protection system (PPS) was disabled to prevent initiation of a scram. To initiate the SHRT-45R test, both primary coolant pumps and the intermediate-loop pump were tripped to simulate an unprotected loss-of-flow accident beginning from full power and flow conditions. The reduction in coolant flow rate caused reactor temperatures to rise temporarily to high, but acceptable levels as the reactor safely terminated the fission process.

The SHRT-17 and SHRT-45R tests are described in detail in the sections that follow.

3.1 The SHRT-17 Test

3.1.1 *Description of the Test*

Prior to the start of SHRT-17, EBR-II was operated at full power and full flow for long enough that temperatures throughout the system had reached an equilibrium state. The full power operation was less than two hours in order to limit decay heat after scram. The control rod drives were active to allow control rod insertion at the start of the transient period.

The SHRT-17 transient was initiated by a trip of the primary and intermediate pumps. The reactor was also instantaneously scrammed. The primary pump trip mode was a breaker trip in which the power to the motor-generator sets and the clutches was simultaneously lost. Each primary pump had its own controller and motor-generator (M-G set). The flow coastdown was governed by the kinetic energy stored in the inertia of the M-G set. While the coastdown shapes for SHRT-17 were designed to be identical for the two primary pumps, intrinsic differences between the two pump drive units caused a difference in stop times. The auxiliary electromagnetic pump in the primary loop was turned off and did not receive power from battery backups as would occur during a total station blackout.

As the SHRT-17 test continued, the reactor decay power decreased due to fission product decay. After the start of the test, no automatic or operator action took place until the test had concluded. Table 3.1.1 summarizes the initial conditions and transient initiators for the SHRT-17 test.

Table 3.1.1.1. SHRT-17 Test Description

Initial Power	57.3 MW (ANL-EBR-132)
Initial Primary Coolant Flow Through Core	8500 gpm at 800°F
Initial Intermediate Coolant Flow	5614.6 gpm at 582°F
Initial Core Inlet Temperature	664.8°F
Primary and Intermediate Pump Coastdown Conditions	Power to motor-generator sets removed
Control Rods	Full insertion at test initiation
Auxiliary EM Pump Conditions	Power to Auxiliary EM Pump removed

3.1.2 *Pre-Transient History*

SHRT-17 occurred during EBR-II Run 129-C. At 12:20 AM on the day of the SHRT-17 test, the SHRT-26 test was concluded and the reactor was shutdown. The reactor remained shutdown until 5:45 AM. Between 5:45 AM and 8:14 AM the reactor was slowly brought back up to power. Between 8:14 and 10:00 AM, EBR-II remained at full power and flow to ensure that temperatures throughout the system had reached equilibrium.

3.1.3 *Initial Conditions*

Figures 3.1.3.1 and 3.1.3.2 show the pre-test calculated powers and flows by core subassembly for the SHRT-17 test. The flow values were obtained as part of the test planning and are the results of calculations from the EBRFLOW code. EBRFLOW was a steady-state thermal-hydraulic design code developed and used by EBR-II project staff to predict flow and outlet mixed mean temperature per subassembly in the reactor. It was based on both EBR-II plant instrument data and data from a separate effects hydraulic rig that was dedicated to obtaining full-scale subassembly pressure drop data for various EBR-II subassembly designs. The ORNL two-dimensional discrete ordinates transport code DOT-III was used to determine individual subassembly power distributions for EBR-II tests. DOT-III calculated both neutron and gamma flux distributions within each subassembly.

Primary sodium heat balance calculations are not available for the SHRT-17 test. According to post run-reports for Run 129-C (ANL-EBR-132), the initial power for the SHRT-17 test was 57.3 MW. Note that Figures 3.1.3.1 and 3.1.3.2 are for Run 129C, not SHRT-17 specifically, and should be renormalized to the appropriate initial power and flow for SHRT-17.

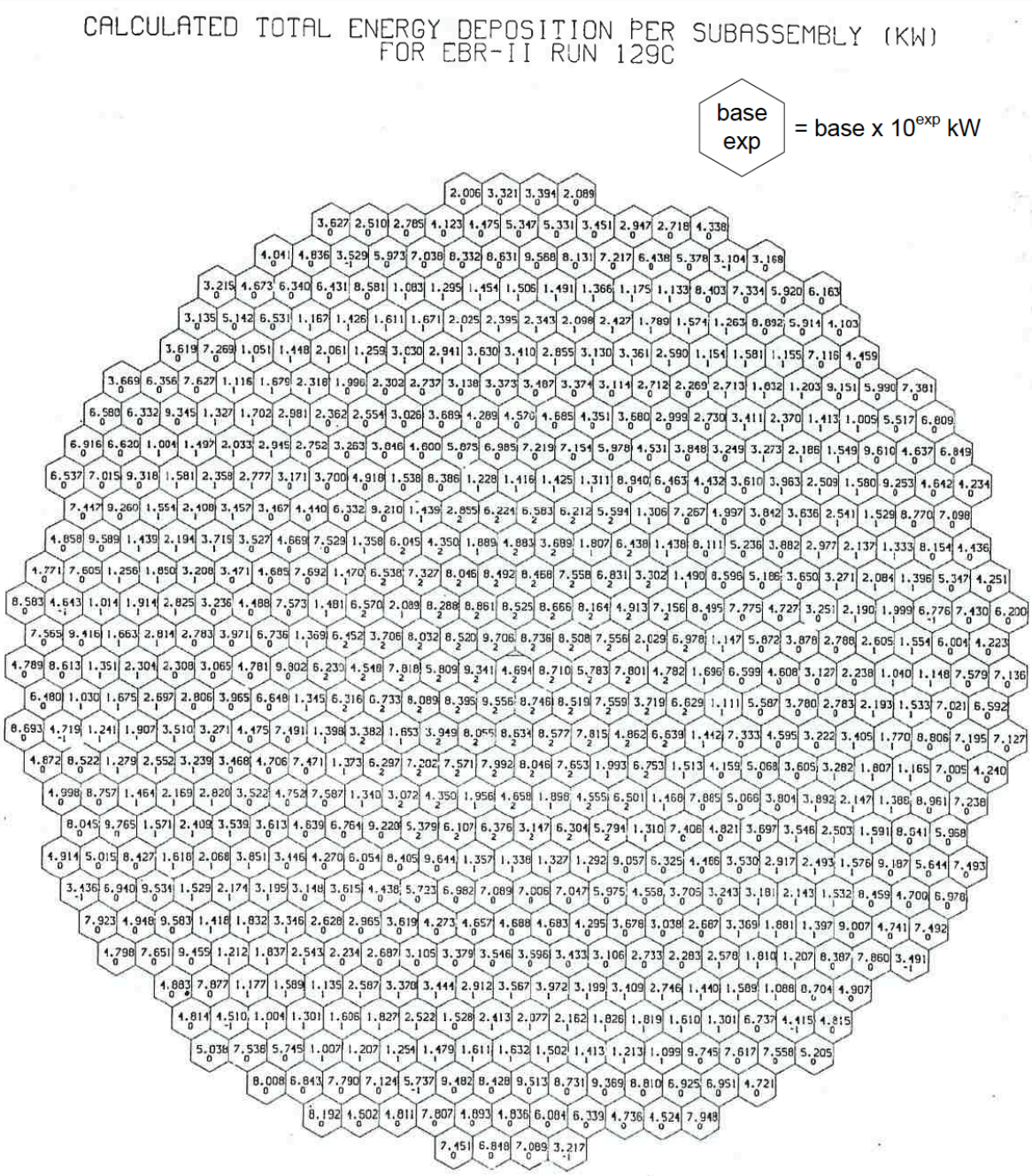

Figure 3.1.3.1. SHRT-17 Power Per Subassembly

The initial core flow rate for the SHRT-17 test was 8500 gpm. Primary sodium flow rates measured in gallons per minute were calibrated at 800°F. Initial flow rates at various locations throughout the primary sodium circuit based on assumed sodium leakage flow rates are discussed in Section 5.3.1. Figure 3.1.3.2 illustrates the subassembly flow distribution based on the proposed core loading pattern as calculated with EBRFLOW. Four different measurements taken of the inlet plena temperatures show that the average core inlet temperature at the start of the SHRT-17 test was 664.8°F.

Pressure measurements taken in EBR-II were calibrated to not include gravity head so that during zero flow conditions, they all read zero. The initial pressure at the discharge of primary sodium pump #1 was 42.9 psi. The initial pressure at the discharge of primary sodium pump #2 was 41.9 psi. At the outlet of the core, the initial upper plenum pressure was 6.36 psi.

The intermediate sodium loop had an initial mass flow rate of 5614.6 gpm. Intermediate sodium flow rates measured in gallons per minute were calibrated at 582°F. The temperature at the inlet to the IHX in the intermediate loop was initially 573.8°F. Pressure measurements at the inlet and the outlet of the intermediate side of the IHX are not available.

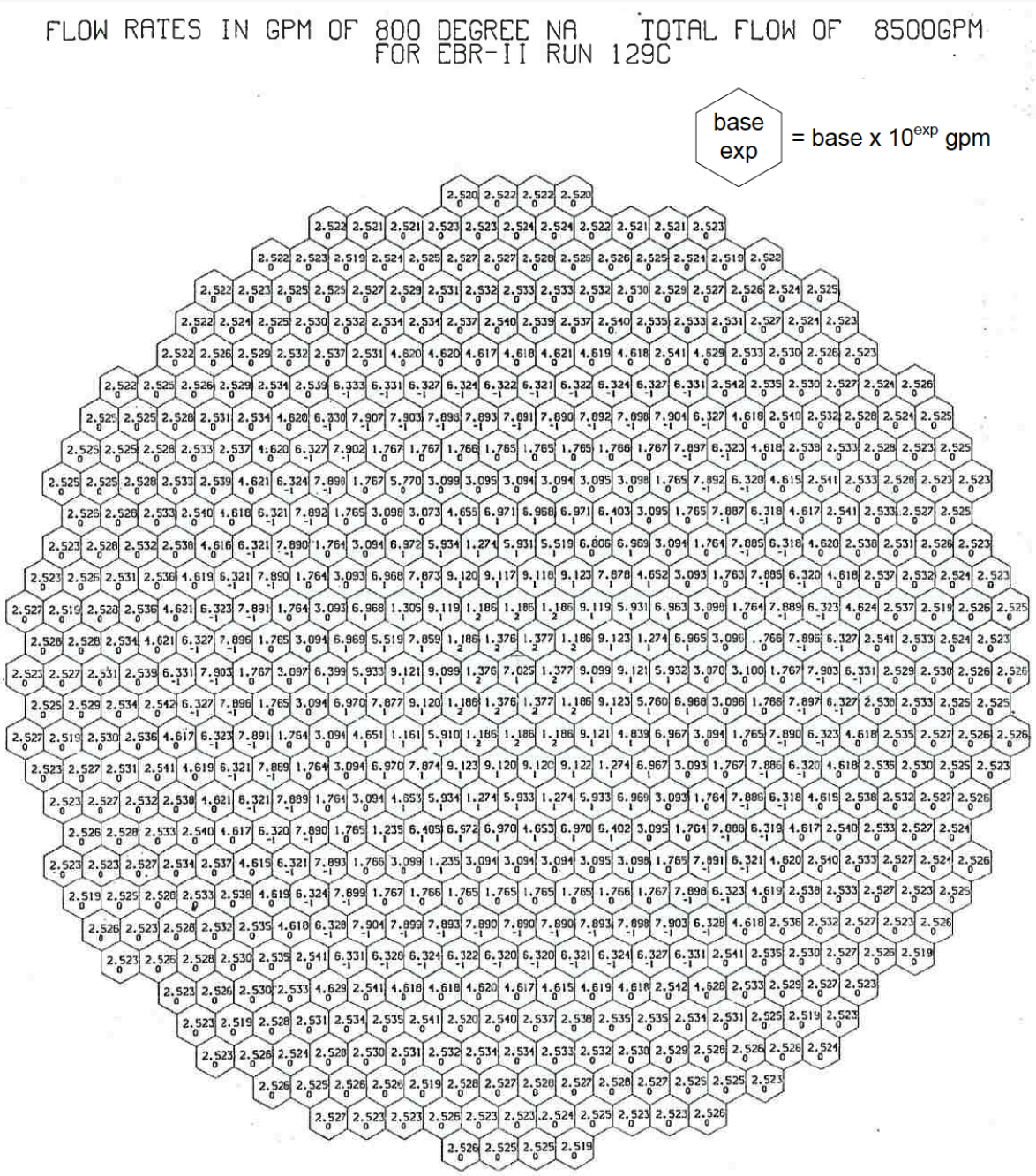

Figure 3.1.3.2. SHRT-17 Flow Per Subassembly at 800°F

3.1.4 *Transient Boundary Conditions*

The boundary conditions for the benchmark specification of SHRT-17 are described in this section. The pump speeds of the two primary sodium pumps are treated as boundary conditions in the primary sodium circuit. In the intermediate sodium loop, the boundary conditions are the flow rate and temperature of the sodium at the inlet of the IHX. The boundary conditions described in this section are consistent with the test procedure described in Section 3.1. These boundary conditions should be sufficient to comprehensively define the benchmark. Data is provided for each of the boundary conditions for the 15-minute duration of the test.

3.1.4.1 *Primary side boundary conditions*

Primary sodium pump speeds are illustrated in Figure 3.1.4.1.1 below and also listed in Table 3.1.4.1.1.

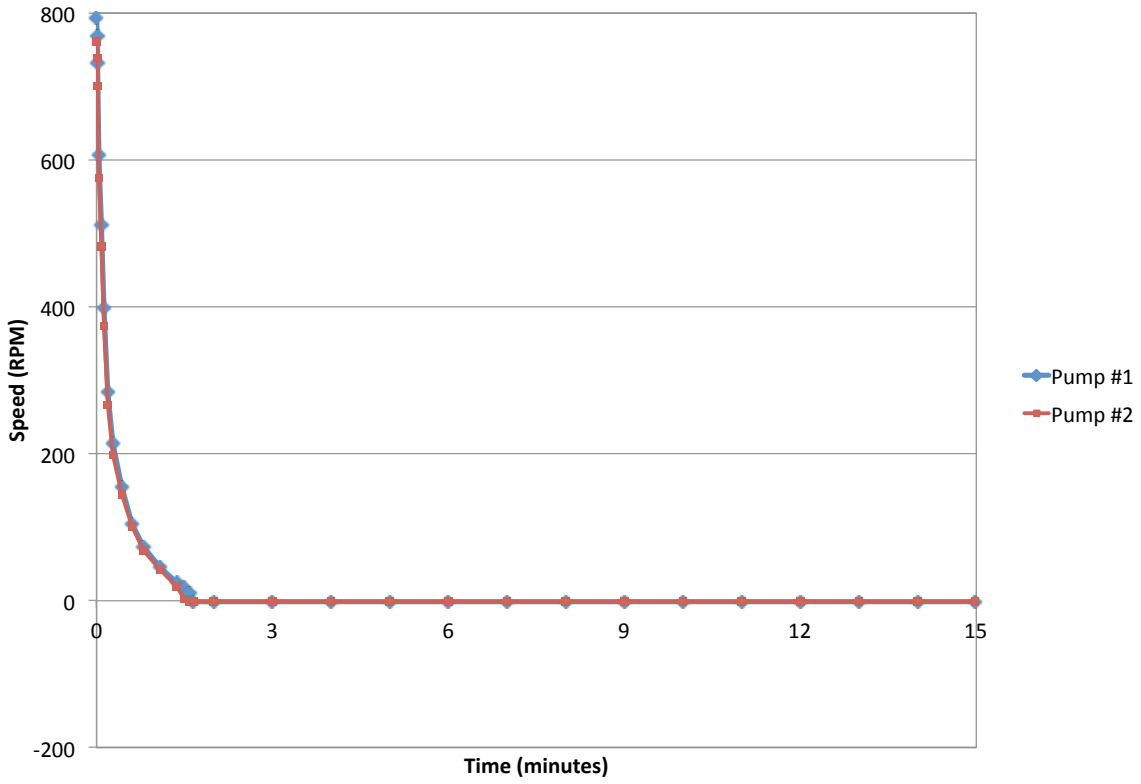

Figure 3.1.4.1.1. Primary Pump Speeds for SHRT-17

Table 3.1.4.1.1. Primary Pump Speeds for SHRT-17

Time (seconds)	Pump #1 (rpm)	Pump #2 (rpm)
0	799.03	764.92
2	727.77	695.42
4	566.79	532.61
6.5	407.49	379.64
9	323.18	301.59
12.5	244.06	230.18
17.5	172.50	167.39
24.5	109.25	113.98
33	56.46	74.62
42	0.69	46.54
51	0.76	2.29
90	0.76	2.44
120	0.61	2.44
180	0.76	2.44
240	0.84	2.59
300	0.61	2.44
360	0.61	2.44
420	0.61	2.44
480	0.61	2.44
540	0.76	2.44
600	0.76	2.75
660	0.69	2.44
720	0.69	2.44
780	0.76	2.59
840	0.76	2.44
900	0.92	2.44

The EBR-II pump model was developed specifically for EBR-II and was implemented in the NATDEMO system simulation code. The pump characteristics in this model are based upon EBR-II experience and can be used together with the pump speed histories above to provide the pump heads during SHRT-17 and SHRT-45R. The pump model is mainly applicable to the first quadrant (positive flow, positive pump speed) and can be used for negative flow. When the user specifies the pump speed as a function of time, the pump head is calculated from the following set of equations.

$$\overline{H} = b_1 \bar{s}^2 + b_2 \bar{s} \overline{w} + b_3 \frac{\overline{w}}{|\overline{w}|} |\overline{w}|^{b_4} \tag{3.1}$$

where

$$\overline{H} = H/H_r \tag{3.2}$$

$$\bar{s} = s/s_r \tag{3.3}$$

$$\overline{w} = w/w_r \tag{3.4}$$

H = pump head

s = pump speed

and

w = coolant flow rate

The r subscript refers to the rated value. The coefficients b_1 and b_2 are constant, but the values of b_3 and b_4 depend on the speed and flow rate, plus several empirical constants defined below:

$$b_3 = \begin{cases} b_{3m} & \text{if } \bar{s} > \epsilon_m \overline{w} \quad (3.5a) \\ b_{3t} & \text{if } \bar{s} \le \epsilon_m \overline{w} \text{ and } \overline{w} \ge \overline{w}_t \quad (3.5b) \\ b_{3\ell} & \text{if } \bar{s} \le \epsilon_m \overline{w} \text{ and } \overline{w} < \overline{w}_t \quad (3.5c) \end{cases}$$

$$b_4 = b_{4t} \text{ if } \bar{s} > \epsilon_m \overline{w} \text{ or } \overline{w} \ge \overline{w}_t \tag{3.6a}$$

$$b_4 = b_{4\ell} \text{ if } \bar{s} \le \epsilon_m \overline{w} \text{ and } \overline{w} < \overline{w}_t \tag{3.6b}$$

Equations 3.5 and 3.6 are based on the idea of using a stopped-rotor pressure drop if $\bar{s} < \in_m \bar{w}$. Also, the stopped-rotor pressure drop is a laminar value if $\bar{w} < \bar{w}_t$, or a turbulent value if $\bar{w} \geq \bar{w}_t$. The default values for the coefficients are:

$$b_1 = 1.1740 \quad (3.7a)$$

$$b_2 = 0.0818 \quad (3.7b)$$

$$b_{3m} = -0.2558 \quad (3.7c)$$

$$b_{3t} = -0.5923 \quad (3.7d)$$

$$b_{3\ell} = -0.0471 \quad (3.7e)$$

$$b_{4t} = 1.9 \quad (3.7f)$$

$$b_{4\ell} = 1.0 \quad (3.7g)$$

$$\bar{w}_t = 0.06 \quad (3.7h)$$

$$\in_m = 0.55 \quad (3.7i)$$

$$H_r = 358{,}530 \text{ Pa} \quad (3.7j)$$

$$w_r = 250.2 \text{ kg/s} \quad (3.7k)$$

and

$$s_r = 14.5 \text{ revolutions/s} = 870 \text{ rpm} \quad (3.7l)$$

This correlation could produce a discontinuity in pump head at the switch from spinning rotor to stopped rotor. With the default values, the pump head is continuous at the transition from turbulent to laminar flow.

Table 3.1.4.1.2 gives the pump parameters to be used for the EBR-II primary side simulation. While EBR-II has two “identical” primary pumps, pump #2 has higher frictional torque losses and stops sooner during the coastdown.

Table 3.1.4.1.2. EBR-II primary pump parameters

Parameter		Rated Condition
N_R (rpm)	rated speed	870.0
H_R (m)	rated head	37.7
Q_R (m^3/s)	rated flow	0.2946
N_s (SI/gp)	specific speed	31.01/1602
I_p ($kg \cdot m^2$)	inertia	16.0
T_R (N·m)	rated torque	1300.0
$T_{f,R}$ (N·m)	friction torque	0.0286 T_R (37.2)

3.1.4.2 *Power Measurement*

The normalized measured fission power for the first twenty seconds of SHRT-17 is illustrated in Figure 3.1.4.2.1. No measurements were taken to effectively measure either the total reactor power or the decay heat power during the transient. To estimate the total reactor power during this test, the decay heat power at the start of SHRT-17 was calculated based on the ANS decay heat standard. The light water reactor decay heat standard was used as there is not yet a fast reactor decay heat standard and also because it is not expected to make a significant difference. For this calculation, the pre-transient power history given in Sections 3.1.2 was assumed leading to a calculated initial decay heat power of 3.36 MW and scale fission power of 53.93 MW at the start of SHRT-17. It should be noted that the decay heat parameters for Run 129C are not available so known decay heat parameters from a later run with very similar core composition, assembly loading pattern and flux shape were used to calculate the initial SHRT-17 decay heat power.

The ANS decay heat standard was used once again to calculate the decay heat power during the transient as a function of the normalized measured fission power given in Figure 3.1.4.2.1. The resulting decay heat power is plotted with the scaled fission power in Figure 3.1.4.2.2 along with the sum of the two for the total reactor transient power. Fission, decay heat and total power data is given in Table 3.1.4.2.1.

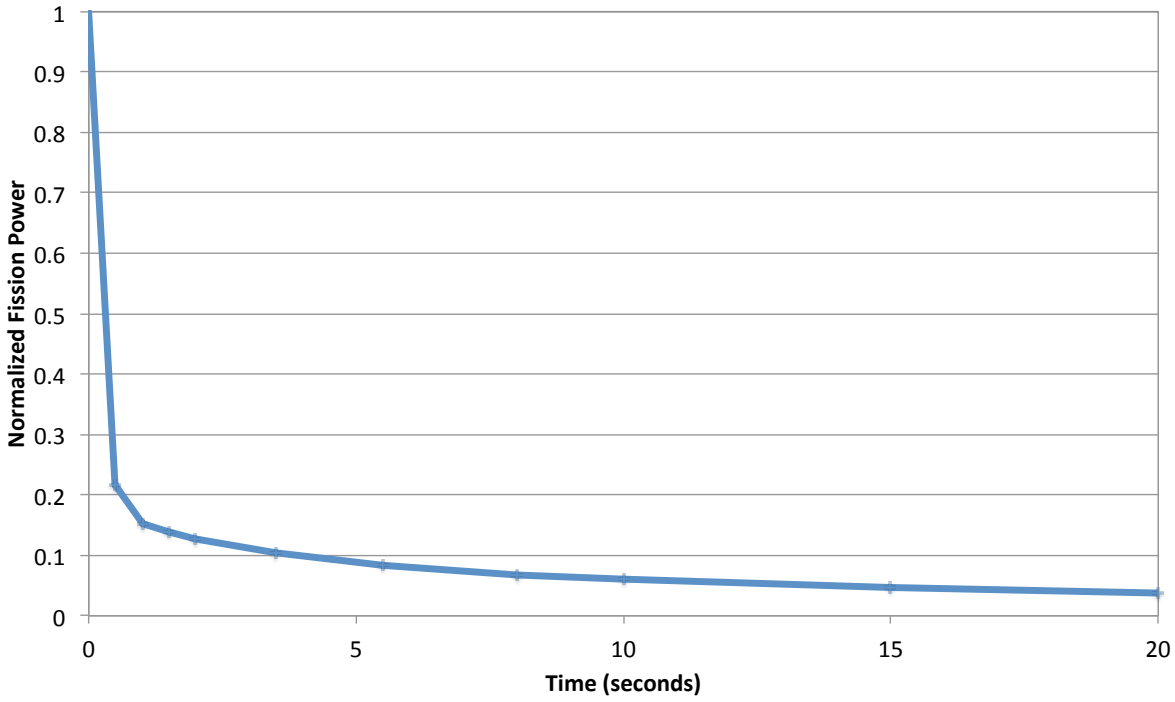

Figure 3.1.4.2.1. Normalized Fission Power During Beginning of SHRT-17

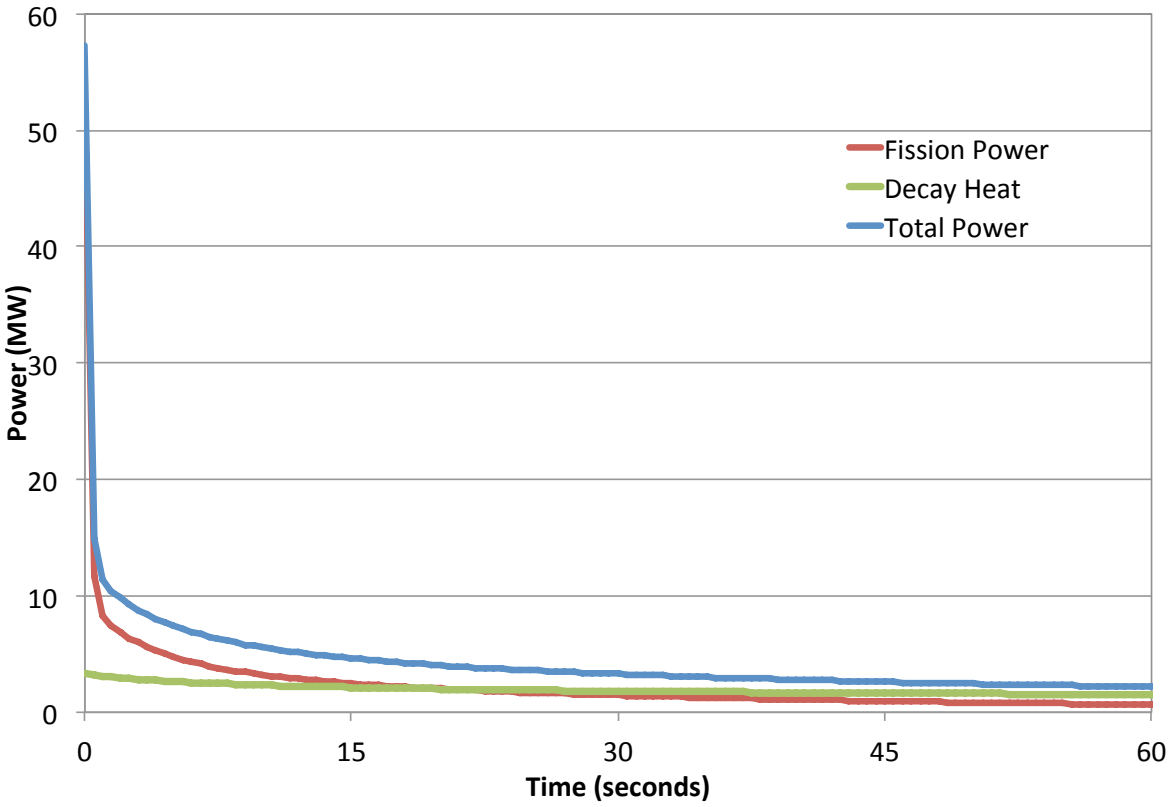

Figure 3.1.4.2.2. Total, Fission and Decay Heat Power During SHRT-17

Table 3.1.4.2.1. SHRT-17 Fission, Decay Heat and Total Power

Time (seconds)	Fission	Decay Heat	Total
0	53.93	3.36	57.29
1	8.24	3.12	11.36
2	6.86	2.95	9.81
3.5	5.61	2.77	8.38
5	4.76	2.63	7.39
7.5	3.82	2.46	6.29
10	3.23	2.33	5.56
15	2.47	2.15	4.62
22.5	1.85	1.95	3.80
30	1.46	1.82	3.28
40	1.10	1.70	2.79
50	0.84	1.60	2.44
60	0.66	1.52	2.19
90	0.38	1.35	1.73
120	0.25	1.24	1.49
180	0.13	1.09	1.22
240	0.10	1.00	1.10
300	0.10	0.93	1.02
360	0.08	0.88	0.96
420	0.08	0.83	0.92
480	0.08	0.80	0.88
540	0.08	0.77	0.84
600	0.08	0.74	0.82
660	0.08	0.71	0.79
720	0.07	0.69	0.76
780	0.08	0.67	0.75
840	0.07	0.65	0.72
900	0.07	0.63	0.70

3.1.4.3 *Intermediate side boundary conditions*

The boundary conditions for the intermediate sodium loop for the SHRT-17 benchmark are the sodium flow rate and temperature at the inlet to the IHX. The IHX inlet sodium flow rate on the intermediate side during SHRT-17 is illustrated in Figure 3.1.4.2.1 and also given in Table 3.1.4.2.1. This flow was driven by the coastdown of the intermediate side EM pump upon trip of the 2400-V breaker to the M-G set. The corresponding IHX inlet sodium temperature is shown in Figure 3.1.4.2.2 and also given in Table 3.1.4.2.2.

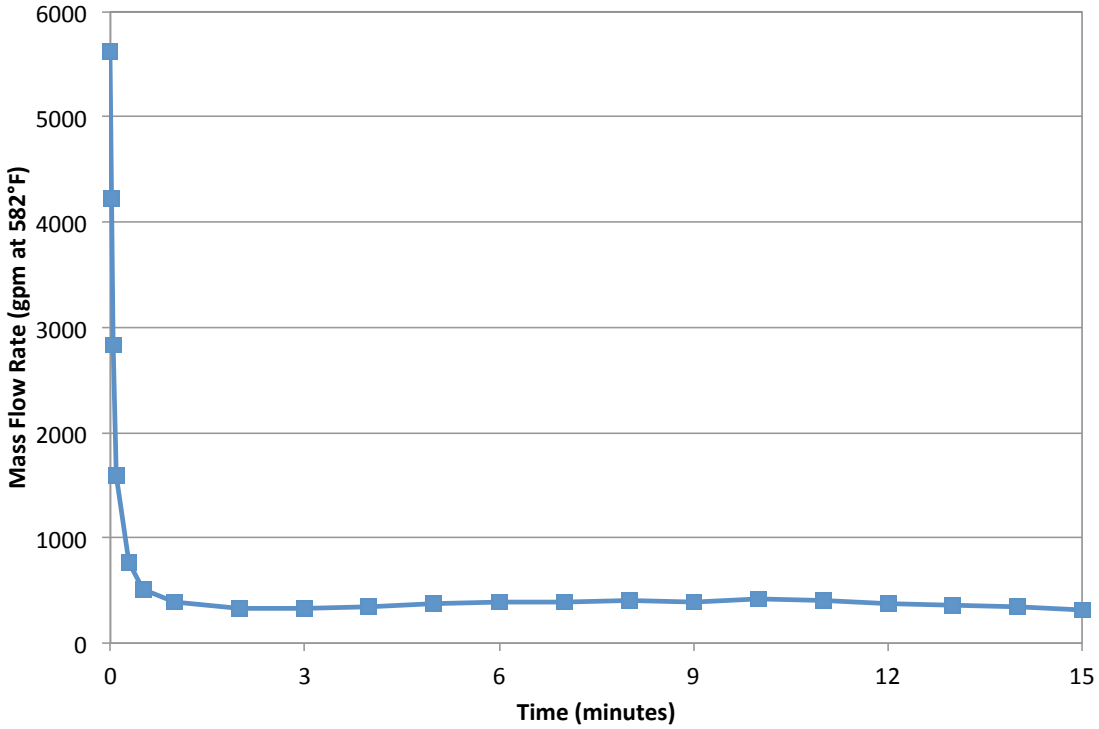

Figure 3.1.4.2.1. Intermediate Heat Exchanger Intermediate Inlet Sodium Mass Flow Rate For SHRT-17

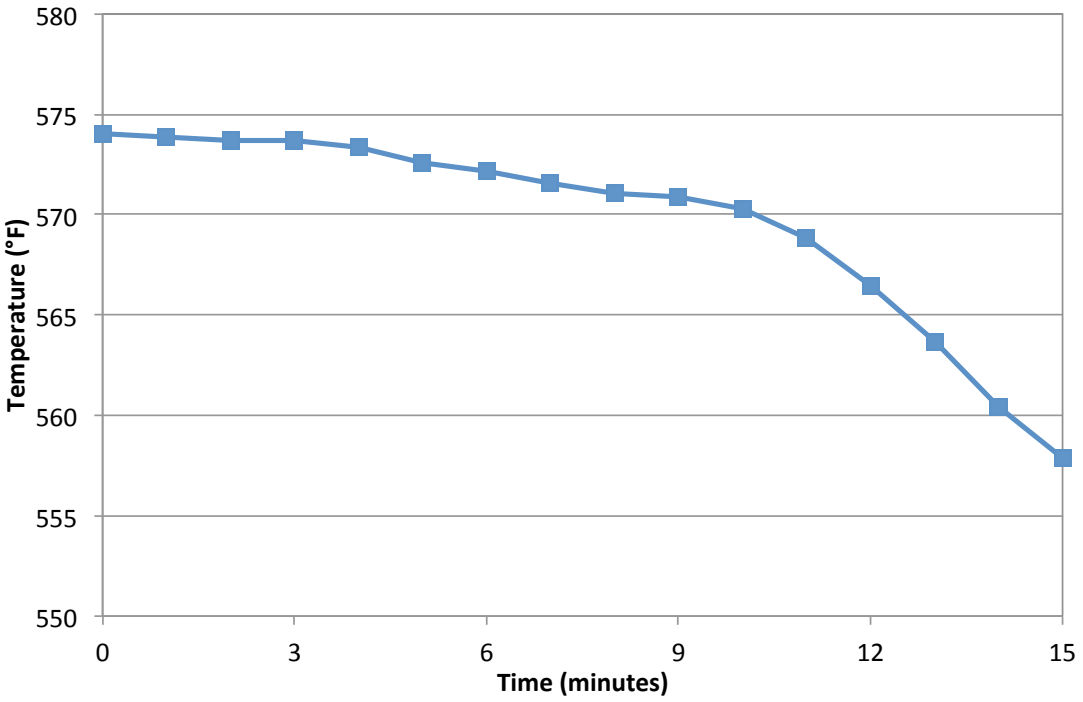

Figure 3.1.4.2.2. Intermediate Heat Exchanger Intermediate Inlet Sodium Temperature For SHRT-17

Table 3.1.4.2.1. Intermediate IHX Inlet Sodium Flow Rate For SHRT-17

Time (seconds)	Flow (gpm at 582°F)
0	5619.55
1	4221.68
2.5	2834.03
6	1593.92
16.5	760.20
30	511.05
60	383.93
120	328.28
180	329.81
240	343.09
300	371.17
360	392.10
420	397.20
480	403.33
540	398.22
600	424.77
660	399.76
720	369.12
780	357.38
840	340.53
900	310.92

Table 3.1.4.2.2. Intermediate IHX Inlet Sodium Temperature For SHRT-17

Time (seconds)	Temperature (°F)
0	574.02
60	573.86
120	573.65
180	573.73
240	573.37
300	572.63
360	572.17
420	571.53
480	571.02
540	570.87
600	570.26
660	568.82
720	566.43
780	563.69
840	560.39
900	557.83

3.1.4.4 *Control Rod/Safety Rod Positions*

EBR-II had two types of control rod designs. The original design, which is designated in this report as the regular worth control rod design, did not include boron carbide poison but essentially consisted of a fuel element pin bundle for the reactivity control. In the High Worth Control Rod (HWCR) design version, the fuel element pin bundle was located below a boron carbide poison pin bundle section. Details can be found in section 4.1.5.

The poison section in the HWCR entered the core region when the fuel element pin bundle section was lowered out of the core. Conversely when the fuel pin bundle section was raised back into the core, this boron pin poison section was raised out of the core, which therefore maximized the reactivity swing. For SHRT-17 the control rods were fully inserted at the beginning of the test such that the bottom of the control rod fuel bundle was 14 inches below the bottom of the fuel bundle of the core driver subassemblies.

The safety rod subassemblies contained 61 fuel elements located in the approximate center of the rod subassembly. Details can be found in section 4.1.6. The safety rod was normally positioned in the reactor with the fuel elements either at the same elevation as the core region or 14 inches lower than the core region to position the fuel element outside the core region. For SHRT-17 the safety rods were fully inserted at the beginning of the test such that the bottom of the safety rod fuel bundle was 14 inches below the bottom of the fuel bundle of the core driver subassemblies.

3.2 The SHRT-45R Test

3.2.1 *Description of the Test*

Prior to the start of SHRT-45R, EBR-II was operated at full power and full flow for long enough that the system had reached an equilibrium state. The initial conditions of EBR-II at the beginning of SHRT-45R are discussed below in Section 3.2.2. Just prior to test initiation, the control rod drives were deactivated to preclude control rod movement during the transient period. This action prevented insertion or withdrawal of the rods by the drive motors, but it did not affect the scram function. In order to protect the reactor from equipment failures during testing, a special scram protection system was implemented just prior to test initiation. This protection was based on in-core temperatures measured with the special XX09 INSAT. Implementation of the special XX09 scram protection also bypassed the normal protection for loss of primary flow, which was a function of low primary flow and high subassembly outlet temperature trips.

The SHRT-45R transient was initiated by opening the 2400 V breaker powering the motor-generator (M-G) set of the primary and intermediate pumps thus removing the power supply to the pumps. Each primary pump had its own controller and M-G set. As is standard practice, the motor of the M-G set is powered by the line voltage. The shaft of the spinning M-G motor then drives the M-G generator shaft through a clutch arrangement. The spinning M-G generator then produces the voltage that powers the pump motor. By varying the coupling of the M-G motor to the M-G generator through the clutch, the power produced by the generator can be varied. During a coastdown when the voltage to the M-G motor is lost, the inertia in the spinning M-G motor and spinning M-G generator is used to extend the pump coastdown.

To obtain the desired extended flow coastdown, less energy was removed from the motor of the M-G set at the beginning of the coastdown. This energy was applied at the end of the coastdown through the coupling of the motor-generator (M-G) set clutch, which retained its power supply. These conditions are similar to those for a station blackout. While the coastdown shapes for SHRT-45R were designed to be identical for the two primary pumps, intrinsic differences between the two pump drive units caused a difference of approximately 5 seconds in stop times. The auxiliary electromagnetic pump in the primary loop continued to receive power from its battery while the rectifier remained tripped, as would occur during a total station blackout.

As the SHRT-45R test continued, the reactor power decreased due to reactivity feedbacks. Once the test was initiated, no automatic or operator action took place until the test had concluded, at which point the reactor was scrammed. Table 3.2.1.1 summarizes the initial conditions and transient initiators for the SHRT-45R test.

Table 3.2.1.1. SHRT-45R Test Description

Initial Power	60.0 MW
Initial Primary Coolant Flow	8971.9 gpm at 800°F
Initial Intermediate Coolant Flow	5474.5 gpm at 582°F
Initial Core Inlet Temperature	650.8°F
Primary and Intermediate Pump Coastdown Conditions	• Power to motor-generator sets removed • Flow coastdown controlled by coupling and decoupling of motor-generator set clutch • Approximately 95 seconds before pump stop
Control Rods	Insertion disabled
Auxiliary EM Pump Conditions	On battery

3.2.2 *Pre-Transient History*

SHRT-45R was conducted during EBR-II Run 138-B. A full, detailed power history of EBR-II during and in the days before Run 138B is not available. For the purposes of calculating decay heat and reactivity feedback coefficients, the following simplified power history has been assumed. Prior to Run 138-B, EBR-II was shut down for approximately a month and a half. Run 138B began 5.67 days before SHRT-45R. At this point, EBR-II was started up and operated at 17.9 MW for 4.03 days. Then 1.64 days before the beginning of SHRT-45R, the power level was increased to 60.0 MW. EBR-II was run at 60.0 MW until SHRT-45R began. During Run 138-B, EBR-II was run for a total of 177 MW-days.

3.2.3 *Initial Conditions*

Figures 3.2.3.1 and 3.2.3.2 show the pre-test calculated subassembly power and flow. The flow values were obtained as part of the test planning and are the results of calculations from the EBRFLOW code. EBRFLOW was a steady-state thermal-hydraulic in-house design code developed and used by EBR-II project staff to predict flow and outlet mixed mean temperature per subassembly in the reactor. It was based on both EBR-II plant instrument data and data from a separate effects hydraulic rig that was dedicated to obtaining full-scale subassembly pressure drop data for various EBR-II subassembly designs. The ORNL two-dimensional discrete ordinates transport code DOT-III was used to determine individual subassembly power distributions for EBR-II tests. DOT-III calculated both neutron and gamma flux distributions within each subassembly.

The values given in Figures 3.2.3.1 and 3.2.3.2 for the predicted power and flow are based on the proposed core-loading pattern for Run 138B. There were a few differences between the proposed loading pattern, upon which these calculations were based, and the loading pattern that was actually used for Run 138B. Those differences will be discussed in Chapter 4. Primary sodium heat balance calculations performed just prior to SHRT-45R showed that EBR-II was operating at 60.0 MW. Note that Figures 3.2.3.1 and 3.2.3.2 are for Run 138B, not SHRT-45R specifically, and should be renormalized to the appropriate initial power and flow for SHRT-45R.

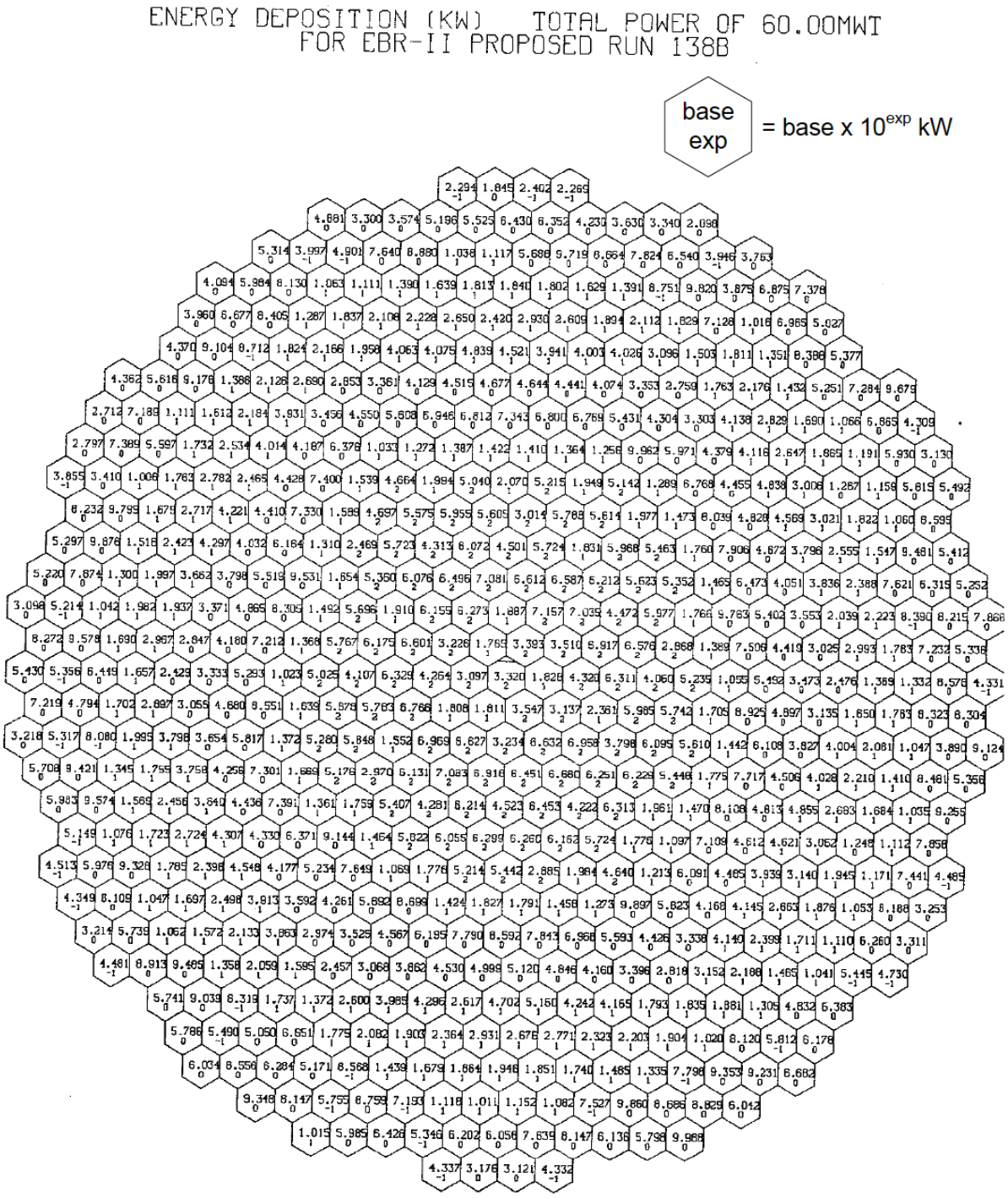

Figure 3.2.3.1. SHRT-45R Power Per Subassembly

Measurements taken before SHRT-45R show that the flow rates for pumps #1 and #2 were 4489.1 gpm and 4482.8 gpm, respectively, for a total primary sodium flow rate of 8971.9 gpm. The measured flow rate at the beginning of the reactor outlet pipe was 8703.2 gpm. The remaining 268.7 gpm was assumed lost to leakage flow paths, which are discussed in Chapter 5. Figure 3.2.3.2 illustrates the subassembly flow distribution as calculated with EBRFLOW. Note that these values are based on a total core flow rate of 9218 gpm and will need to be scaled down to the actual sodium flow rate through the core, which was 8766.6 gpm. Four different measurements taken of the inlet plena temperatures show that the average core inlet temperature at the start of the SHRT-45R test was 650.8°F. Primary sodium flow rates measured in gallons per minute were calibrated at 800°F.

Pressure measurements taken in EBR-II were calibrated to not include gravity head so that during zero flow conditions, they all read zero. The initial pressure at the discharge of primary sodium pump #1 was 41.84 psi. Unfortunately, no pressure measurement is available for the discharge of primary sodium pump #2 so for this benchmark specification, it is assumed both pumps had the same initial discharge pressure. At the outlet of the core, the initial upper plenum pressure was 6.51 psi.

The intermediate sodium loop had an initial mass flow rate of 5474.5 gpm. Intermediate sodium flow rates measured in gallons per minute were calibrated at 582°F. The temperature at the inlet to the IHX in the intermediate loop was initially 552.1°F. Pressure measurements at the inlet and the outlet of the intermediate side of the IHX are not available.

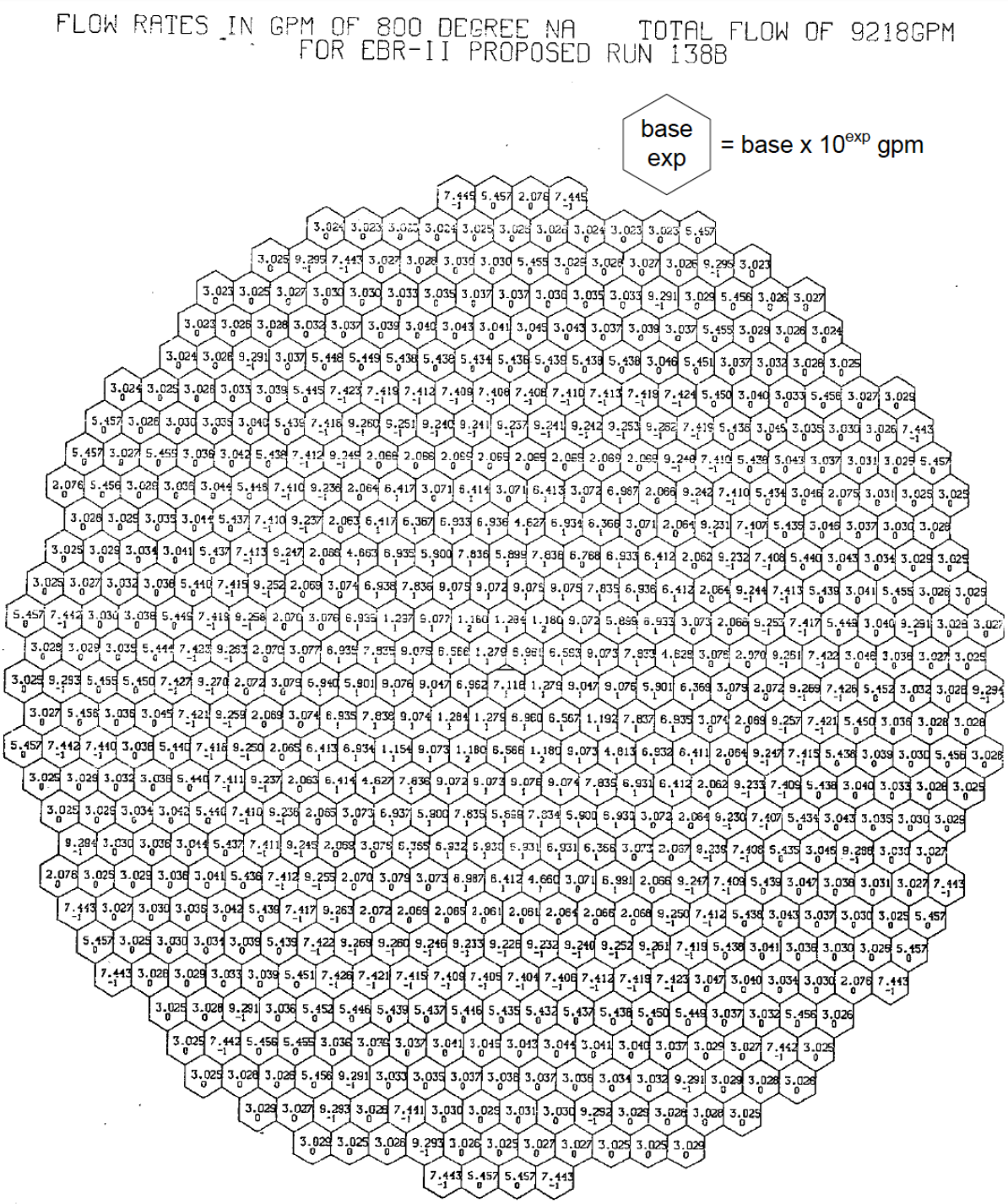

Figure 3.2.3.2. SHRT-45R Flow Per Subassembly at 800°F

3.2.4 *Transient Boundary Conditions*

The pump speeds of the two primary sodium pumps are treated as boundary conditions in the primary sodium circuit. In the intermediate sodium loop, the boundary conditions are the flow rate and temperature of the sodium at the inlet of the IHX. The boundary conditions described in this section are consistent with the test procedure described at the beginning of Section 3.2. Suggestions are provided regarding the modeling of the auxiliary EM pump in the primary circuit during SHRT-45R. These boundary conditions are sufficient to define the benchmark. Data is provided for each of the boundary conditions for the 15-minute duration of the test.

3.2.4.1 *Primary side boundary conditions*

Data for the pump speed of the two primary sodium pumps is illustrated in Figure 3.2.4.1.1 below and also listed in Table 3.2.4.1.1. A description of the Argonne EBR-II pump model is provided in Section 3.1.4.1 above for SHRT-17. This pump model is also be used for SHRT-45R.

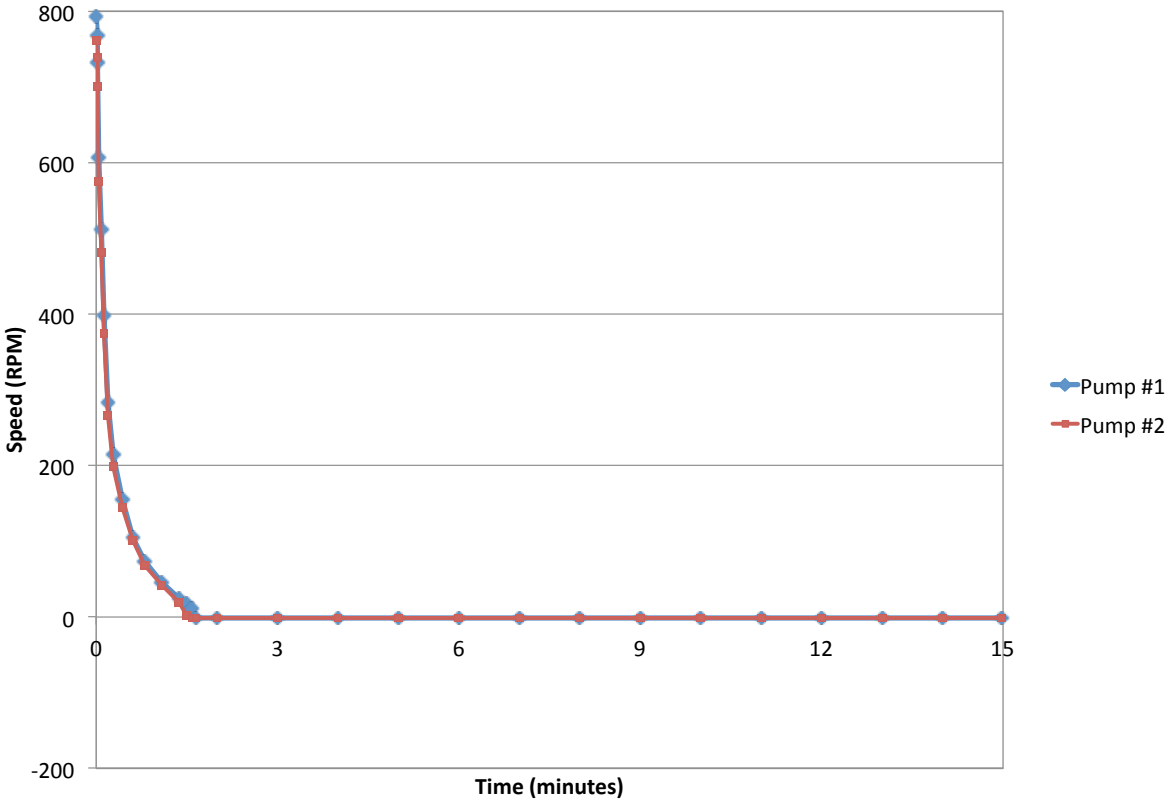

Figure 3.2.4.1.1. Primary Pump Speeds for SHRT-45R

Table 3.2.4.1.1. Primary Pump Speeds for SHRT-45R

Time (seconds)	Pump #1 (rpm)	Pump #2 (rpm)
0	792.05	762.27
1	769.10	739.07
1.5	731.19	701.21
3	606.46	575.65
4.5	511.19	482.21
7	397.55	373.96
11	283.90	266.69
17	213.66	198.62
25.5	154.38	144.98
36.5	105.14	100.40
48.5	72.67	68.91
64.5	46.45	42.42
82	25.45	19.69
90	17.13	1.38
95	10.39	-0.67
98.5	-0.67	-0.67
120	-1.06	-0.99
180	-0.72	-0.67
240	-0.67	-0.53
300	-1.26	-1.23
360	-1.53	-1.38
420	-0.87	-0.77
480	-0.70	-0.50
540	-1.60	-1.50
600	-1.55	-1.57
660	-1.55	-1.50
720	-1.33	-1.31
780	-0.96	-0.87
840	-1.72	-1.62
900	-1.28	-1.14

The auxiliary EM pump in the primary system was a conduction-type DC electromagnetic unit that operated in series with the main pumps. When the two main sodium pumps were operating, the auxiliary EM pump had no appreciable effect on the primary coolant flow. The auxiliary EM pump was installed on the outside of the 14-inch reactor outlet pipe without changing either the shape or diameter of the inside of the pipe.

The magnetic field for the auxiliary EM pump was supplied by a permanent magnet, which surrounded the outside of the pipe. The auxiliary EM pump current, terminal voltage, rectifier voltage, and impedance histories during the SHRT-45R test are provided in Table 3.2.4.1.2 and Figures 3.2.4.1.1-4.

The auxiliary EM pump characteristics are such that the pump provides a head of 0.25 psi at a flow rate of 500 gpm (calibrated for 900°F sodium) with a rectifier voltage of 1.4 volts and a current of 9000 amps. Figure 3.2.4.1.5 illustrates the relationship between the auxiliary pump flow rate and current after the pump begins operating on battery power.

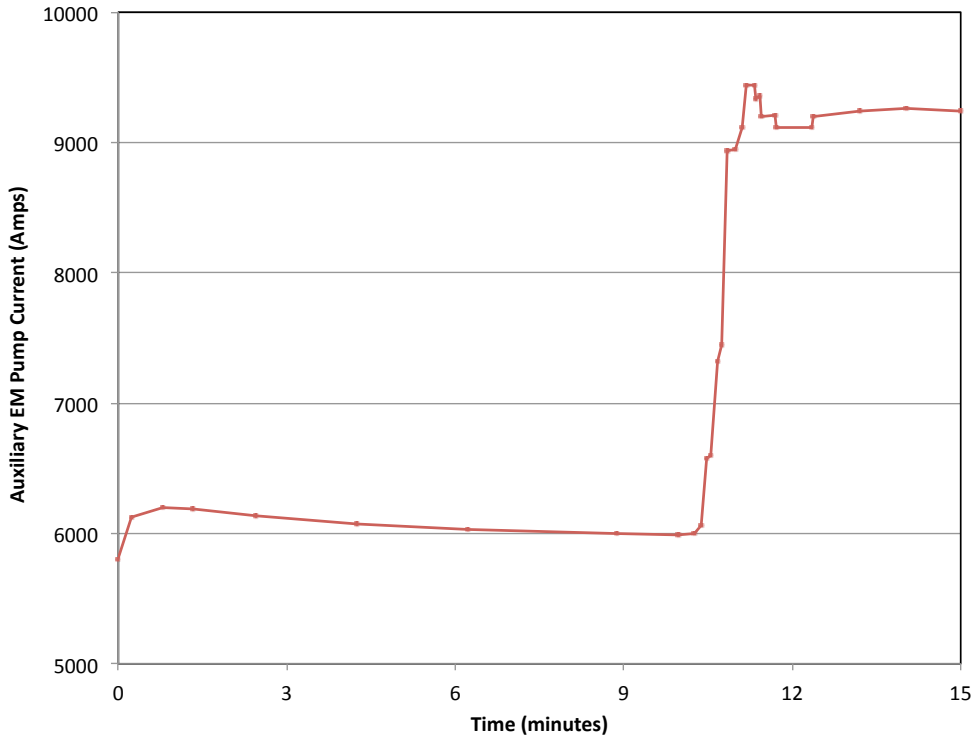

Figure 3.2.4.1.1. Auxiliary EM Pump Current For SHRT-45R

Table 3.2.4.1.2. Auxiliary EM Pump Data During SHRT-45R

Time (s)	Current (Amps)	Rectifier Voltage (V)	Terminal Voltage (V)	Impedance (μOhms)
0.0	5797.14	0.784	0.234	40.04
13.5	6121.30	0.761	0.207	34.11
47.0	6200.54	0.749	0.188	30.41
79.5	6186.53	0.743	0.181	29.18
121.5	6167.36	0.737	0.167	27.07
123.2	6172.51	0.738	0.188	30.48
147.0	6130.74	0.735	0.186	30.24
254.5	6075.52	0.724	0.178	29.48
372.5	6026.88	0.712	0.174	29.96
532.0	5999.42	0.700	0.168	28.36
597.5	5989.97	0.692	0.170	28.38
616.0	6002.85	0.691	0.172	28.57
623.0	6064.94	0.702	0.175	28.68
628.0	6579.34	0.794	0.195	29.88
633.0	6597.94	0.794	0.199	30.04
640.5	7322.64	0.918	0.231	31.29
644.5	7445.66	0.943	0.237	31.95
651.0	8936.83	1.205	0.305	34.05
659.5	8945.13	1.210	0.305	34.07
667.0	9119.65	1.239	0.309	34.26
671.5	9438.08	1.293	0.323	34.61
680.0	9442.66	1.295	0.325	34.65
681.5	9335.09	1.279	0.323	34.55
685.0	9359.97	1.280	0.324	34.33
686.5	9203.76	1.253	0.314	34.37
701.5	9210.34	1.254	0.315	34.40
702.5	9111.64	1.240	0.311	33.82
741.0	9118.79	1.243	0.312	34.29
743.0	9203.19	1.255	0.316	34.31
792.0	9244.39	1.264	0.318	34.03
842.0	9261.55	1.268	0.311	33.45
899.5	9238.09	1.265	0.311	33.59

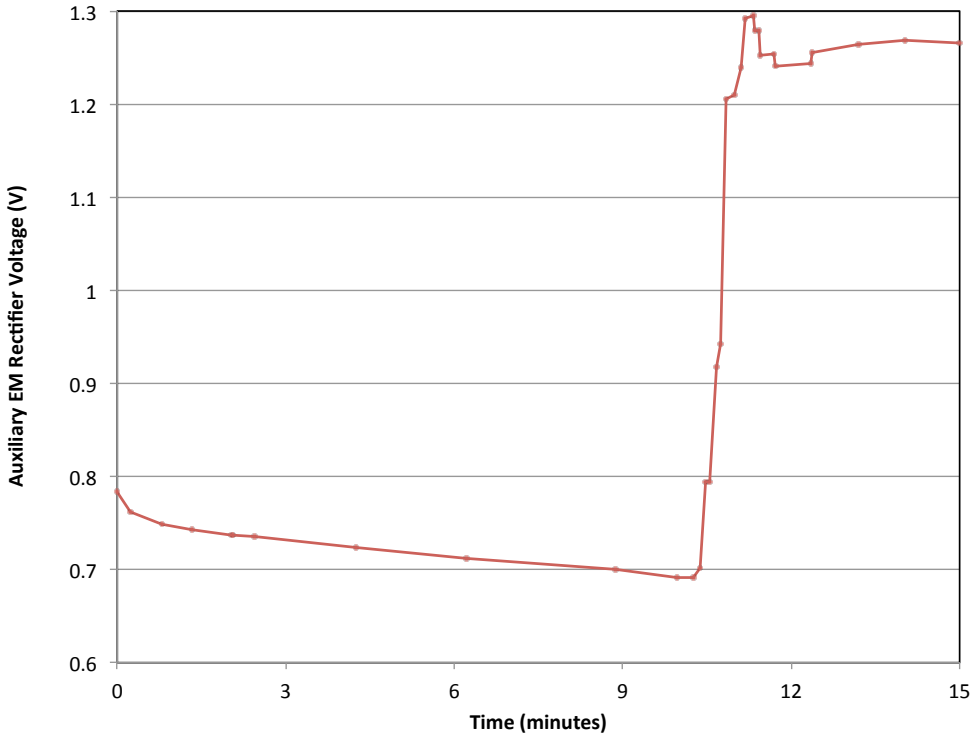

Figure 3.2.4.1.2. Auxiliary EM Pump Rectifier Voltage For SHRT-45R

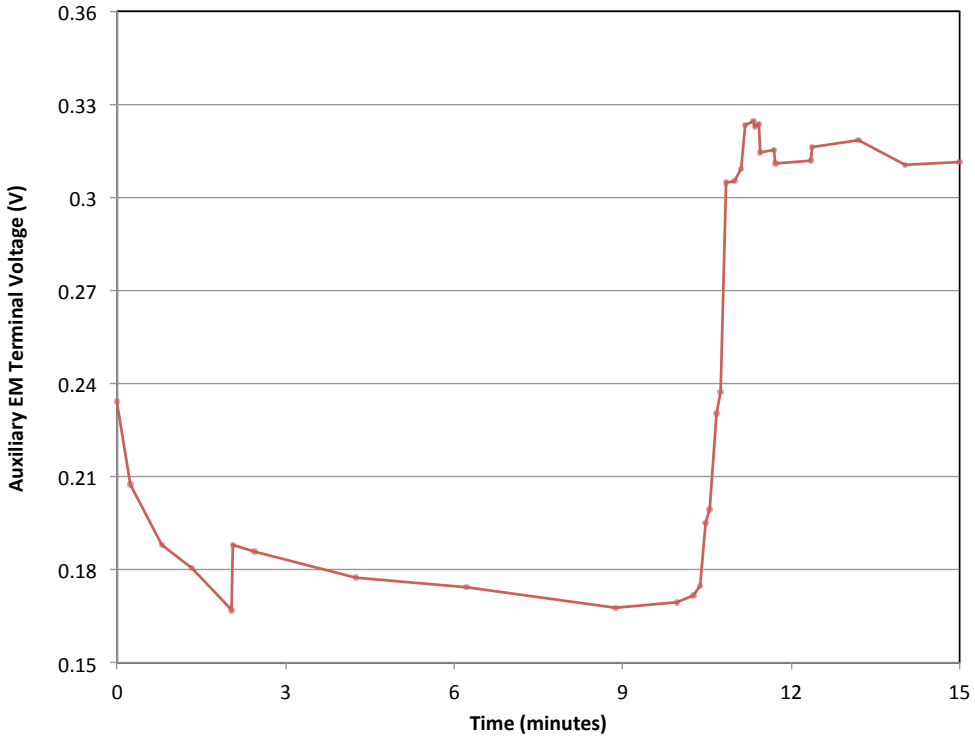

Figure 3.2.4.1.3. Auxiliary EM Pump Terminal Voltage For SHRT-45R

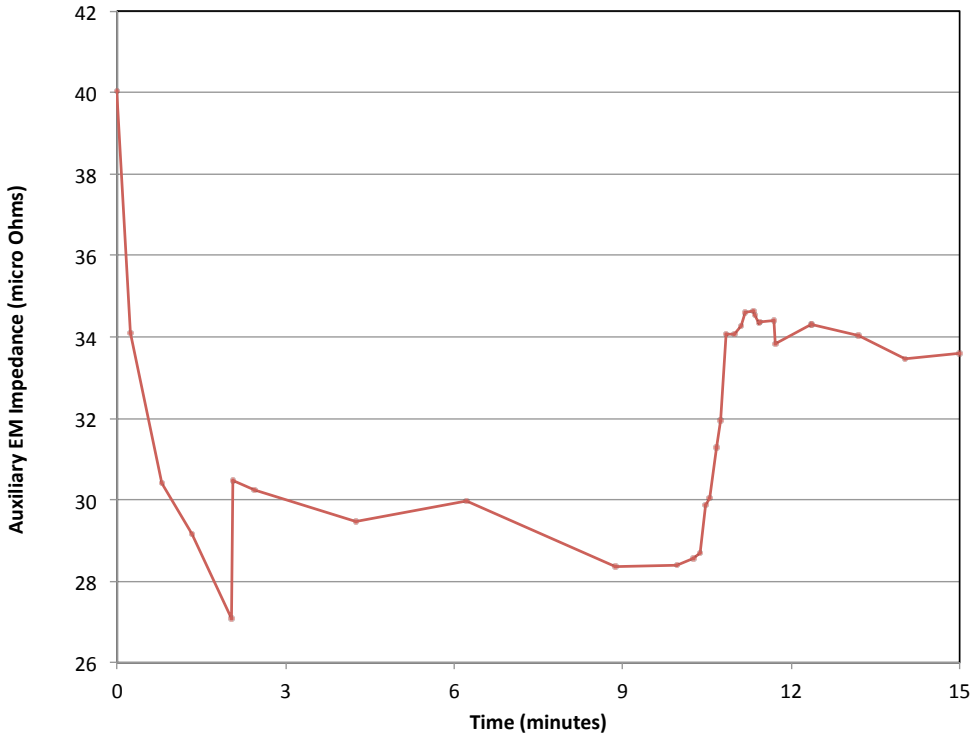

Figure 3.2.4.1.4. Auxiliary EM Pump Impedance For SHRT-45R

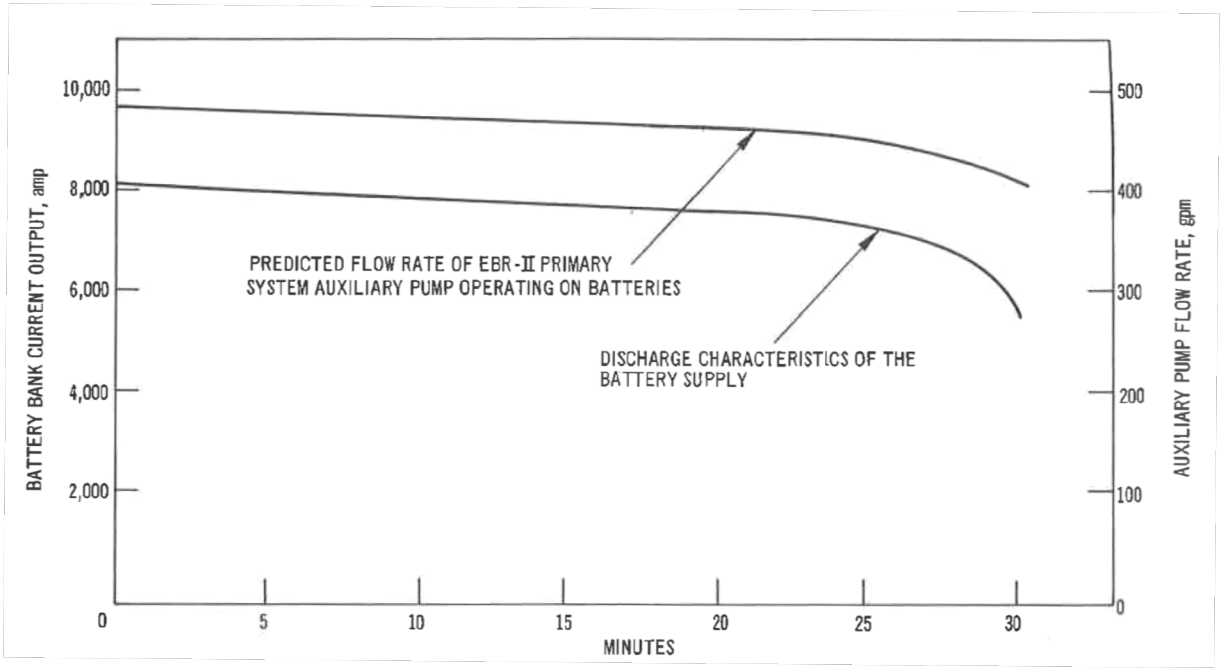

Figure 3.2.4.1.5. Auxiliary Pump Flow on Battery

3.2.4.2 *Intermediate side boundary conditions*

The boundary conditions for the intermediate sodium loop are the sodium flow rate and temperature at the inlet to the IHX. The IHX inlet sodium flow rate on the intermediate side is illustrated in Figure 3.2.4.2.1 and also given in Table 3.2.4.2.1. Flow was driven by the coastdown of the intermediate side EM pump upon trip of the 2400-V breaker to the M-G set. The corresponding IHX inlet sodium temperature is shown in Figure 3.2.4.2.2 and given in Table 3.2.4.2.2.

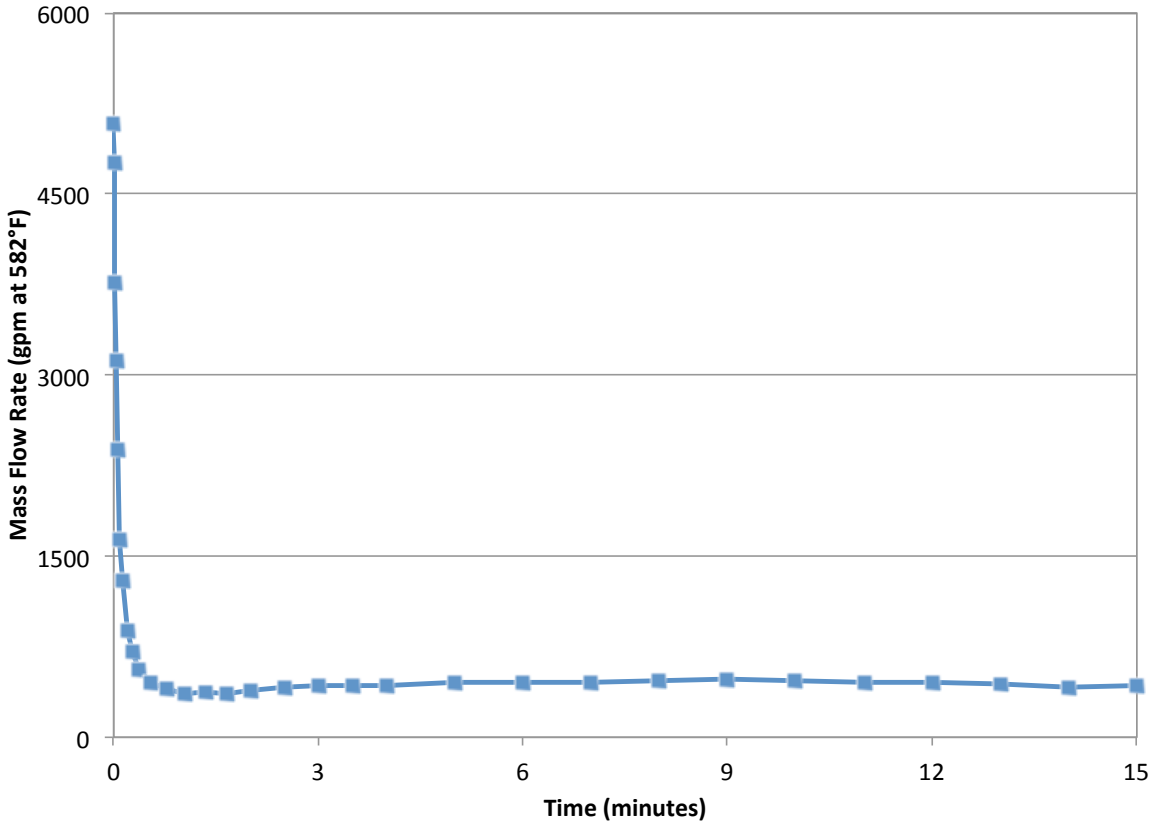

Figure 3.2.4.2.1. Intermediate Heat Exchanger Intermediate Inlet Sodium Mass Flow Rate For SHRT-45R

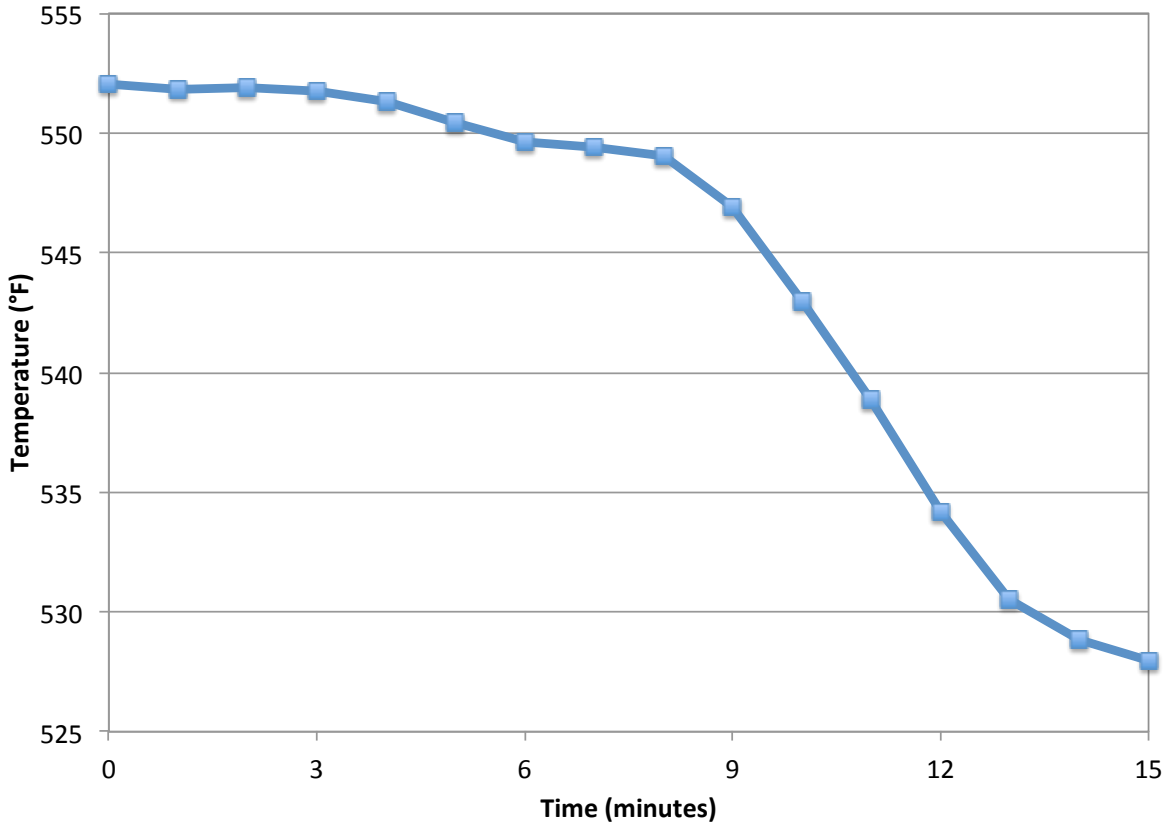

Figure 3.2.4.2.2. Intermediate Heat Exchanger Intermediate Inlet Sodium Temperature For SHRT-45R

Table 3.2.4.2.1. Intermediate IHX Inlet Sodium Flow Rate For SHRT-45R

Time (seconds)	Flow (gpm at XX°F)
0	5079.5
0.5	4756.0
1	3772.6
1.5	3118.3
3	2382.0
5	1632.5
7.5	1297.4
12	886.9
16	709.6
22.5	562.4
32	456.2
46	398.3
62.5	361.0
80	371.7
98.5	360.1
120	382.9
150	411.4
180	422.0
210	430.8
240	433.5
300	457.8
360	455.5
420	450.8
480	463.3
540	482.1
600	472.8
660	455.4
720	449.5
780	442.7
840	418.2
900	429.9

Table 3.2.4.2.2. Intermediate IHX Inlet Sodium Temperature For SHRT-45R

Time (seconds)	Temperature (°F)
0	552.1
60	551.8
120	551.9
180	551.7
240	551.3
300	550.5
360	549.6
420	549.4
480	549.1
540	546.6
600	543.0
660	538.8
720	534.2
780	530.6
840	528.8
900	527.9

3.2.4.3 *Control Rod/Safety Rod positions*

A brief description of the possible positions for the control and safety rods is given previously in Section 3.1.4.3. For SHRT-45R the control rods were partially inserted such that the bottom of the control rod fuel bundle was 8.29 inches below the bottom of the fuel bundle of the core driver subassemblies. The safety rods were inserted 6.29 inches below the bottom of the fuel bundle of the core driver subassemblies during the test.

4 EBR-II Reactor Core

The EBR-II reactor vessel grid plenum assembly accommodated 637 hexagonal subassemblies, which were installed in one of three regions: central core, inner blanket or outer blanket. The central core comprised the 61 subassemblies in the first five rows. Two of these positions contained safety-rod subassemblies and eight positions contained control-rod subassemblies. The remaining central core subassemblies were either driver-fuel or experimental-irradiation subassemblies of varying types. Rows 6 and 7 formed the inner blanket regions. The inner blanket region did not contain any blanket assemblies. It was named as such because it originally housed blanket subassemblies. The subassemblies in Rows 8-16 formed the outer blanket region.

SHRT-17 was conducted on June 20, 1984 during Run 129-C. Figures 4.1 and 4.2 provide illustrations of the core-loading pattern for Run 129-C. Figure 4.1 only shows the subassemblies in the first 8 rows. Figure 4.2 shows all subassembly positions in EBR-II. During Run 129-C, a large variety of subassembly types were utilized: driver, blanket, reflector, steel, experimental, control and safety. Each of these subassembly types is discussed in detail in Section 4.1 below. Two types of driver subassemblies were used for SHRT-45R but for SHRT-17 only the MARK-II AI type driver subassembly as denoted by the letter D in Figure 4.1 was used.

In Figure 4.1, P indicates a partial driver. Partial drivers are driver subassemblies where approximately half of the fuel elements are replaced by steel elements. In Figure 4.1, those subassemblies whose label begins with the letter K were steel subassemblies. HFD in Figure 4.1 refers to a high-flow driver, all of which were located in Row 6. Row 6 is the start of the inner blanket region and forms the expanded core, which contains driver-fuel and irradiation subassemblies. A high flow driver subassembly was the basic driver subassembly with extra inlet flow holes drilled into the subassembly inlet nozzle region to allow higher subassembly coolant flow.

In the central core region, two positions in row 3 held safety-rod subassemblies and eight positions in row 5 contained control-rod subassemblies. These subassemblies are identified by the letters S and C, respectively, in Figure 4.1. The remaining subassemblies in Figure 4.1 are all experimental or driver-irradiation type subassemblies and they will be discussed in Section 4.1.8.

Figure 4.2 illustrates the rest of the core in detail. The subassemblies in Figure 4.2 where no identification label is provided are reflector type subassemblies. Additionally, those subassemblies with identification labels of 9888 are also reflector type subassemblies. In Figure 4.1, reflector subassemblies are identified as R. The subassemblies in Rows 11-16 that are not labeled 9888 are blanket type subassemblies. Table 4.1 summarizes the different types of subassemblies in the core loading for SHRT-17 and SHRT-45R and the various labels used for each type of subassembly.

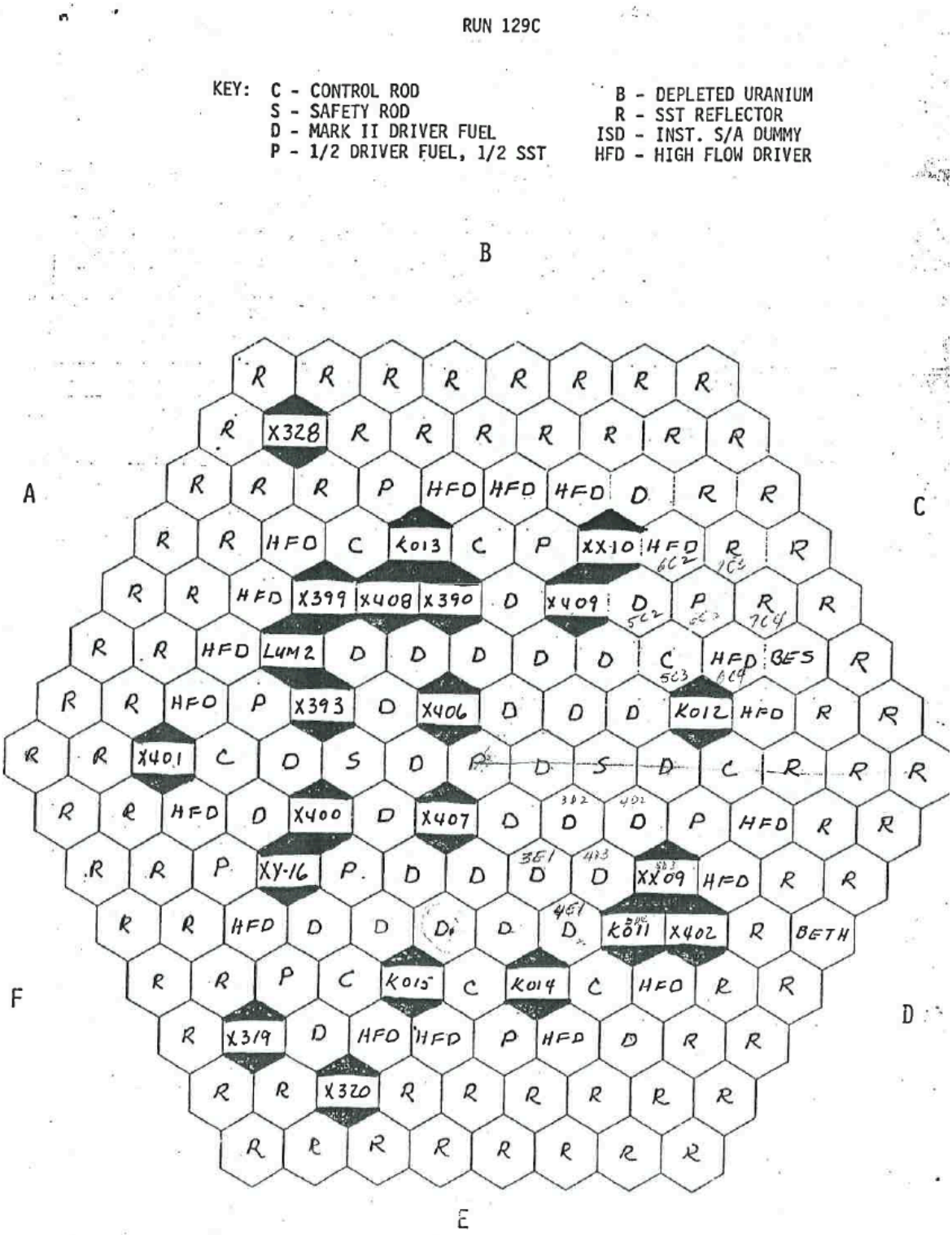

Figure 4.1. SHRT-17 Core Loading Pattern (First 8 Rows)

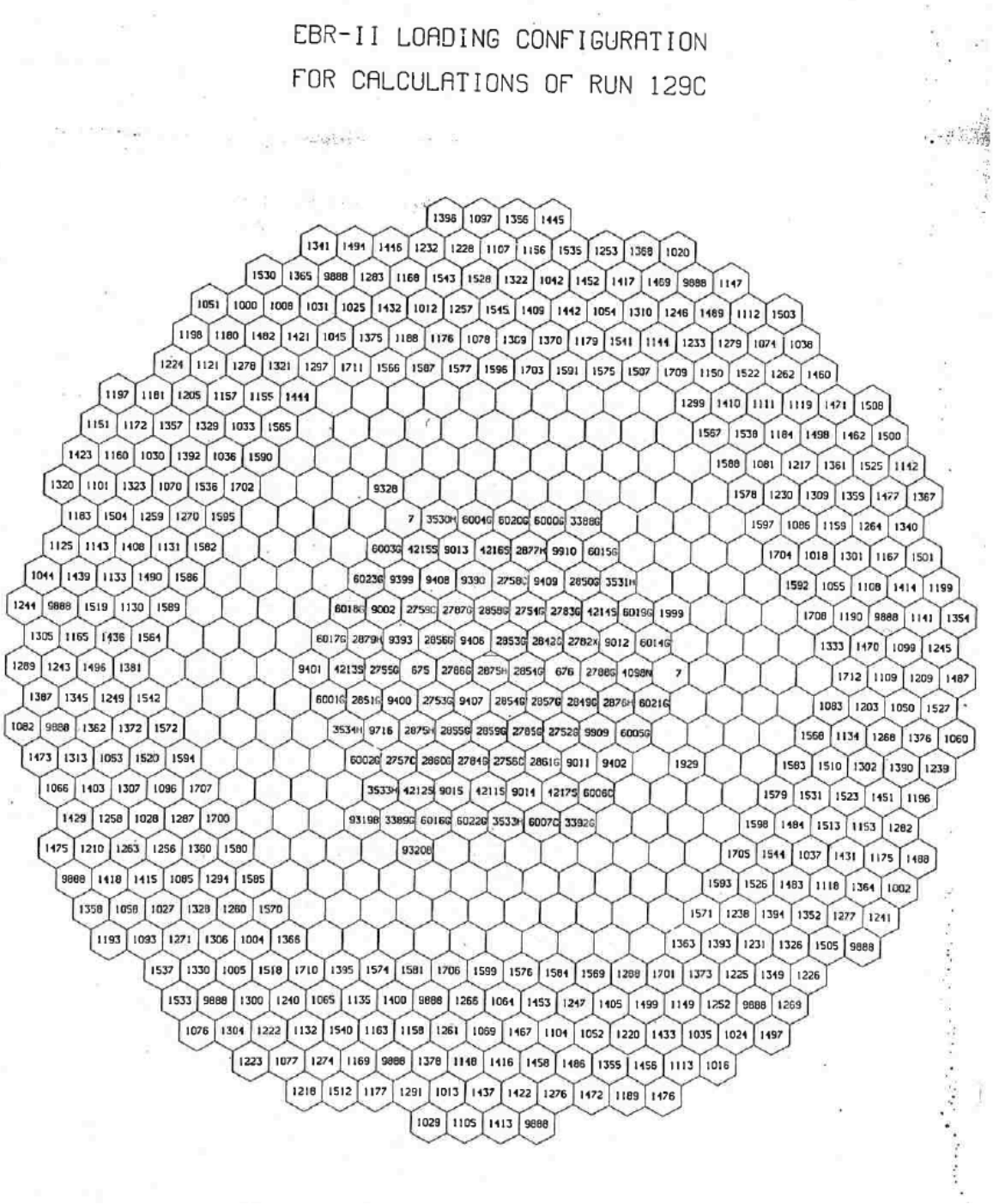

Figure 4.2. SHRT-17 Core Loading Pattern (All Rows)

The SHRT-45R test was performed as part of Run 138-B. Run 138-B began on March 28th, 1986 and ended on April 3rd, 1986. Figures 4.3-4.5 provide various illustrations of the core-loading pattern for Run 138-B. Figures 4.3 and 4.4 show the proposed core-loading pattern while Figure 4.5 shows the actual core-loading pattern. Figures 4.3 and 4.5 only show the subassemblies in the first 8 rows. While the loading pattern shown in Figure 4.3 was not the final loading pattern that was implemented for Run 138-B, it is easier to read than the actual loading pattern shown in Figure 4.5. The differences between the actual and proposed loading patterns are described below. Figure 4.4 shows all subassembly positions in EBR-II.

During Run 138-B, a large variety of subassembly types were utilized: driver, blanket, reflector, steel, experimental, control and safety. Each of these subassembly types is discussed in detail in Section 4.1 below. Two types of driver subassemblies were used for Run 138-B. The first was the MARK-II fuel manufactured by Atomics International (AI), denoted as MARK-II AI. It is referred to in Figure 4.5 as MK2AI. The second driver type was MARK-II A fuel, referred to in Figure 4.5 as MK2A. A detailed discussion of these two driver fuel types is presented below in Section 4.1.

Several variations of the basic driver subassemblies were also used. Standard MARK-II A and MARK-II AI subassemblies are both referred to in Figure 4.3 as 'D.' In Figure 4.3, 'P' refers to the partial driver subassemblies where approximately half of the fuel elements were replaced with steel elements. In Figure 4.3, 'HFD' refers to high-flow driver subassemblies. These subassemblies were the same as standard driver subassemblies but with extra inlet flow holes drilled in the subassembly inlet nozzle to allow for high coolant flow.

Steel subassemblies are identified in Figure 4.3 as 'K' (e.g. K013) and in Figure 4.5 as SST. Control-rod subassemblies are identified in Figure 4.3 as 'C' and in Figure 4.5 as either 'CONTROL' or 'HW CNTR,' which refers to high-worth control rod design subassembly option. There is only one CONTROL subassembly (regular-worth control rod) in the SHRT-45R core loading pattern. This CONTROL subassembly is disregarded as a separate subassembly type for this benchmarking exercise. Subassemblies X320, X411 and X412 were experimental-irradiation subassemblies. EBR-II was loaded with four test facility subassemblies for Run 138-B: XY-16, XX09, XX10 and LUM-2. XY-16 was a steel subassembly. XX09 and XX10 were instrumented subassemblies (INSATs) and LUM-2 was similar to the K-type steel subassemblies. Figure 4.5 lists one subassembly in Row 4 as C2776A XETAGS. This subassembly was a MARK-II AI subassembly with Xenon tag gas.

Reflector subassemblies are identified as 'R' in Figure 4.3, 'SSR' in Figure 4.5 and are left blank in Figure 4.4. The remaining subassemblies in Rows 8-16 were depleted uranium outer blanket subassemblies. Table 4.1 summarizes the different types of subassemblies in the core loading for SHRT-17 and SHRT-45R and the various labels used for each type of subassembly.

For SHRT-45R, the proposed and actual core-loading patterns are nearly identical but there are a few small differences. Figure 3.2.3.1 gives the power per subassembly and Figure 3.2.3.2 gives the flow per subassembly. Values in both of these figures were calculated based on the proposed core loading pattern. The necessary corrections to the proposed SHRT-45R loading pattern given in Figure 4.3 are listed below as well as suggested changed to Figures 3.2.3.1 and 3.2.3.2 to properly account for these changes in the power and flow per subassembly values:

- The subassembly in position 7B6 was a K-type steel subassembly. The difference between a reflector and a steel subassembly in this position is expected to be small so no changes are necessary to Figures 3.2.3.1 and 3.2.3.2 for this subassembly position.
- The subassembly in position 5B4 was not the experimental subassembly X411 but rather a standard MARK-II A driver subassembly. No changes are necessary to Figures 3.2.3.1 and 3.2.3.2 for this subassembly position.
- The subassembly in position 6E4 was a P-type partial-driver subassembly. Use a power of 297.0 kW and a flow of 46.27 gpm for the subassembly in this position.
- The subassembly in position 7E3 was a reflector subassembly. Use a power of 19.61 kW and a flow of 3.072 gpm for the subassembly in this position.
- The subassembly in position 8D6 was the source subassembly, S1951. As is standard engineering practice, an external neutron source is required in a reactor core to produce the initial neutrons to start the fission process. In EBR-II, this external neutron source was contained in the source subassembly. This source subassembly and the reflector subassembly were similar in geometry and composition so the subassembly in this position should be treated as a reflector subassembly with no changes necessary to Figures 3.2.3.1 and 3.2.3.2 for this subassembly position.

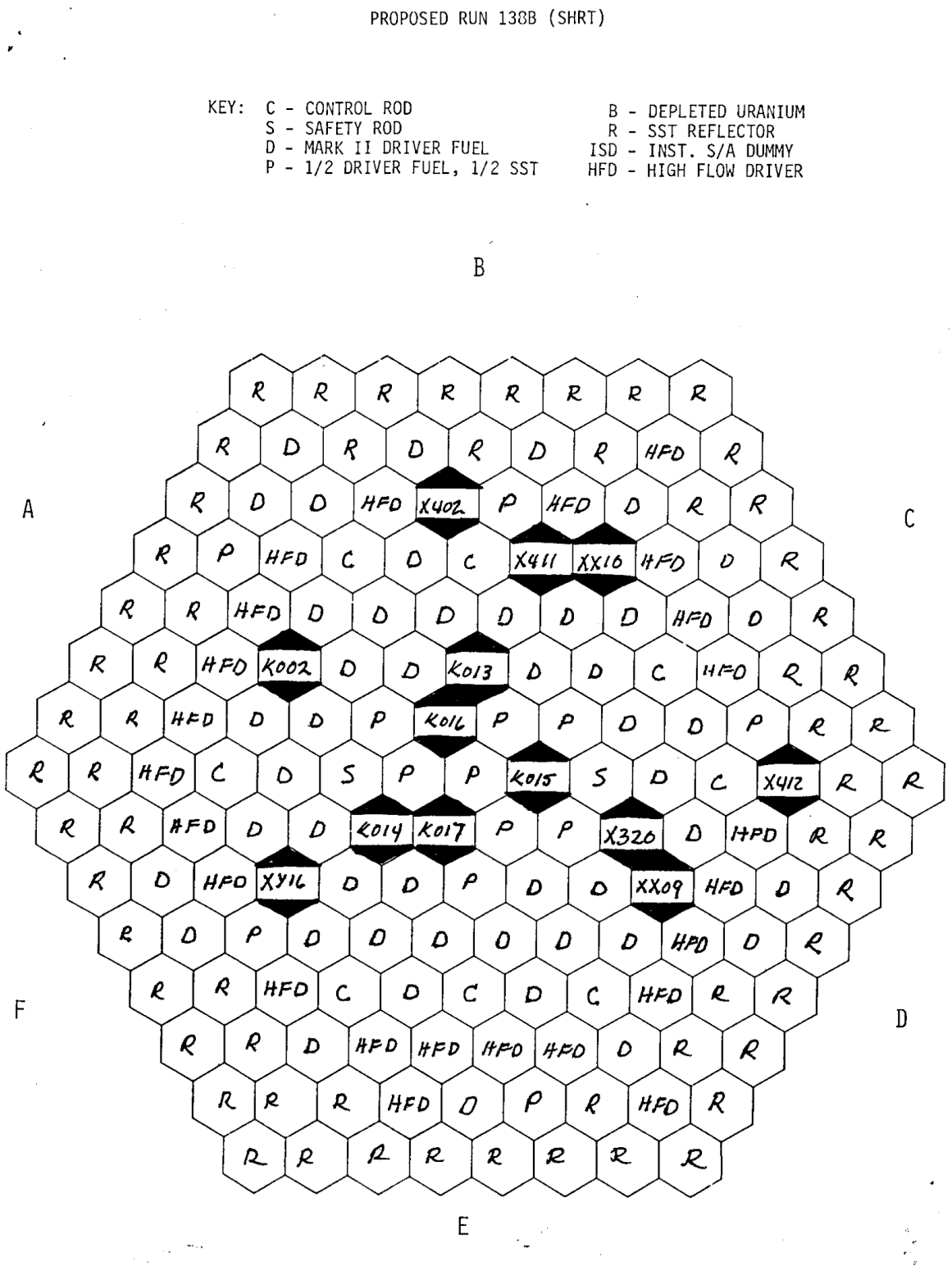

Figure 4.3. Proposed SHRT-45R Core Loading Pattern (First 8 Rows)

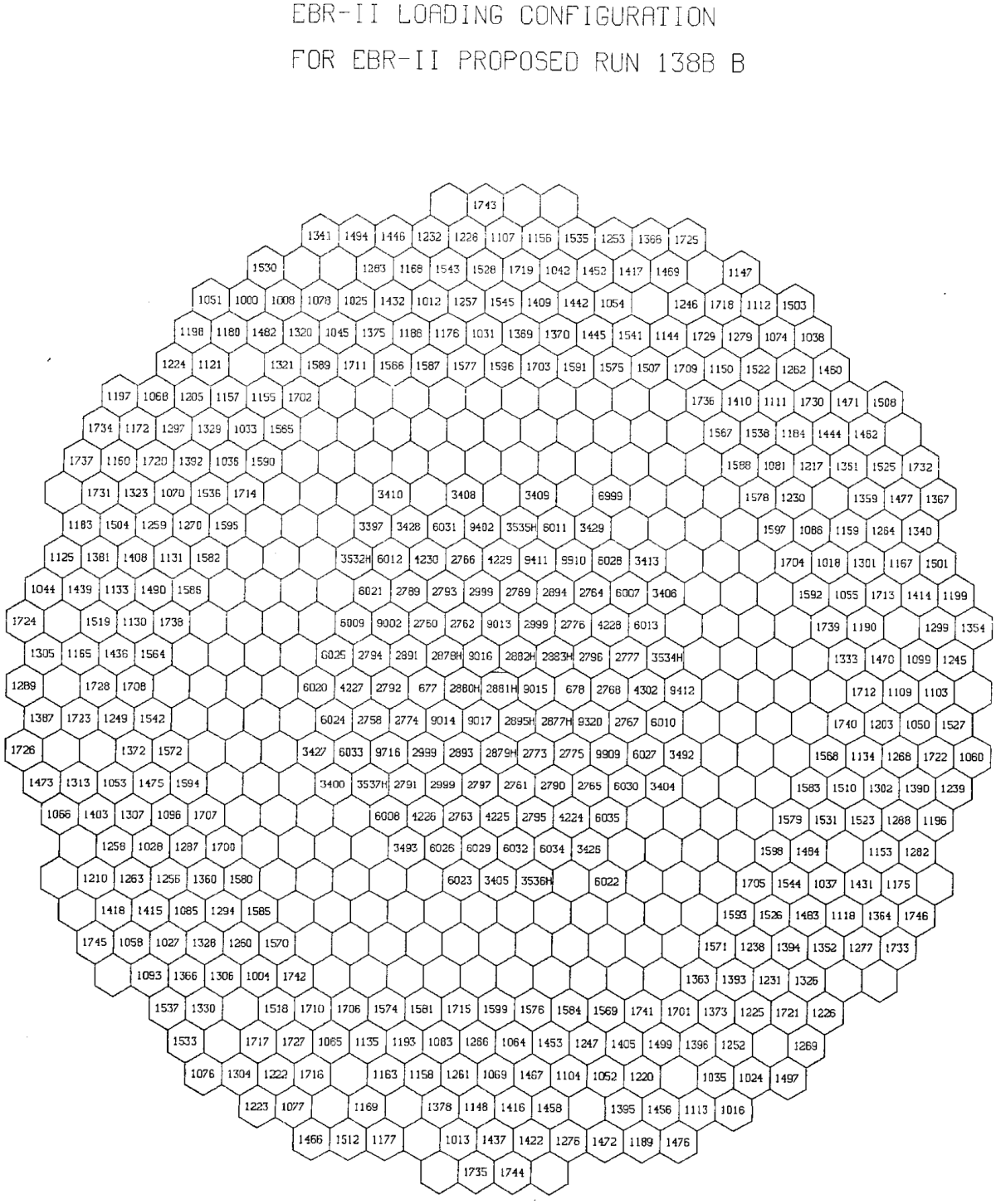

Figure 4.4. Proposed SHRT-45R Core Loading Pattern (All Rows)

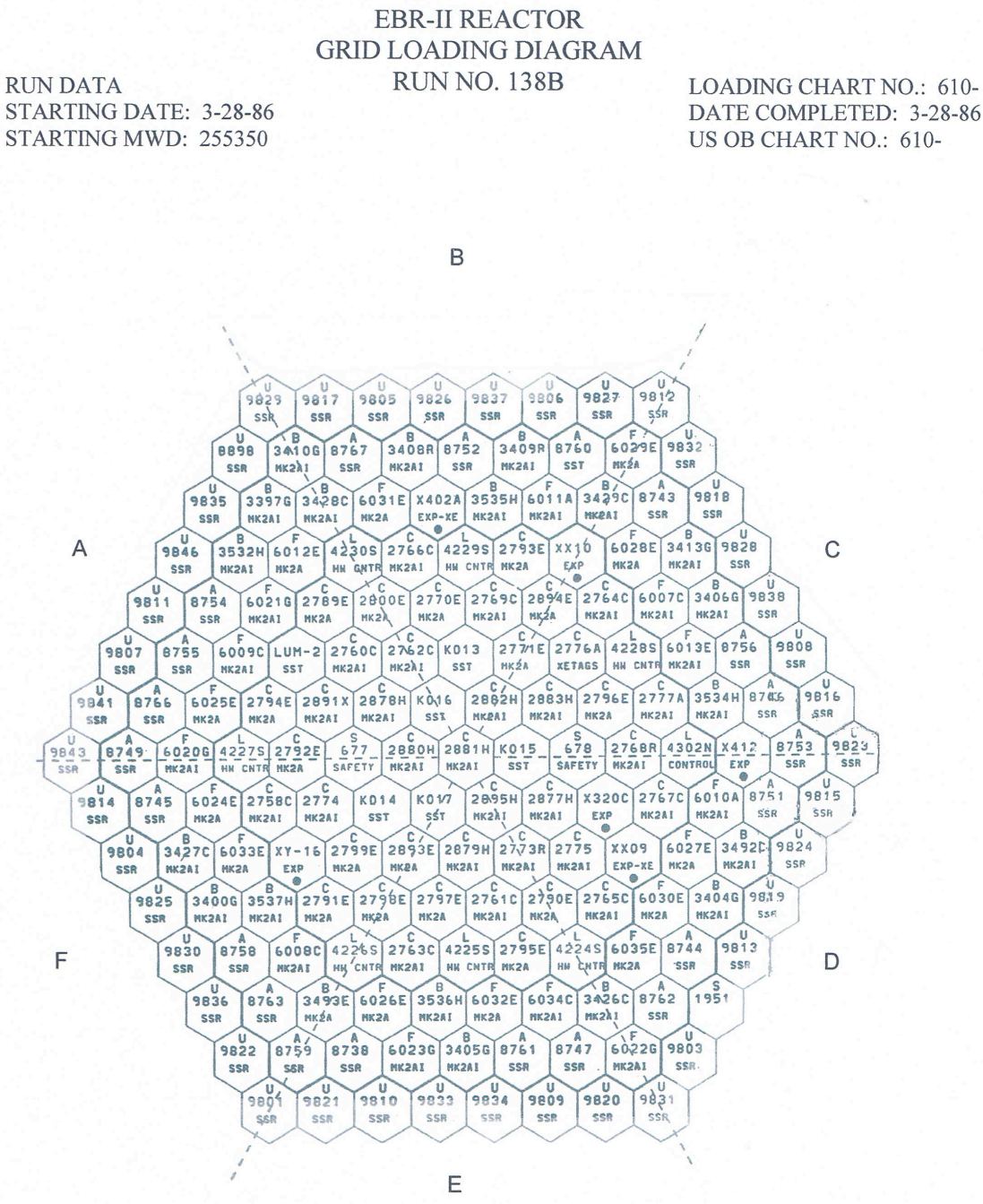

Figure 4.5. Actual SHRT-45R Core Loading Pattern (First 8 Rows)

Table 4.1. SHRT-17 and SHRT-45R Subassembly Types

Subassembly Type	Figure 4.1/4.3 Identifiers	Figure 4.5 Identifiers
MARK-II AI (P, D)	P, D	MK2AI
MARK-II A (D)†	D	MK2A
Stainless Steel	K, XY-16	K SST, LUM-2, SST, XY-16
Stainless Steel Reflector	R	U SST, A SST
Outer Blanket	N/A	N/A
Control	C	CONTROL, HW CNTR
Safety	S	SAFETY
Instrumented	XX09, XX10	XX09, XX10
SHRT-17 Experimental	X319, X320, X328, X390, X393, X399-X402, X406-X409	
SHRT-45R Experimental	X320, X402, X412	X320C, X402A, X412, XETAGS

† MARK-II A subassemblies were not used in SHRT-17

Each subassembly was composed of primarily three sections: upper adapter, center hexagonal ducted section and lower adapter. The upper adapter for each subassembly was identical so that they could each be handled by the same fuel-handling components. Different types of lower adapters were used to prevent improper positioning of the subassembly on the reactor grid. Also, different orifices were used to ensure appropriate amounts of coolant flow. For example, inner and outer blanket subassemblies had different lower adapter designs. Driver subassemblies had different lower adapters depending on whether they were loaded in the central core or inner blanket regions. These various lower adapter designs determined the amount of coolant flow through the subassemblies by blocking a different number of flow holes drawing sodium from in the lower plena. In the figures that follow illustrating each type of subassembly, (E) indicates that a dimension is an estimate taken in inches and converted to centimeters.

4.1 Subassembly Geometry

The outer configuration of all subassemblies was very similar. The upper adapter was formed to fit the top of the hexagonal outer tube of the central region and the top part of the upper adapter was slotted to adjust the orientation of the subassembly within the reactor grid. The lower surface of the mushroom-shaped head on the upper adapter provided a solid surface for grasping during fuel handling with gripper devices.

The center region of each subassembly was surrounded by a hex tube, which created an independent flow channel for each subassembly. Each face of the hexagonal tube contained a spacer button, formed by dimpling the tube wall outward. The buttons served to prevent the subassemblies from touching if bowing were to occur.

The lower adapter positioned the subassembly within the reactor grid and determined the amount of coolant flow through the subassembly. Subassemblies that were to be positioned in Rows 1 through 5 had core-type lower adapters. The core-type lower adapter was a stainless

steel, machined cylindrical nozzle. The upper portion had a rounded shoulder, which sat in the hole of the upper grid plate of the reactor grid plenum. The bottom was slotted to fit on key bars below the lower grid plate in the core region. The core region lower adapters had four sets of coolant flow holes. Depending on the row in which the subassembly was position, a different number of flow holes were covered by the various step sizes of the lower grid plate. These step sizes are discussed in more detail in Chapter 5.

The expanded core-type lower adapter was used for driver fuel in Row 6 and irradiation subassemblies located in Rows 6 or 7 of the reactor. The inner blanket lower adapter with two sets of flow holes was used for the subassemblies, other than driver fuel type, located in Rows 6 or 7. The outer blanket lower adapter was used for subassemblies in Rows 8-16. These adapters fit into stainless steel tubes that interconnected the upper and lower grid plates of the reactor grid assembly to provide a flow path from the low-pressure plenum. Yet another type of lower adapter was used for the control rod and safety rod subassemblies and guide thimbles.

The inner configuration of the center section of a subassembly varied depending upon the specific subassembly type. Figure 4.1.1 shows an isometric view of the inner configuration of a MARK-II AI subassembly. The center section of the MARK-II AI subassembly consisted of an upper shield, a core bundle of fuel elements and a lower shield. For each subassembly type, geometric details are provided in the following subsections for the inner configuration of each of the different types of subassemblies loaded in the reactor core for the SHRT-17 and SHRT-45R tests. For those subassembly types that include fuel elements, Table 4.1.1 presents the nominal design parameters of the fuel element by type.

These two tables give design data for the wire-wrapped cladded fuel elements for a number of fuel element types. The MARK-II AI and MARK-II A fuel elements were part of the central core driver and expanded core driver subassembly designs. In both Tables 4.1.1 and 4.1.2, the numbers in parentheses are for the MARK-II A fuel element. All the other numbers in the columns are common to both the MARK-II AI and the MARK-II A designs. The MARK-II S element was used in the high worth control rod design. The MARK-II AI element was utilized in the safety rod design. Each fuel element clad tube contained a single metal fuel slug. U-5Fs is the fissium fuel alloy uniquely developed and fabricated for the Argonne EBR-II reactor. The relevant material properties of the fissium fuel are provided in Section 4.2.1.

The fuel elements were sodium bonded. Above the sodium bond level was a fission gas plenum that was initially filled with an inert gas until fission gas was produced. The inert gas used was Helium with Xenon tracer isotopes added for tagging a leaking fuel element. Wire wrap diameters are also included by fuel element type in the tables. The number of fuel elements in each subassembly type is included in both tables.

Table 4.1.2 presents the nominal design parameters for the subassembly hexagonal duct wall. Elevation and plane view figures are shown in the following sections for each subassembly type. The schematics describing the subassemblies in the following sections are not to scale and are engineering simplifications of the original blueprints.

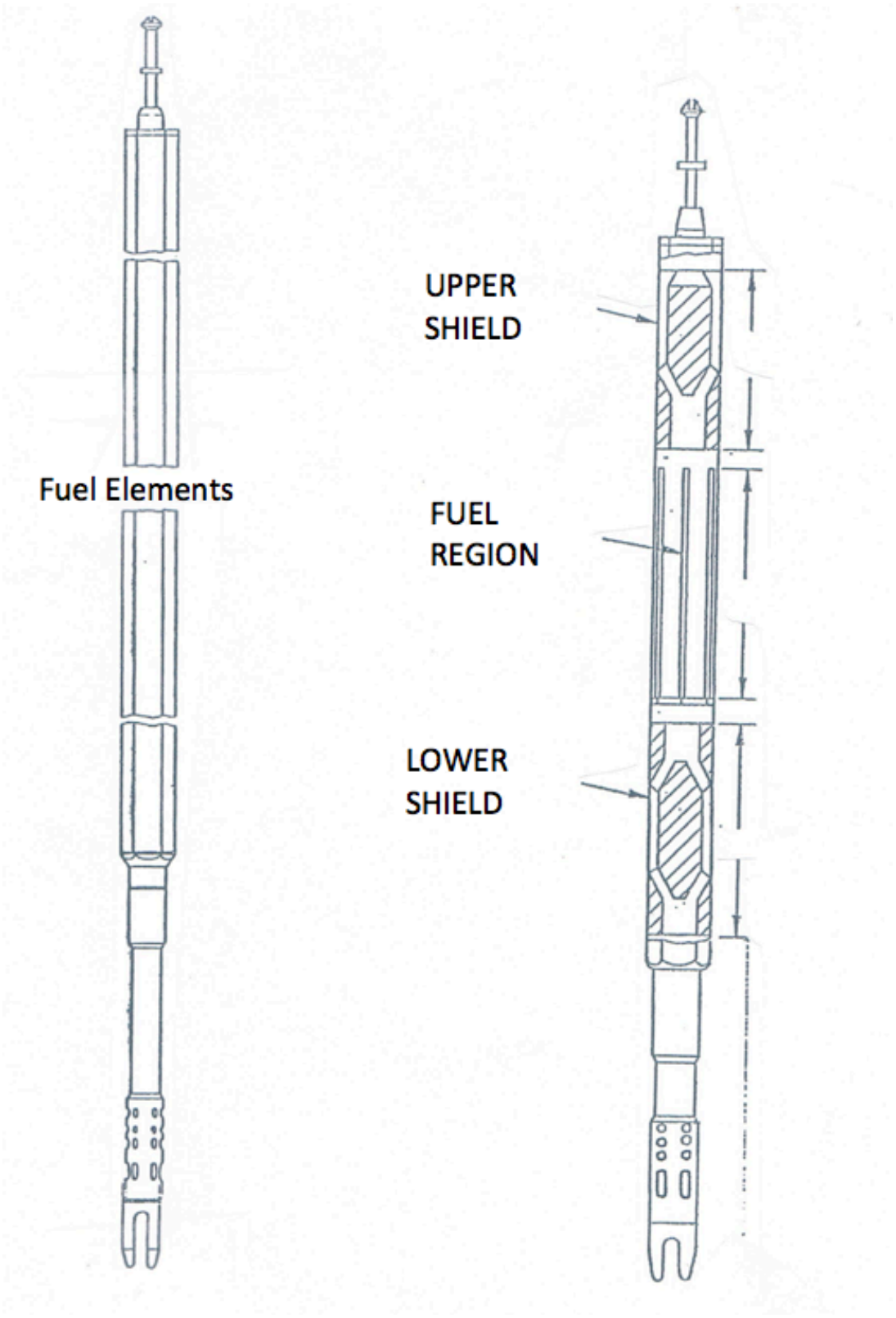

Figure 4.1.1. MARK-II AI Subassembly Configuration

Table 4.1.1. Design parameters (nominal) of EBR-II subassembly fuel elements (metric units)

Item	MARK-II AI (A)	MARK-IIS	XX09	XX10	Outer Blanket
Fuel alloy, wt %	U-5Fs	U-5Fs	U-5Fs	Stainless Steel	Depleted U
Enrichment weight, % ^{235}U	67	67	67	N/A	~0.0
Number of Elements	91 (91) [a]	61	59 of 61	18	19
Fuel-slug length, m	0.3429	0.3429	0.3429	N/A	1.397
Fuel-slug diameter, mm	3.36	3.36	3.36	N/A	11.09
Cladding-wall thickness, mm	0.315	0.315	0.315	Solid rod	0.457
Cladding-wall OD, mm	4.41	4.41	4.41	8.81	12.52
Element length, m	0.6108 (0.6362) [a]	0.5334	0.6108 (0.6494)[†]	0.6108 (0.6951)[†]	1.575
Restrainer height above fuel, mm	12.7	12.7	12.7	None	N/A
Sodium level above fuel, mm	31.75 (6.35) [a]	6.35	31.75	N/A	30.48
Plenum gas	Inert gas	Inert gas	Inert gas	N/A	Inert Gas
Cladding material	316	316	316	316	304
Spacer-wire diameter, mm*	1.24	1.24	1.24	1.24	None
Spacer-wire material	316	316	316	316	N/A

[†]With top instrument adapter

[*]Spacer wire pitch = 0.1524 m

[a]Value in parentheses refers to MARK-II A subassembly

Table 4.1.2. Design parameters (nominal) for EBR-II subassembly structure

	MARK-II AI/MARK-II A	XX09/XX10	Safety/HWCR	Reflector/Uranium Blanket
Pitch center to center mm (in.)	58.93 (2.32)	58.93 (2.32)	58.93 (2.32)	58.93 (2.32)
Outer Hex Tube				
Flat-to-flat outside mm (in.)	58.17 (2.29)	58.17 (2.29)	58.17 (2.29)	58.17 (2.24)
Flat-to-flat inside mm (in.)	56.1 (2.21)	56.1 (2.21)	56.1 (2.21)	56.1 (2.21)
Material	316SS	304SS	316SS	304SS
Inner Hex Tube				
Flat-to-flat outside mm (in.)		48.4 (1.908)	48.4 (1.908)	
Flat-to-flat inside mm (in.)		46.4 (1.827)	46.4 (1.827)	
Material		304SS	304SS	
Upper Adapter/Fixture	304SS		304SS	304SS
Upper Axial Shield	304SS		304SS	
Lower Axial Shield	304SS		304SS	
Lower Adapter	304SS		304SS	304SS

4.1.1 *Driver Subassemblies*

Figure 4.1.1.1 shows the axial cross-section view of subassembly type MARK-II AI (MK2AI), which was used in the core driver region. This figure illustrates the upper and lower axial shields, pin bundle, lower adapter (nozzle) and upper adapter regions. The location of the driver subassembly hex tube is indicated in Figure 4.1.1.1 by the thick line. The driver subassembly hex tube extends from the top of the lower adapter to section A-A in Figure 4.1.1.1. Several important axial locations A-A through N-N are indicated in this figure. Plane sections of the subassembly at these axial locations are illustrated in Figures 4.1.1.2 and 4.1.1.3. Elevation views of the upper and lower shield sections are also illustrated in detail in Figure 4.1.1.3. In Figure 4.1.1.3 and the corresponding figures for other types of driver subassembly, (E) indicates that a dimension is an estimate taken in inches and converted to centimeters. The top elevation view is of the upper shield while the bottom elevation view is of the lower shield. The gap between the bottom of the upper shield and the top of the pin bundle is neglected in Figure 4.1.1.1.

The elevation view of Figure 4.1.1.1 does not show the detailed geometry of the top fixture nor the gap between the top fixture and the upper axial shield. For the benchmark calculations, the fixture is ignored.

Section A-A at the outlet of the hex tube shows the flow area and the hex tube structure dimensions. The materials that were used are given in Table 4.1.2. Section B-B is at the top of the upper shield. The upper part of the shield was a cylinder made of Type 304 stainless steel. Below this the upper axial shield became an annulus. Section C-C shows that in the transition region between the top and lower parts of the upper axial shield, six flow holes were drilled. This drilling face was sloped at 30° to the horizontal with flow hole diameters of 0.0150876 m. The flow hole-to-hole pitch was 0.0445 m. The annular region of the upper shield is shown in section D-D as well as the flow annulus diameter. Despite distortion in the figures, all flow holes are intended to be circular.

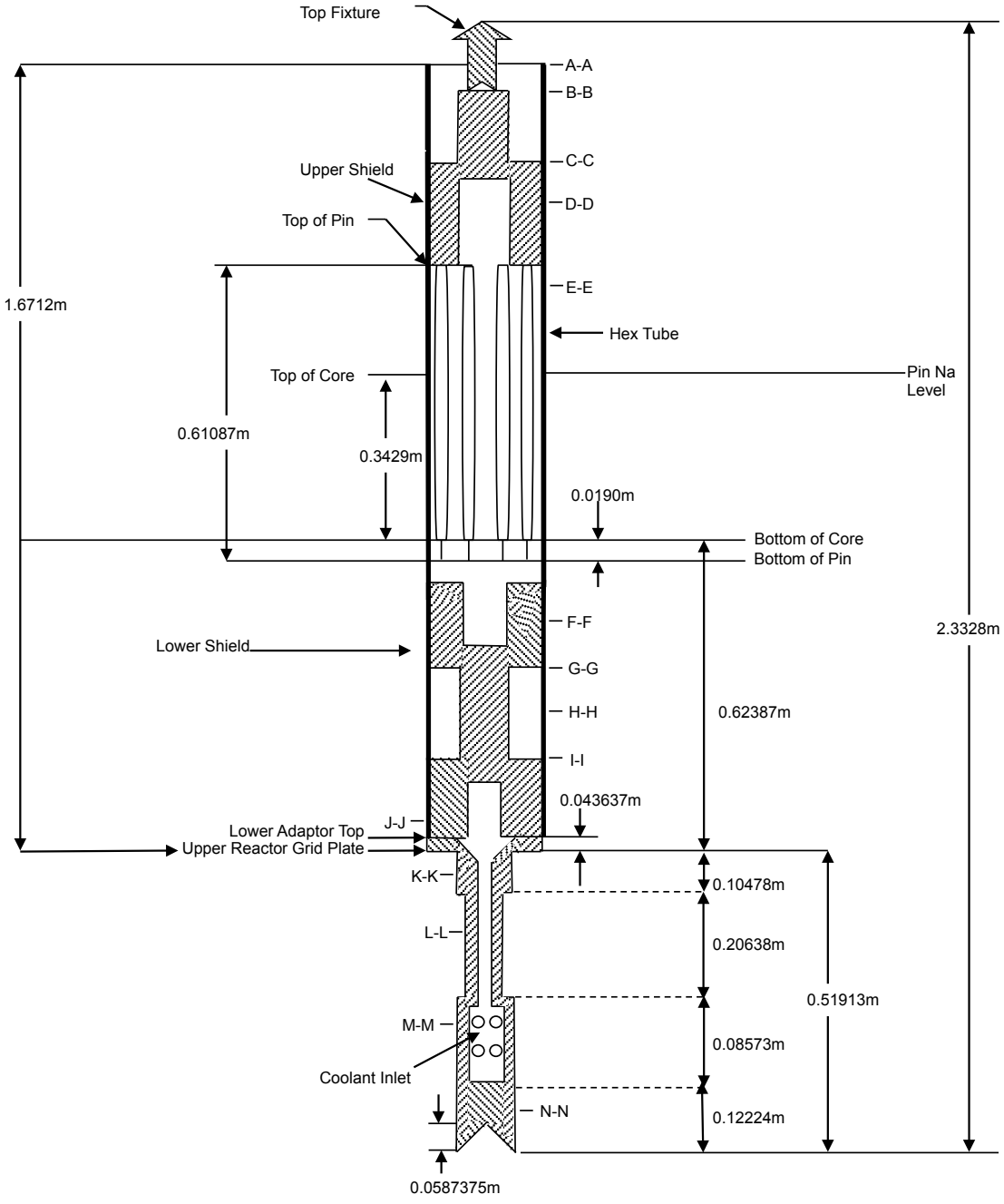

Figure 4.1.1.1. MARK-II AI Core Driver axial section

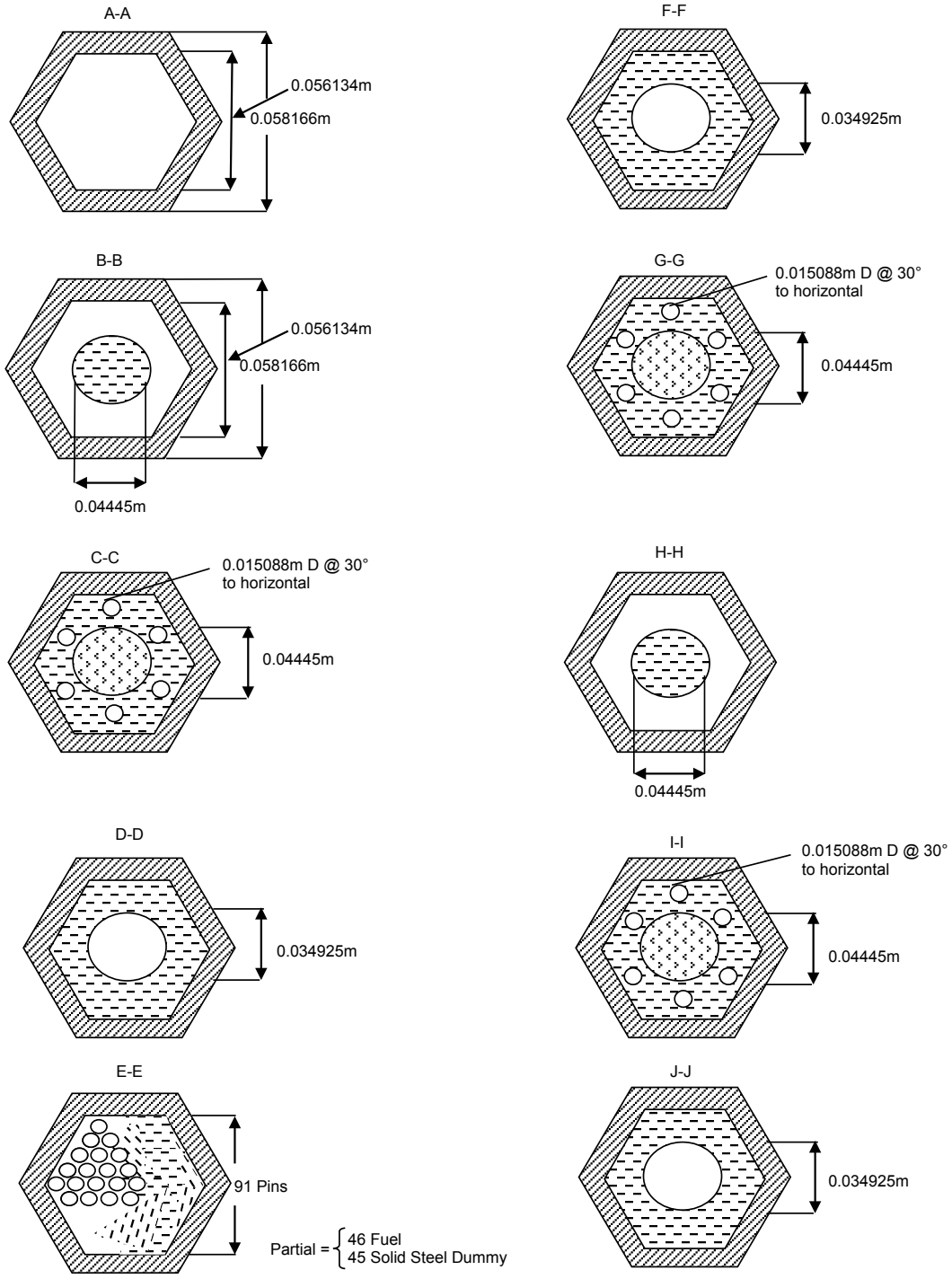

Figure 4.1.1.2. MARK-II AI Core Driver plane sections

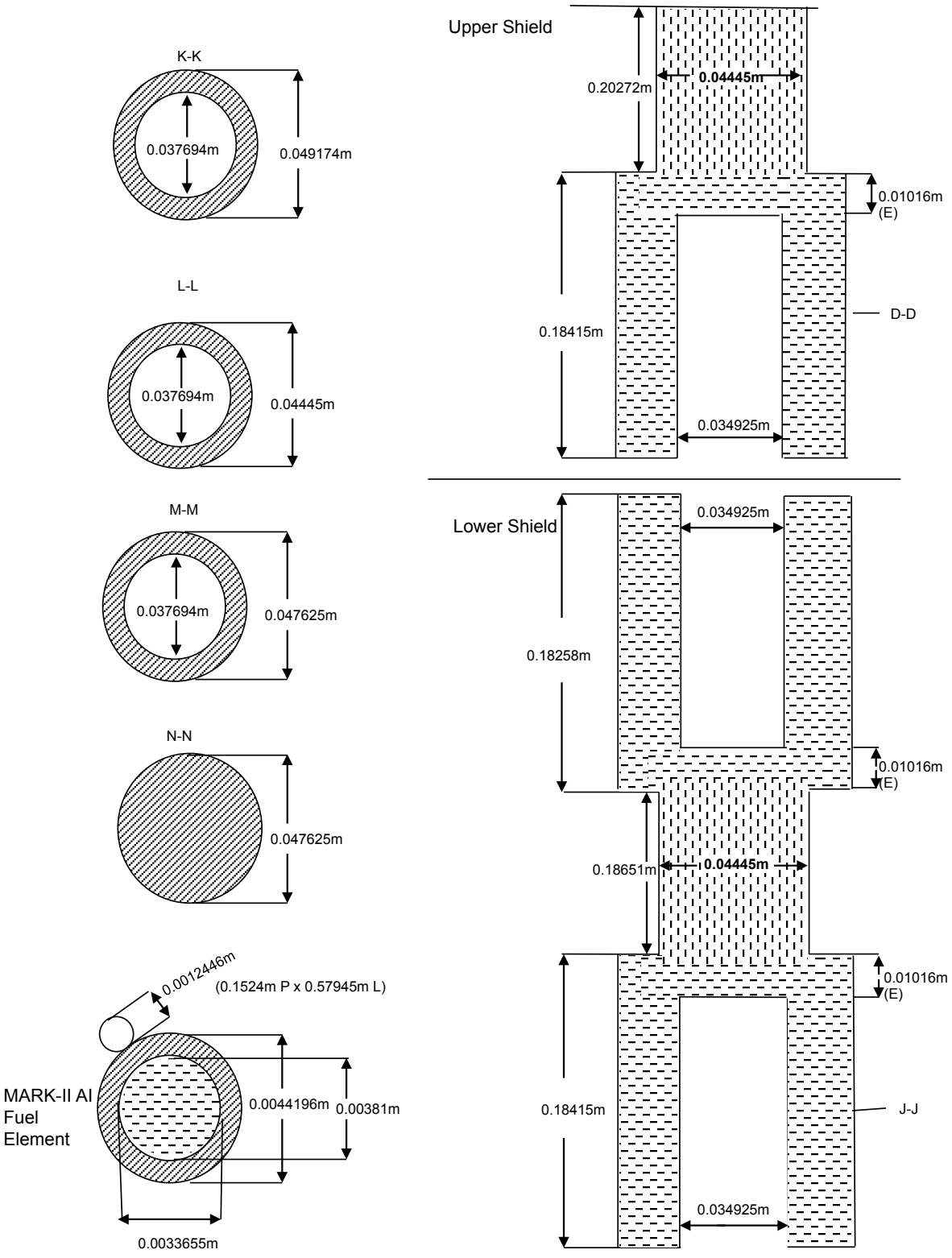

Figure 4.1.1.3. MARK-II AI Core Driver axial and plane sections

Section E-E displays a cross-section through the wire-wrapped pin bundle of the MARK-II AI subassembly. Details are available in Table 4.1.1 for the MARK-II AI pin bundle element. Those MARK-II A pin bundle element design numbers that are different from the MARK-II AI pin bundle element design numbers are shown in parentheses in Table 4.1.1. For the fully fueled subassemblies, the 91 pins were the MARK-II AI fuel elements. Figure 4.1.1.3 also shows a cross-section through a wire-wrapped fuel element.

For the partially fueled assemblies that had the P designation, 45 of the element positions were occupied by wire-wrapped solid 316 stainless steel elements with the same dimensions as the fueled elements. The locations of the fuel and steel elements within the subassembly are illustrated below in Figure 4.1.1.4. The orientation of the subassembly within the core is not known. The top of the fuel slugs that form the top of the core is depicted in the elevation view in Figure 4.1.1.1. There was one fuel slug in each fuel element and the "Top of Core" label in Figure 4.1.1.1 is the top of this fuel slug.

For details regarding the fuel slugs and the sodium level, reference should be made to Table 4.1.1. The bottom of the core, which was the bottom of the fuel slug, is taken to be the bottom of the element without regard to the element end cap. The element bottom locator tip, which was part of the end cap, is shown to be 0.0190 m long. The locator tip helped to position the fuel element in the fuel bottom support plate.

Below the fuel bottom support plate, there was a gap and then the top of the lower axial shield. The lower axial shield was similar in concept to the top axial shield and can be thought of as two upper axial shields joined top-end to top-end. Section F-F towards the top of the lower axial shield was equivalent to section D-D of the upper shield while sections G-G and H-H were equivalent to sections C–C and B-B, respectively. Towards the bottom of the lower shield, sections I-I and J-J were the equivalent of sections C-C and D-D, respectively.

Figure 4.1.1.3 also includes additional axial dimension information for the upper and lower shield. At the bottom of the lower shield is the boundary between the hex tube and the lower adapter. Plane sections K-K to N-N are sections in the lower adapter. Figure 4.1.1.3 shows the details of the geometry of the lower adapter required for the core driver region. The unique outer configuration of the lower adapter included design features to minimize subassembly misloadings. The outer diameters varied according to position along the lower adapter. The coolant inlet was composed of flow holes drilled into the lower adapter at section M-M. Hole dimensions are not provided as assembly flows and pressure drops are provided in Sections 3.1.3 and 3.2.3 at steady-state conditions.

Details of the solid end of the adaptor beyond section N-N are not given, since these only pertain to the subassembly hold-down on the orientation bars located at the bottom of the lower grid plate.

Figure 4.1.1.5 shows the axial cross-section view of subassembly type MARK-II A (MK2A), which was used in the core driver region. As with Figure 4.1.1.1 for the MARK-II AI subassembly type, Figure 4.1.1.5 shows the top and bottom axial shields, the pin bundle region and the lower adapter (nozzle). Further detailed geometry information for the upper shield, lower shield and the MARK-II A fuel element may be found in Figures 4.1.1.6 and 4.1.1.7.

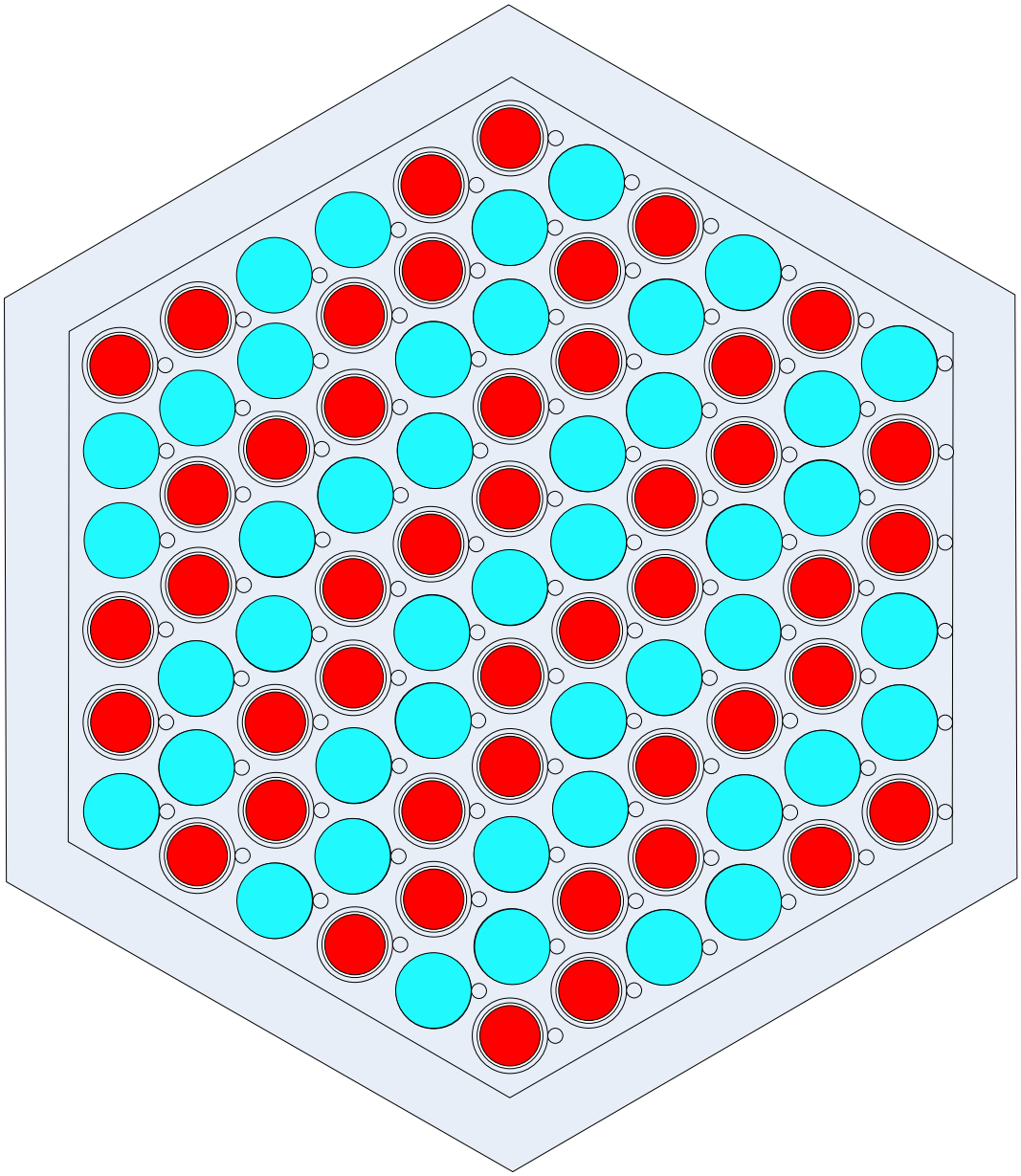

Figure 4.1.1.4. Partial Driver Fuel (red) and Steel (blue) Pins

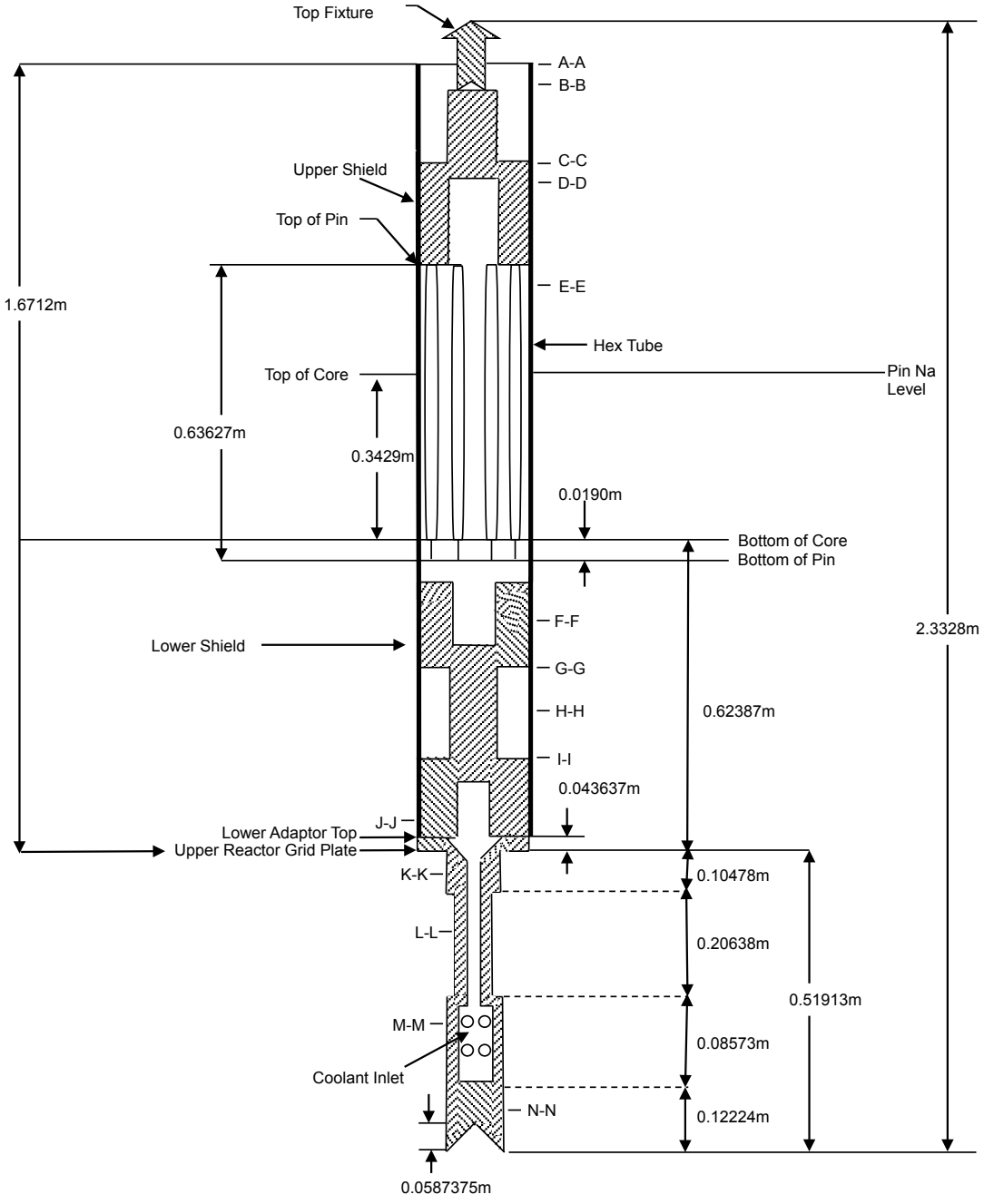

Figure 4.1.1.5. MARK-II A Core Driver axial section

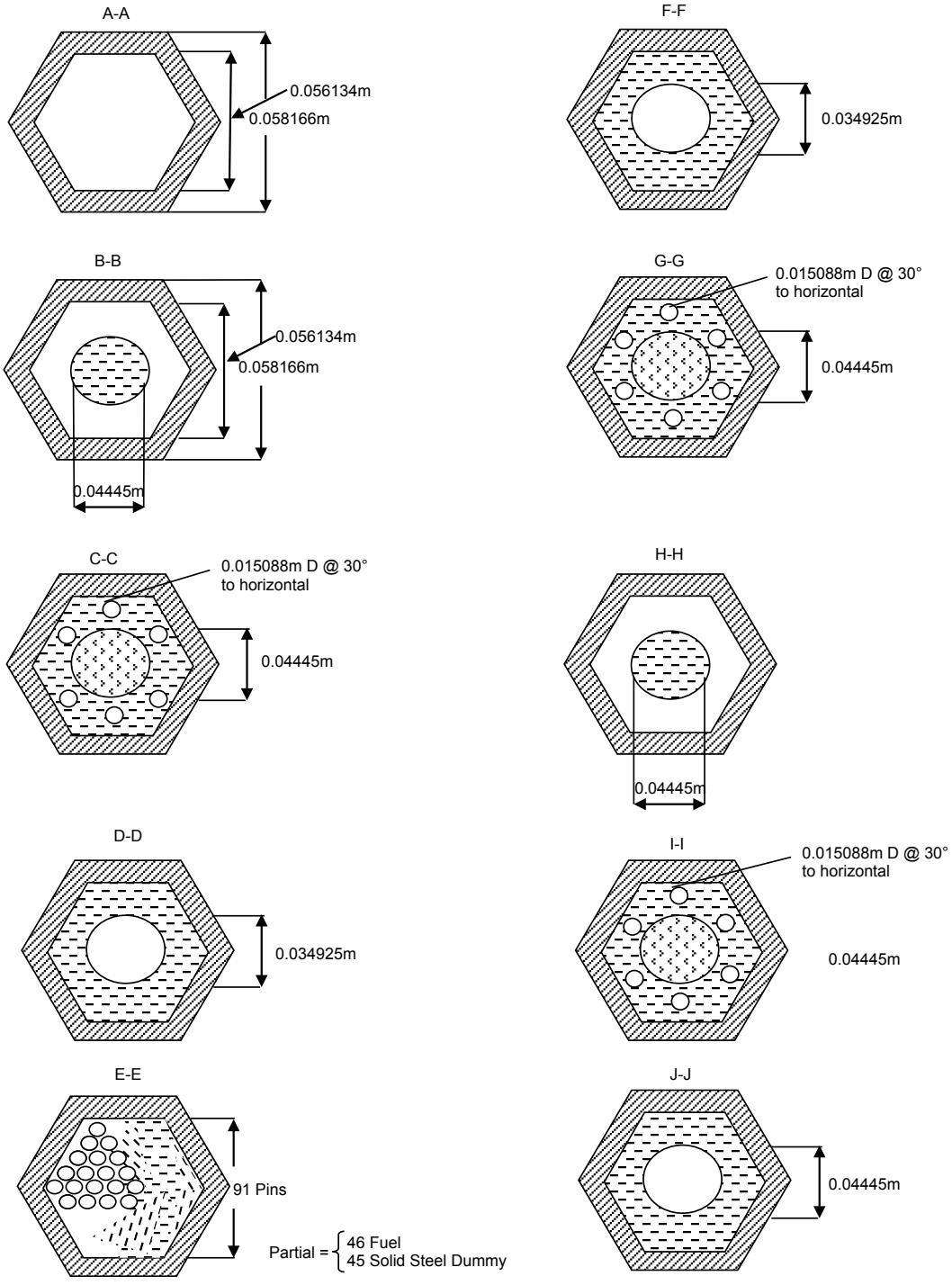

Figure 4.1.1.6. MARK-II A Core Driver plane sections

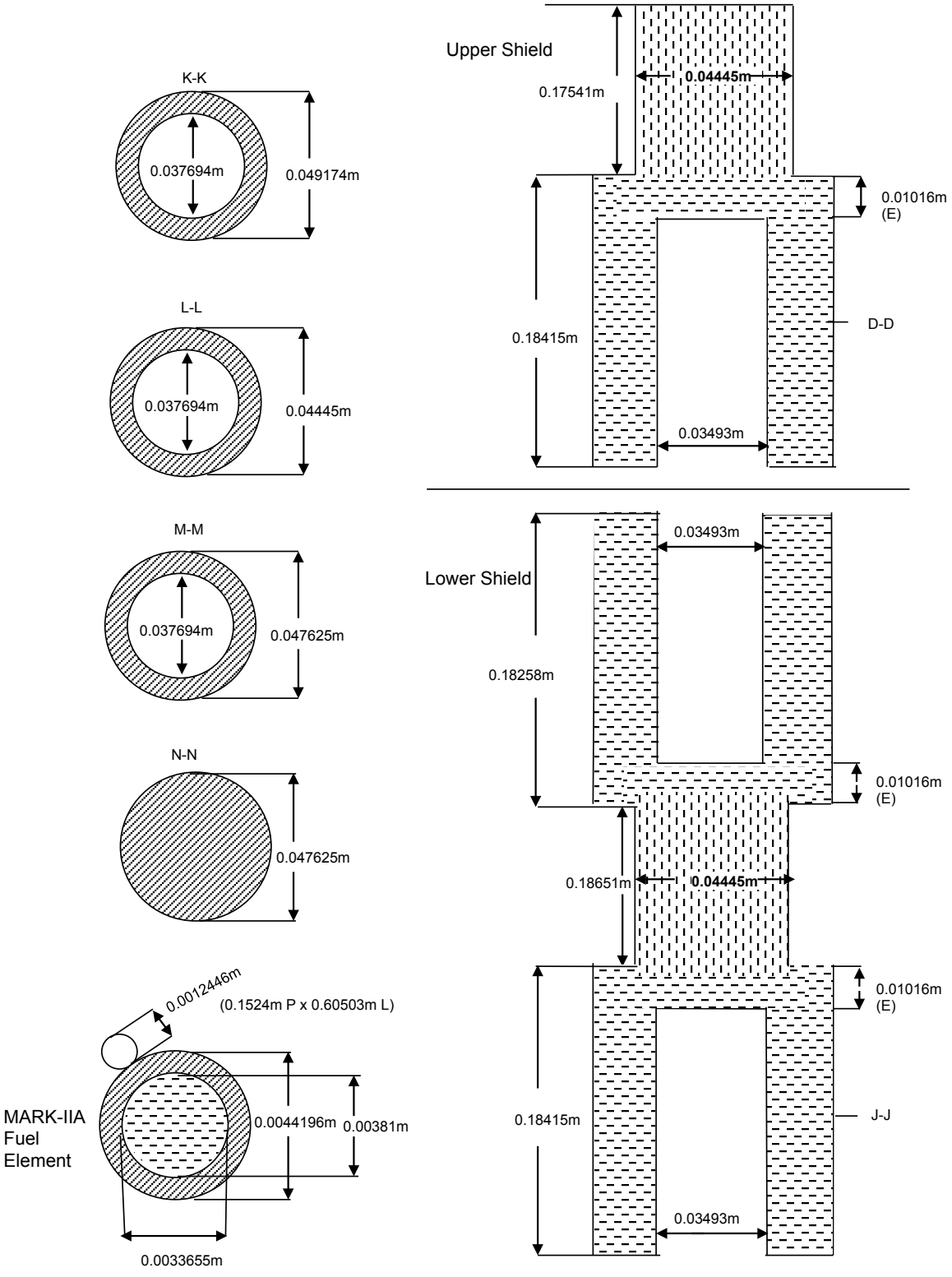

Figure 4.1.1.7. MARK-II A Core Driver elevation and plane sections

There were only two differences between the MARK-II AI and the MARK-II A subassemblies. The first difference was in the length of the fuel elements. This led to the second difference, which was in the length of the corresponding upper axial shields. All the other dimensions and features of the two subassemblies were the same so reference should be made to the discussion given for the MARK-II AI subassembly for a description of the corresponding elevation and plane cross-section views. These views are illustrated for the MARK-II A subassembly in Figures 4.1.1.6 and 4.1.1.6.

When the MARK-II AI and MARK-II A subassemblies were loaded into the external core region (Rows 6-7) as external core drivers, the lower adapters were changed to those specifically designed for the external core region. Figures 4.1.1.8-4.1.1.10 show axial and plane cross-section views of the subassembly type MARK-II AI that was loaded in the external core region as an expanded core driver. Figures 4.1.1.11-4.1.1.13 are given for the MARK-II A external core driver subassemblies.

The high flow driver (HFD) subassembly found in the external core region was either a MARK-II AI external core driver or a MARK-II A external core driver. These subassemblies had extra flow holes cut into the lower adapters to allow higher coolant flow rates but were otherwise unchanged.

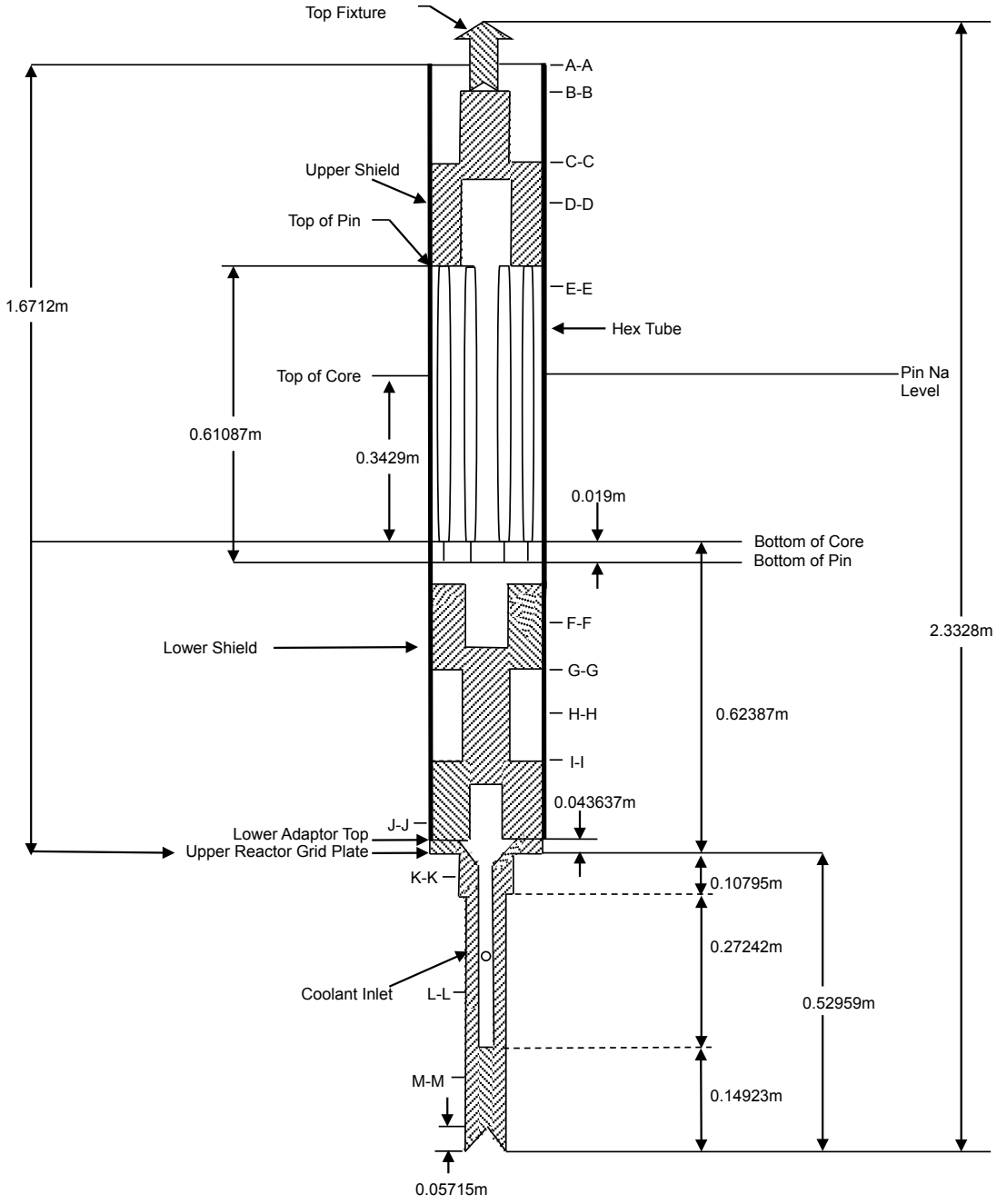

Figure 4.1.1.8. MARK-II AI External Core Driver (including HFD) axial section

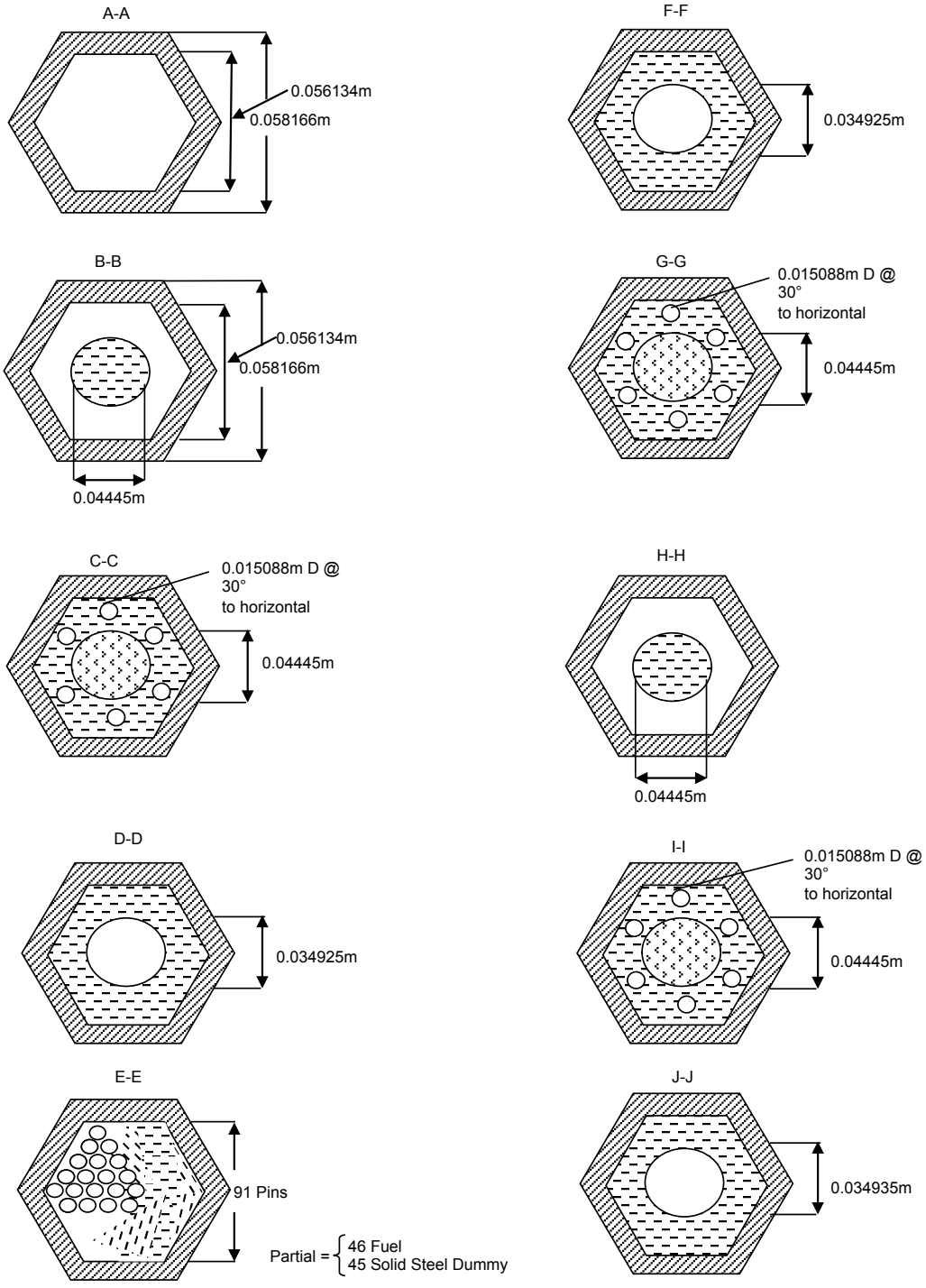

Figure 4.1.1.9. MARK-II AI External Core Driver (including HFD) plane sections

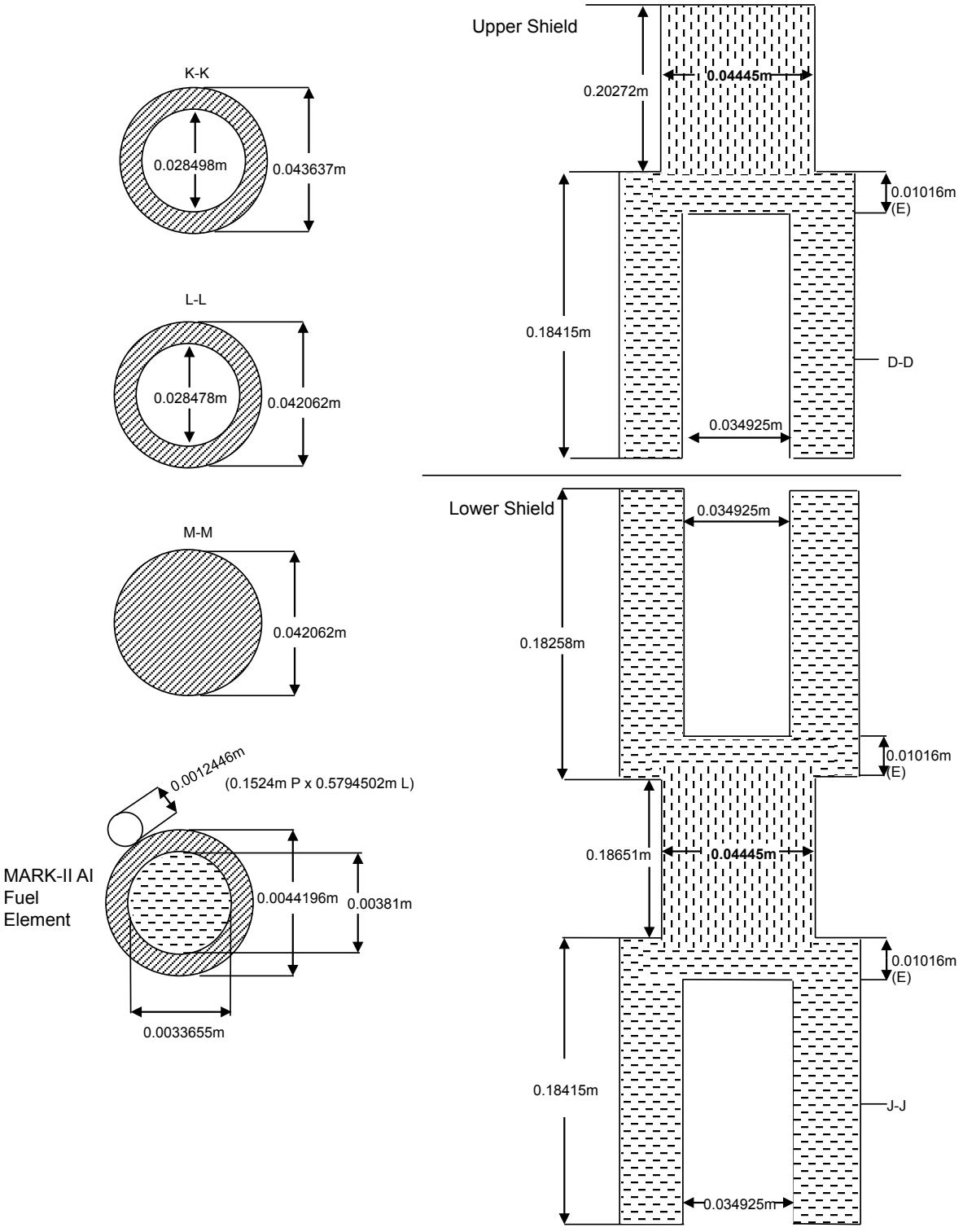

Figure 4.1.1.10. MARK-II AI External Core Driver (including HFD) elevation and plane sections

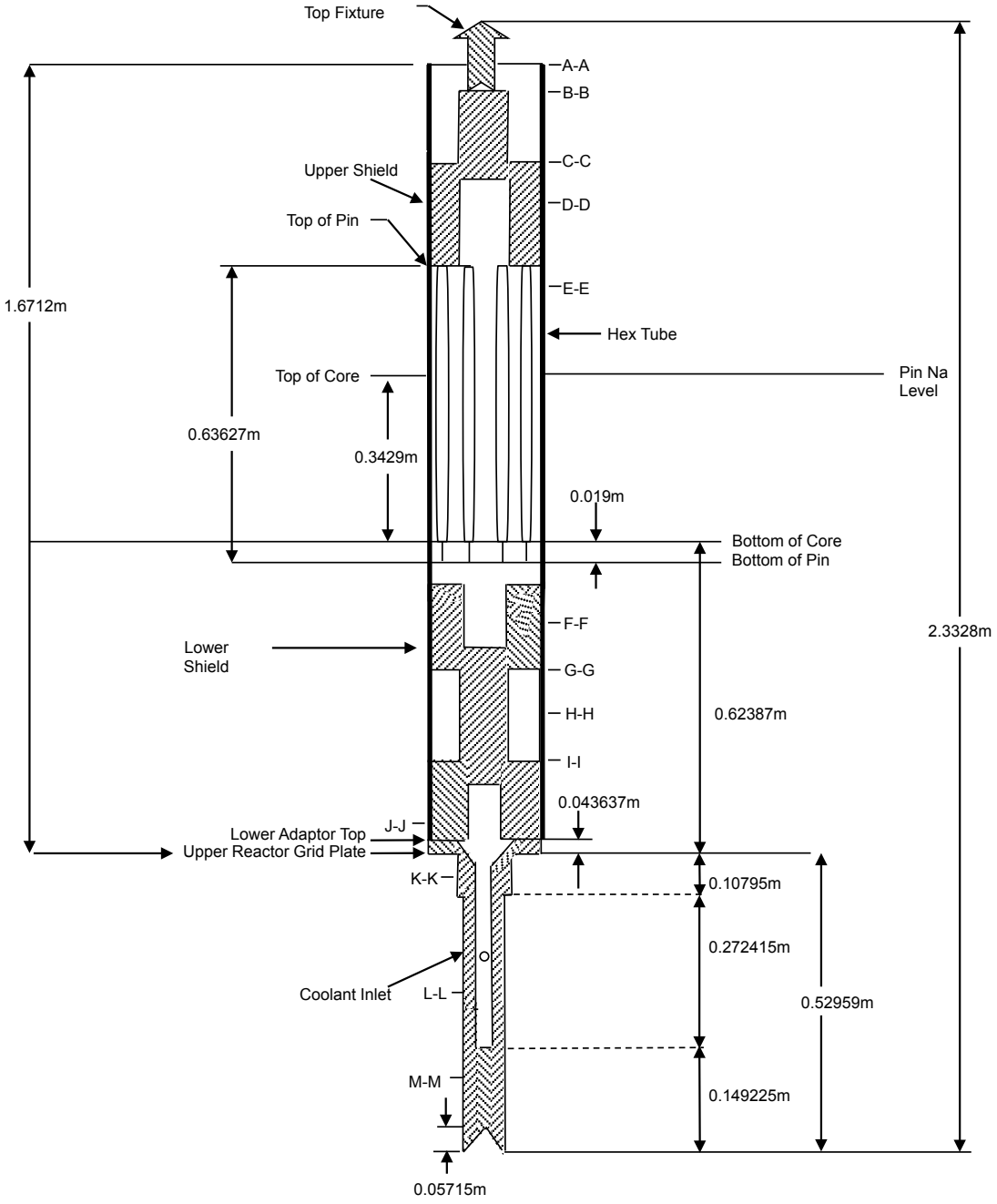

Figure 4.1.1.11. MARK-II A External Core Driver (including HFD) axial section

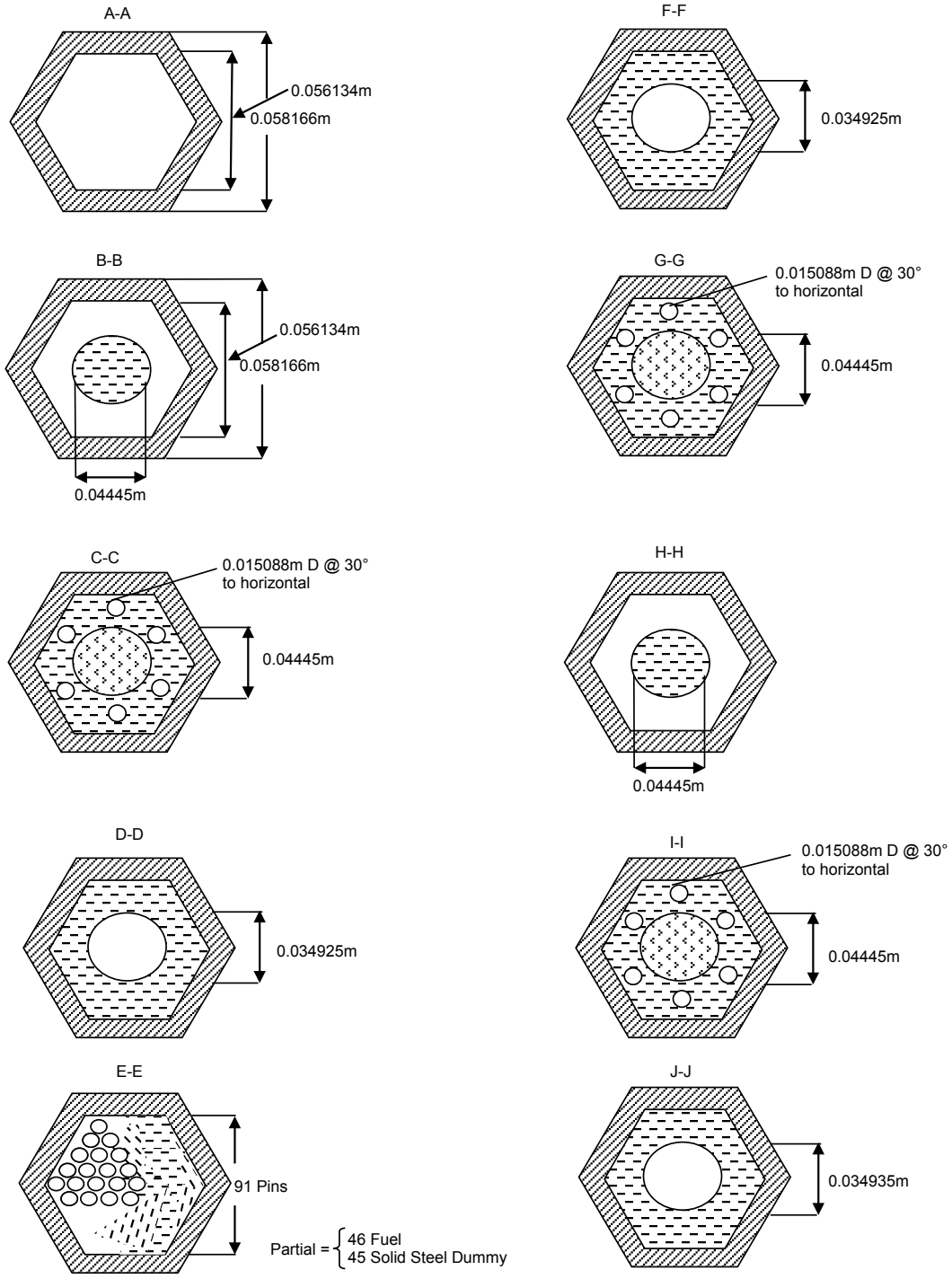

Figure 4.1.1.12. MARK-II A External Core Driver (including HFD) plane sections

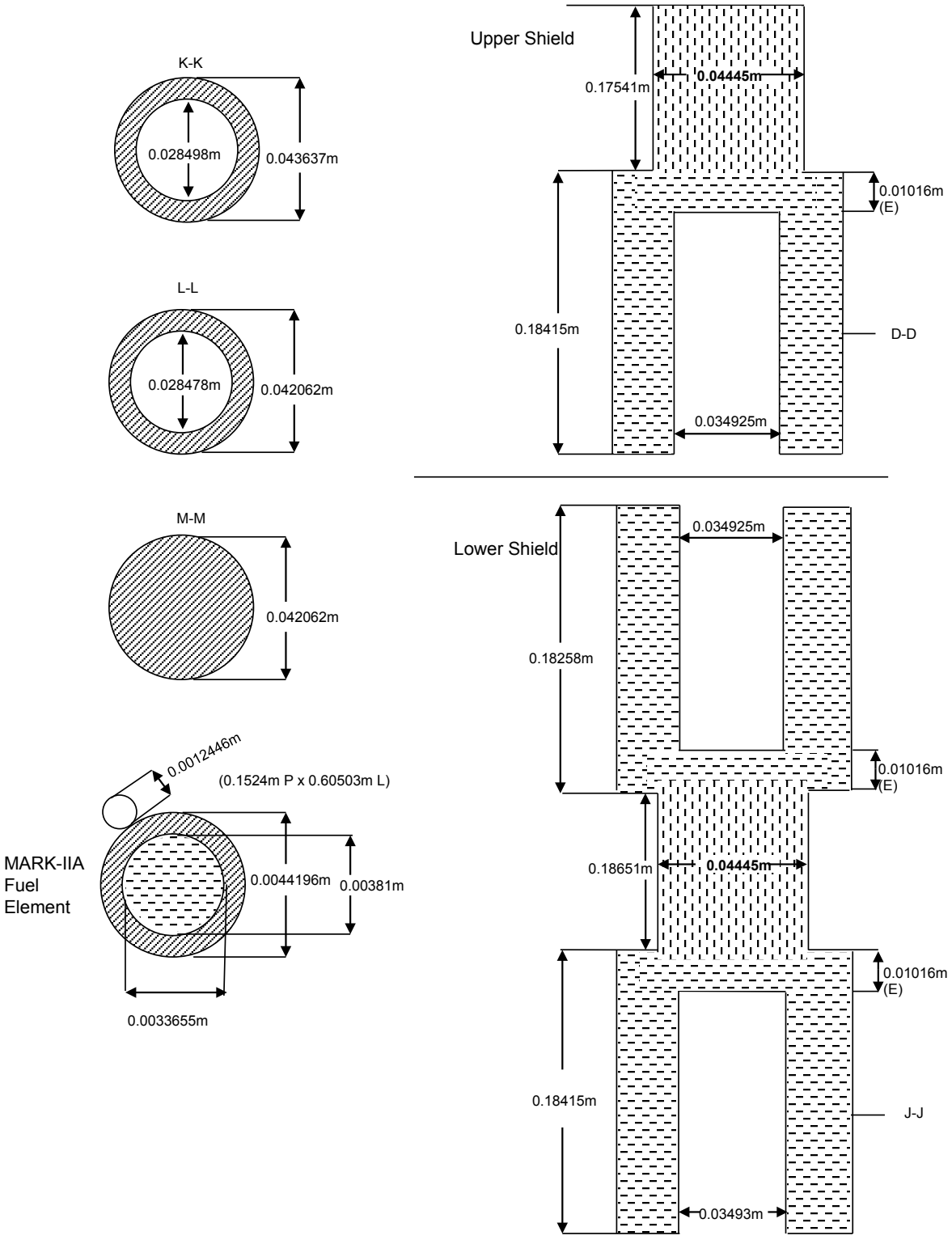

Figure 4.1.1.13. MARK-II A External Core Driver (including HFD) elevation and plane sections

4.1.2 *Steel Subassemblies*

Figures 4.1.2.1 and 4.1.2.2 show axial and plane cross-section views of the subassembly type Steel K (SST) used in the core driver region. These figures show the upper adapter with the fuel handling fixture, center hexagonal tube region, and lower adapter (nozzle). The location of the steel subassembly hex tube is indicated in Figure 4.1.2.1 by the thick line. The steel subassembly hex tube extends from the bottom of the locator pin to section A-A in Figure 4.1.2.1. The elevation view of Figure 4.1.2.1 does not show the detailed geometry of the fixture nor the gap between the top fixture and the top of the stainless steel rod bundle. This fixture is ignored in the benchmark calculation.

Section A-A at the outlet of the hex tube shows the flow area and the hex tube structure dimensions. Materials used are given in Table 4.1.2. Section B-B displays a cross-section through the 7-pin stainless steel rod bundle of the K subassembly. Details are also shown in Figure 4.1.2.2 for the stainless steel rod element. The bottom of the bundle is taken to be the bottom of the stainless steel rods without regard to the element end caps. The element bottom locator tip is shown to be 0.0419 m long. Details are not shown for the locator tips.

Below the locator tips, there was a gap and then the top of the lower adapter. Plane sections C-C to F-F are in the lower adapter. Figure 4.1.2.1 shows the details of the geometry of the lower adapter. The unique outer configuration of the lower adapter structure shown in sections C-C to F-F had design features to minimize subassembly misloadings. The outer diameters varied according to position along the lower adapter. The coolant inlet was composed of flow holes drilled into the lower adapter at section E-E. Hole dimensions are not provided as assembly flows and pressure drops are provided in Sections 3.1.3 and 3.2.3 at steady-state conditions. Details of the solid end of the adaptor beyond section F-F are not given, since these only pertain to the subassembly hold-down on the orientation bars located at the bottom of the lower grid plate.

For the purposes of this benchmark, the LUM-2 subassembly will be treated as a stainless steel subassembly. There is only one LUM-2 subassembly and it is a 19-pin, as opposed to 7-pin, steel element rod subassembly in a control rod position.

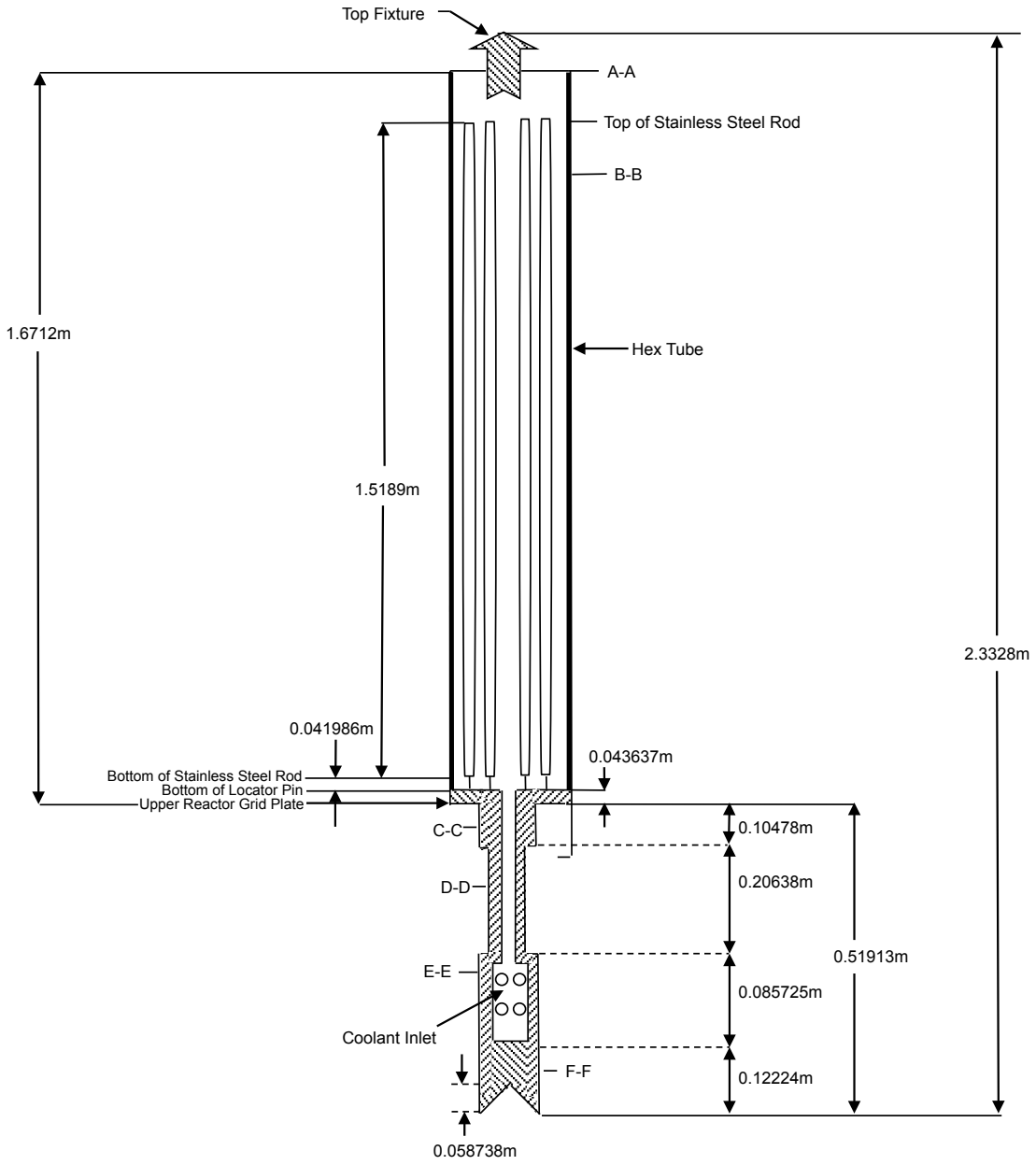

Figure 4.1.2.1. Core Steel axial section

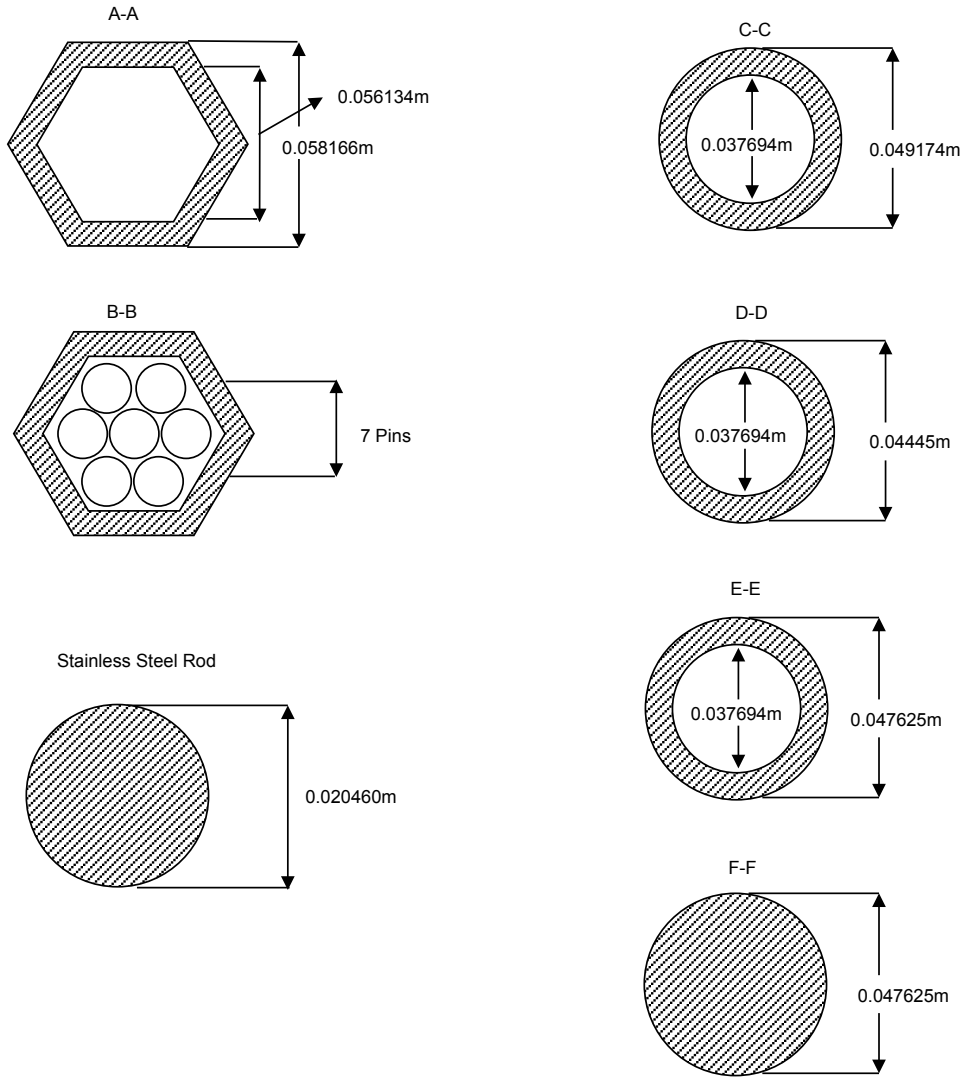

Figure 4.1.2.2. Core Steel plane sections

4.1.3 *Reflector Subassemblies*

Figures 4.1.3.1 and 4.1.3.2 show axial and plane cross-section views of the stainless steel reflector (A, SSR) subassembly used in the expanded core region. These figures show the upper adapter with the fuel handling fixture, center hexagonal tube region, and lower adapter (nozzle). The elevation view of Figure 4.1.3.1 neglects the detailed geometry of the fixture and the gap between the top fixture and the top of the stacked hexagonal blocks that form the stainless steel reflector. The fixture is ignored in the benchmark calculation. The location of the reflector subassembly hex tube is indicated in Figure 4.1.3.1 by the thick line. The reflector subassembly hex tube extends from the top of the lower adapter to section A-A in Figure 4.1.3.1.

Section A-A at the outlet of the hex tube shows the flow area and the hex tube structure dimensions. Materials that were used are given in Table 4.1.2. Below section A-A, section B-B displays a cross-section through one of the six hexagonal blocks of the subassembly. Six slots were cut into each block, with a slot width of 0.0015748 m and a length of 0.011913 m, as indicated in Figure 4.1.3.2. The bottom end of each block was machined to a rounded shape to permit bowing but these details, as simplifications made for the benchmark, are not provided. Dimples in the hex tube provided centering and played a role in the bowing but this is also omitted.

The bottom of the stack of blocks rested on a support plate. Below that support plate, three orifice plates were welded onto the top of the lower adapter. The simplification for this bottom geometry is shown in Figure 4.1.3.1 as the stack bottom resting on one orifice plate.

Plane sections C-C to F-F are sections in the lower adapter. Figure 4.1.3.2 shows the cross-section details of the geometry of the lower adapter required for a non-driver subassembly in the expanded core region. The unique outer configuration of the lower adapter structure shown in sections C-C to F-F has design features to minimize subassembly misloadings. The outer diameters vary according to position along the lower adapter. Section C-C is a plane section through the rounded shoulder of the lower adapter at the top of the reactor upper grid plate as it narrows down to the cylindrical nozzle region. The coolant inlet was composed of flow holes drilled into the lower adapter near section E-E. Hole dimensions are not provided as assembly flows and pressure drops are provided in Sections 3.1.3 and 3.2.3 at steady-state conditions. Details of the solid end of the adaptor beyond section F-F are not given, since these only pertain to the subassembly hold-down on the orientation bars located at the bottom of the lower grid plate.

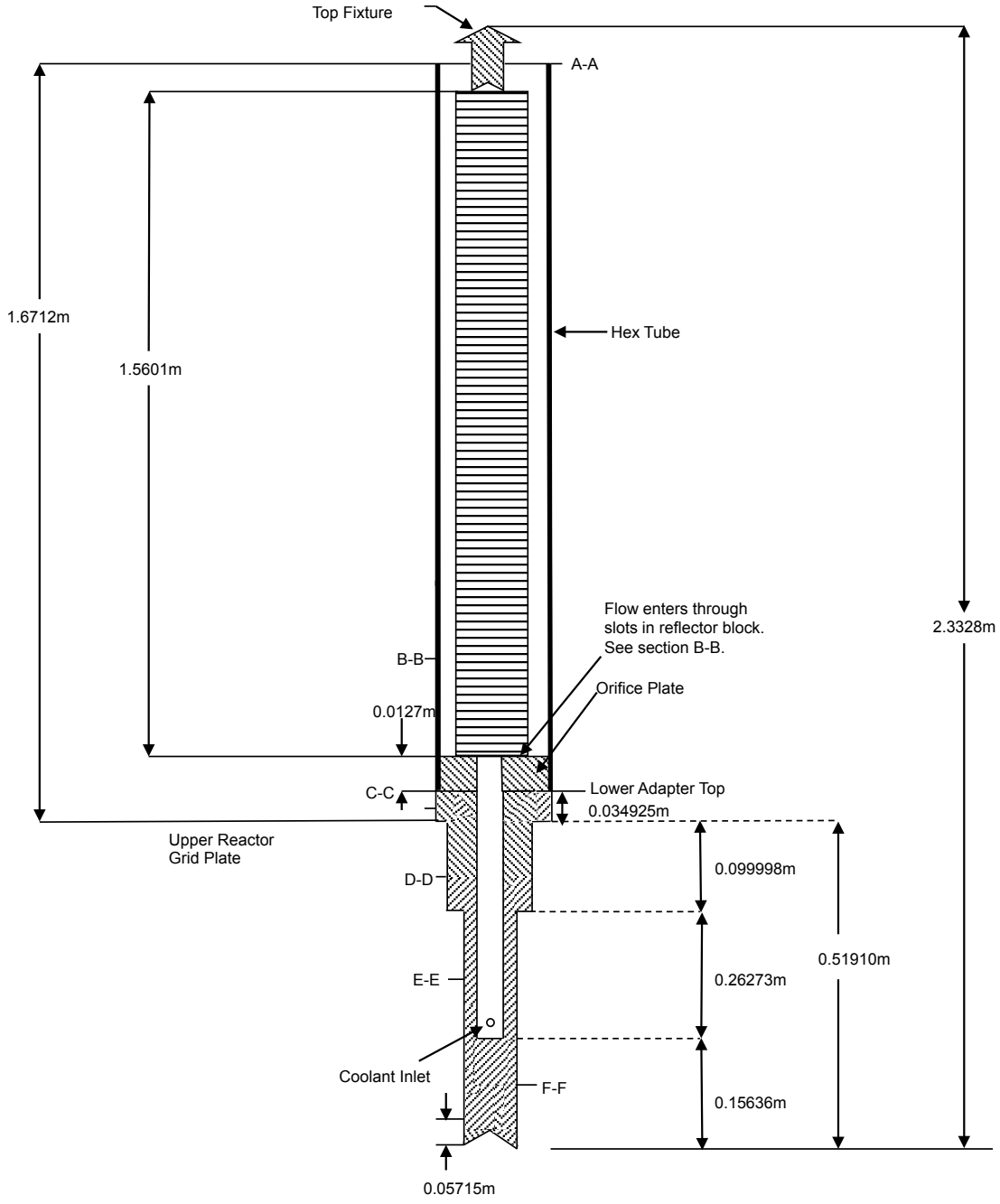

Figure 4.1.3.1. Stainless Steel Reflector axial section for the Expanded Core Region

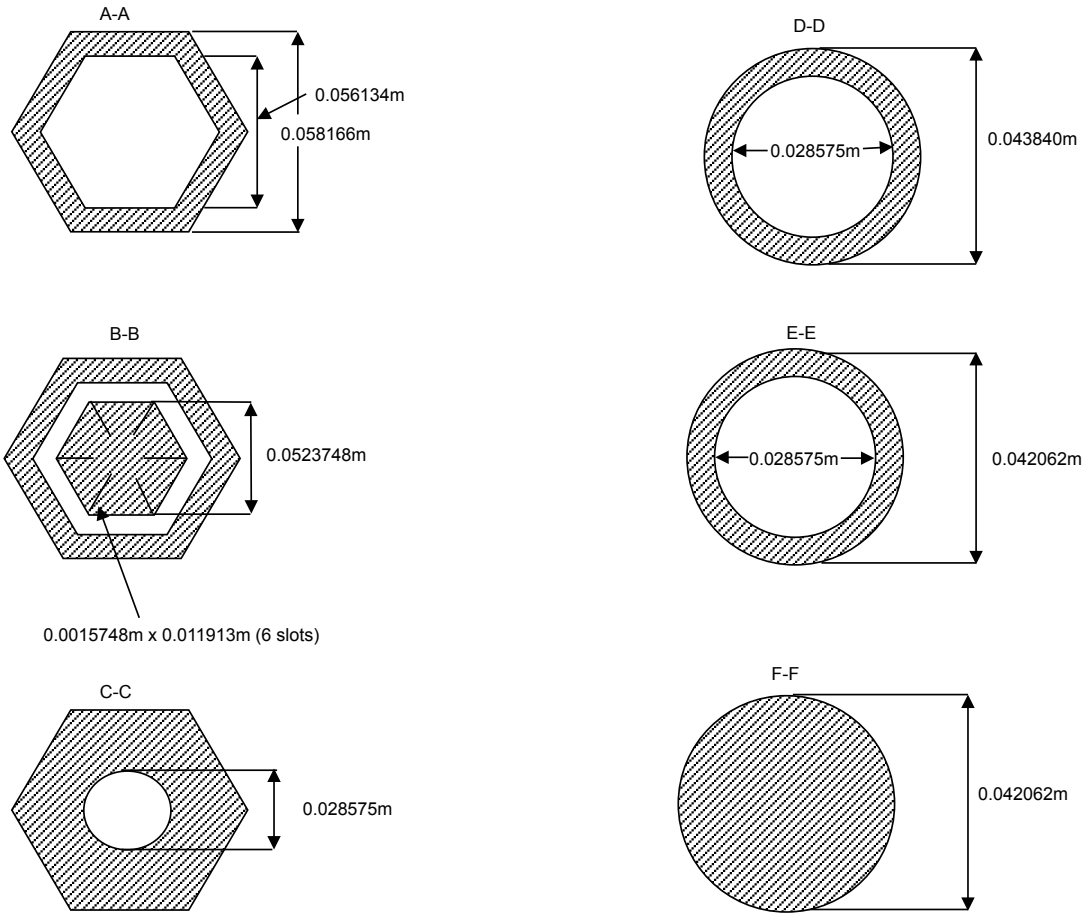

Figure 4.1.3.2. Stainless Steel Reflector plane sections for the Expanded Core Region

Figures 4.1.3.3 and 4.1.3.4 show axial and plane cross-section views of the stainless steel reflector (A, SSR) subassembly type used in the outer blanket region. These figures show the upper adapter, center hexagonal tube region and lower adapter (nozzle). The differences between the outer blanket reflector and expanded core reflector are in the lower adapter. Otherwise, the two types of reflector subassemblies were identical. Plane sections C-C to G-G are sections in the lower adapter. In Figure 4.1.3.4, (E) indicates that a dimension is an estimate taken in inches and converted to centimeters.

Figure 4.1.3.3 shows the details of the geometry of the lower adapter required for a subassembly in the outer blanket region. The unique outer configuration of the lower adapter structure shown in sections C-C to G-G had design features to minimize subassembly misloadings. The outer diameters varied according to position along the lower adapter. Section C-C is a plane section through the rounded shoulder of the lower adapter at the top of the reactor upper grid plate as it narrows down to the cylindrical nozzle region.

Unlike the lower adapter suited for the expanded core region, there were no flow holes/slots cut into the side of the nozzle for coolant feed from the inlet plenum. The coolant inlet consisted of the flow hole drilled into the bottom of the lower adapter past section G-G. Coolant flow from the low-pressure inlet plenum was fed upwards into the outer blanket subassembly region through the flow hole. Flow hole dimensions are not provided as assembly flows and pressure drops are provided in Sections 3.1.3 and 3.2.3 at steady-state conditions. Details of the solid end of the adaptor beyond section G-G are not given, since these only pertain to the subassembly hold-down on the orientation bars located at the bottom of the lower grid plate.

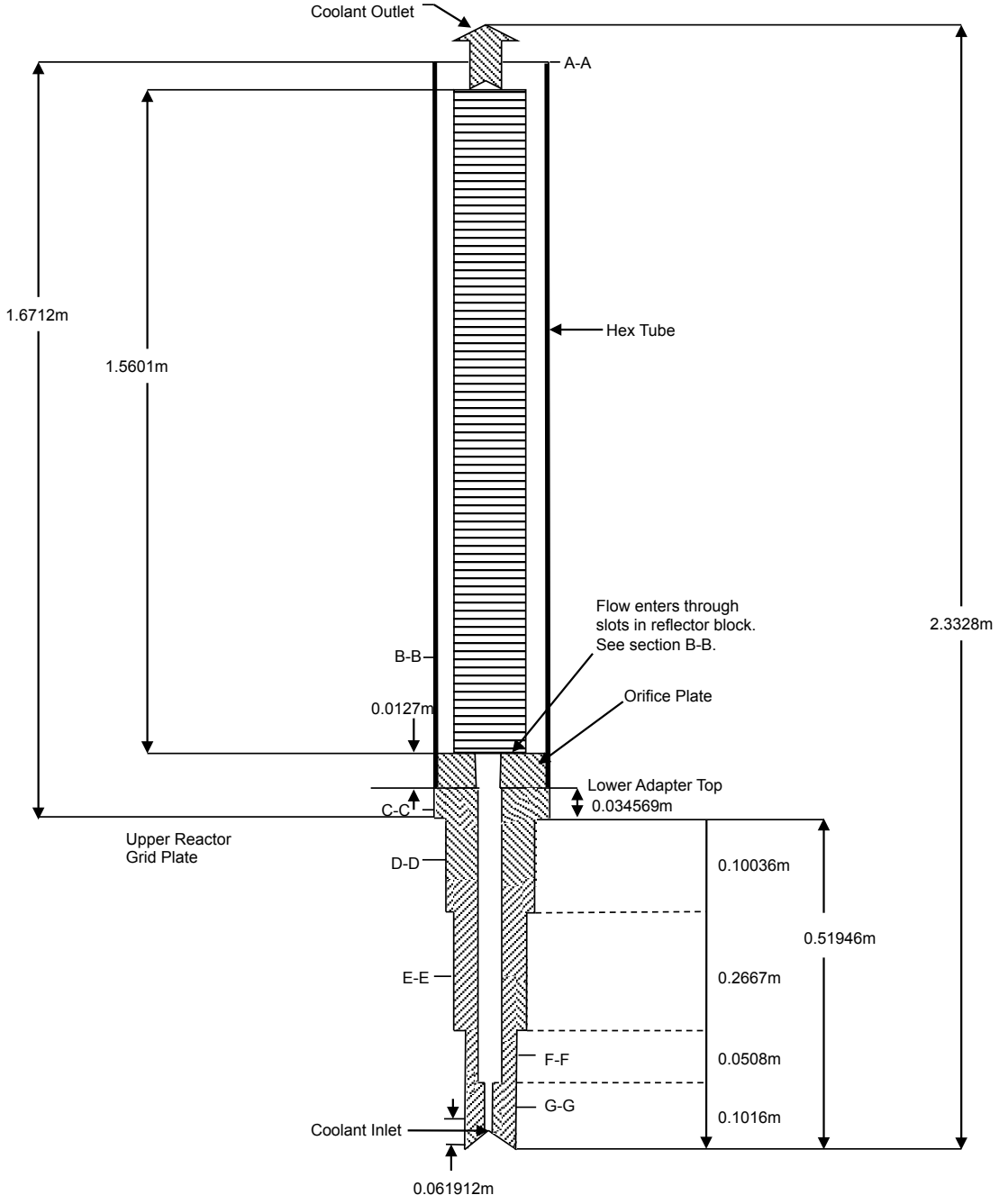

Figure 4.1.3.3. Stainless Steel Reflector axial section for the Outer Blanket Region

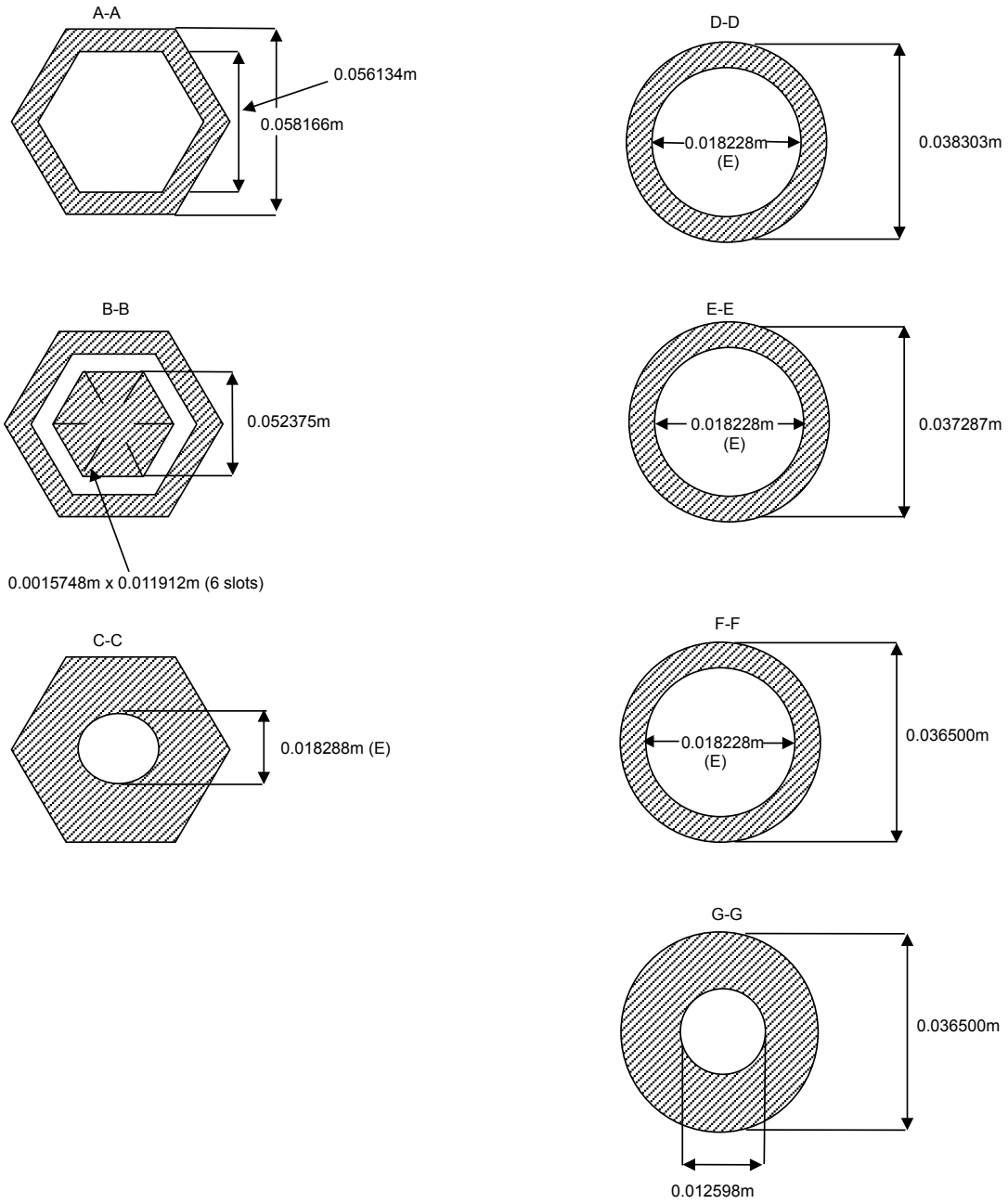

Figure 4.1.3.4. Stainless Steel Reflector plane sections for the Outer Blanket Region

4.1.4 *Uranium Blanket Subassemblies*

Figures 4.1.4.1 and 4.1.4.2 show axial and plane cross-section views of the depleted uranium (SST) subassembly type used in the outer blanket region. These figures show the upper adapter with the fuel handling fixture, center hexagonal tube region and lower adapter (nozzle). The location of the blanket subassembly hex tube is indicated in Figure 4.1.4.1 by the thick line. The hex tube extends from the bottom of the pin to section A-A in Figure 4.1.4.1. The elevation view of Figure 4.1.4.1 does not show the detailed geometry of the fixture nor the gap between the top fixture and the top of the depleted uranium element bundle. The fixture is ignored in the benchmark calculation. In Figure 4.1.4.2, (E) indicates that a dimension is an estimate taken in inches and converted to centimeters.

Section A-A at the outlet of the hex tube shows the flow area and the hex tube structure dimensions. The materials that were used are given in Table 4.1.2. Section B-B displays a cross-section through the 19-element depleted uranium bundle. Table 4.1.1 contains dimensions for the depleted uranium bundle element. The blanket elements were in contact with neighboring elements. Figure 4.1.4.2 shows a cross-section through a fuel element.

The top of the depleted uranium slugs, which defines the top of the core, is depicted in the elevation view. The top compression spring within each element that holds the fuel slugs in place is not depicted in Figure 4.1.4.1. There were five depleted uranium slugs in each blanket element and the “Top of Blanket” label in Figure 4.1.4.1 is the top of these depleted uranium slugs. For details regarding the fuel slugs and the sodium bond level, reference should be made to Table 4.1.1. The bottom of the blanket, which was the bottom of the depleted uranium slug, is taken to be the bottom of the element without regard to the element end cap. The element bottom locator tip, which was part of the end cap, is shown. The locator tip helps to position the fuel element in the bottom grid plate, which was welded to the lower adapter. Details are not shown regarding the locator tips and the bottom grid plate attached to the lower adapter.

The lower adapter of this subassembly type and the lower adapter of the reflector subassembly in the outer blanket region were identical (compare Figures 4.1.4.1 and 4.1.3.3). A single lower adapter design applied to all the positions in the outer blanket region. Plane sections C-C to G-G were sections in this lower adapter design.

Like the stainless steel reflectors in the outer blanket region, there were no flow holes/slots cut into the side of the nozzle for coolant feed from the inlet plenum. The coolant inlet consisted of a flow hole drilled into the bottom of the lower adapter through section G-G. Coolant flow from the low-pressure inlet plenum fed upwards into this outer blanket subassembly through this flow hole. Flow hole dimensions are not provided as assembly flows and pressure drops are provided in Sections 3.1.3 and 3.2.3 at steady state conditions. Details of the solid end of the adaptor beyond section G-G are not given, since these only pertain to the subassembly hold-down on the orientation bars located at the bottom of the lower grid plate.

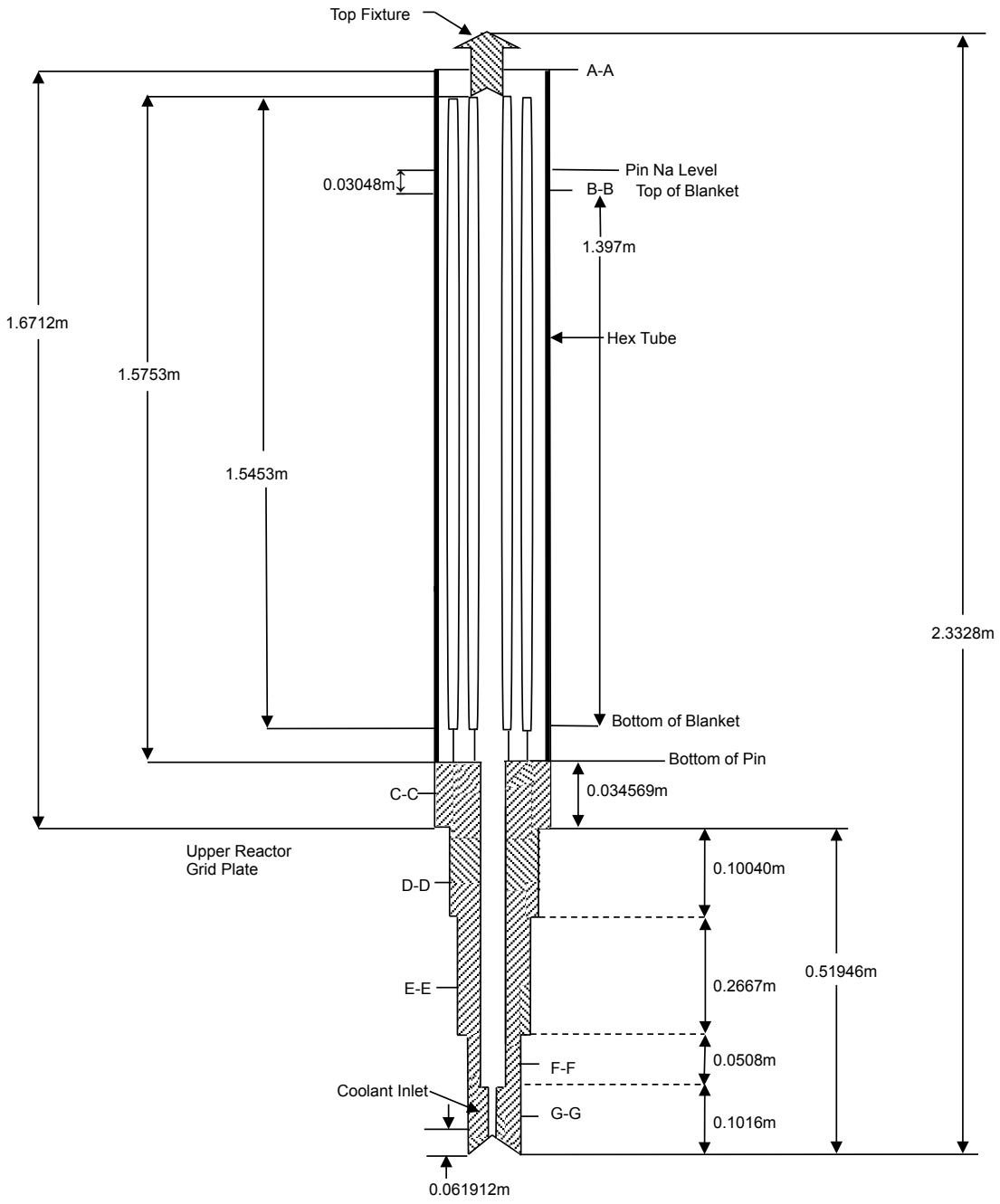

Figure 4.1.4.1. Uranium Outer Blanket axial section

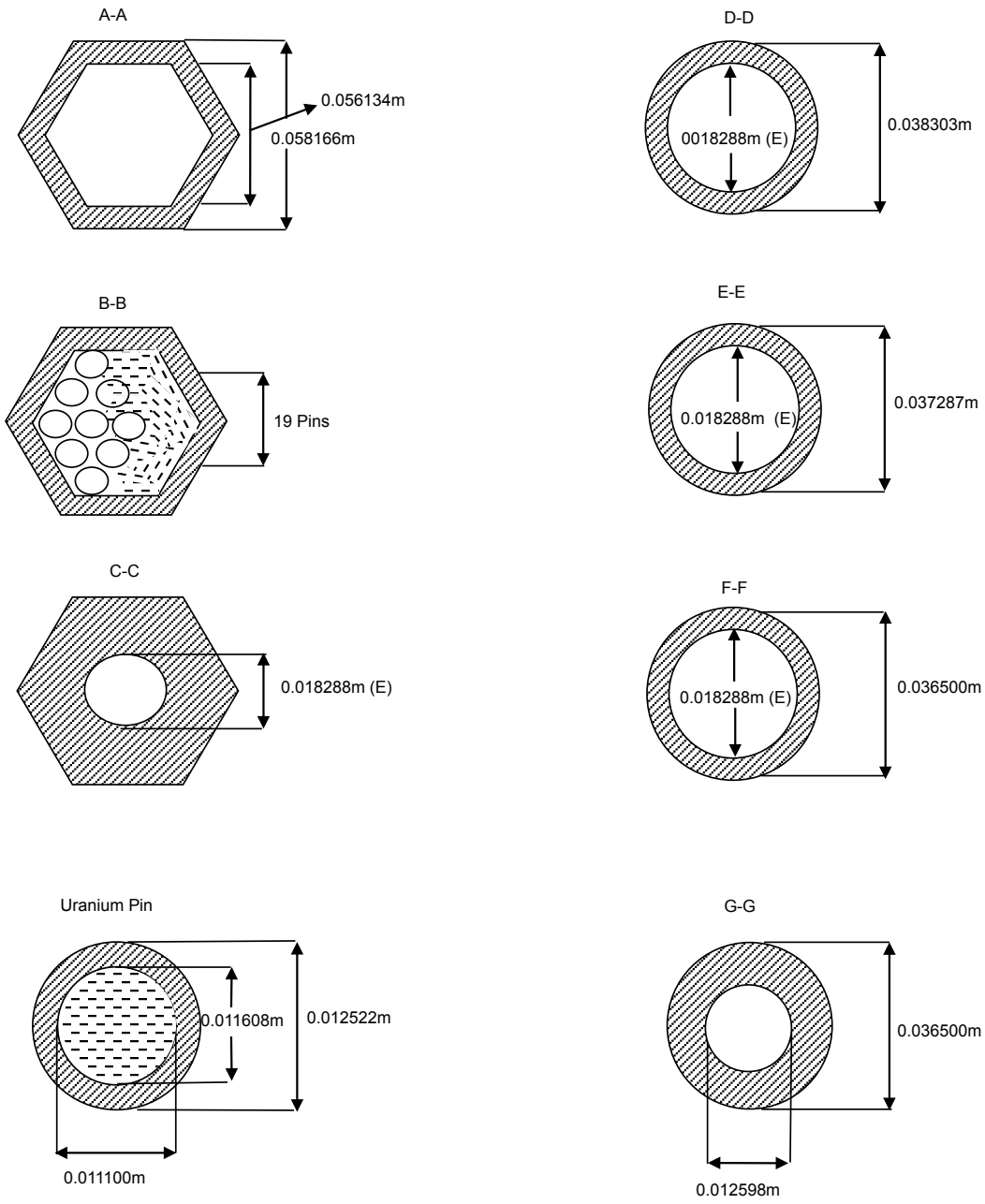

Figure 4.1.4.2. Uranium Outer Blanket plane sections

4.1.5 *Control Subassemblies*

There were eight control subassemblies located in Row 5 of the core. Each consisted of a fixed hexagonal tube, called a guide thimble, and a moveable control rod. The guide thimble was similar in outward configuration to the other subassemblies and was semi-permanently installed and secured to an adapter on the reactor grid plate. The control rod contained fuel elements near the center. It was fitted at the top end with a handling adapter and at the bottom end with a tubular adapter that fit into the lower part of the guide thimble.

The control rod was designed to be moved vertically within the guide thimble over a range of 35.56 cm (14 inches). When the control rod was lowered to its bottom position, the fuel elements were below the bottom of the reactor core elevation and contributed minimum reactivity to the core. When the control rod was raised to its uppermost position, the fuel elements were fully inserted into the reactor core and contributed maximum reactivity. In the High Worth Control Rod (HWCR) design version of the control rod, a boron carbide poison pin bundle section was located above the fuel element pin bundle. This poison section in the HWCR entered the core region when the fuel element pin bundle section was lowered out of the core. Conversely, when the fuel pin bundle section was raised back into the core, this boron pin poison section was raised out of the core. This maximized the reactivity swing for these types of control rods. For SHRT-45R, the control rod insertion depth at the initiation of the test was such that the bottom of the control rod fuel bundle was 21.29 cm below the bottom of the fuel bundle of the core driver subassemblies.

Figures 4.1.5.1-4.1.5.3 show axial and plane cross-section views of the HWCR subassembly type and its guide thimble used in the core driver region. These figures show the top boron carbide poison pin bundle section, fuel pin bundle region and lower adapter (nozzle) with the bottom axial shield. The upper adapter with the top fuel handling fixture is also shown. The location of the control subassembly inner hex tube is indicated in Figure 4.1.5.1 by the thick line. The hex tube extends from the bottom of the pin to section A-A in Figure 4.1.5.1. The elevation view of Figure 4.1.5.1 does not show the detailed geometry of the fixture nor that of the gap between the top fixture and the top wire-wrapped boron carbide poison pin bundle. The fixture is ignored in the benchmark calculation.

Section A-A at the outlet of the hex tube shows the flow area and the hex tube structure dimensions. Materials that were used are given in Table 4.1.2. Section B-B is a cut through the top boron carbide poison pin bundle, which was composed of seven poison pins that were clad in stainless steel. An axial section cut through a poison pin stainless steel tube is also shown in Figure 4.1.5.3. The top end plug, which had a complicated geometry, is shown simplified as a right cylinder. Below the end plug was a gas space followed by an upper part that was a shield cylinder made of stainless steel. This was sitting on an inconel spring.

Below the inconel spring were the 14 boron carbide (B_4C) pellets and then the bottom end plug. Figure 4.1.5.3 gives the dimensions of the stainless steel shield cylinder, the boron carbide pellets and the inconel spring. The seven poison pins were positioned at the bottom end in a grid assembly, which is depicted by a horizontal line in Figure 4.1.5.1. This grid is ignored in the benchmark analysis.

There was then a gap between this poison bundle grid plate and the top of the core fuel pin bundle. Section C-C shows that in the fuel pin bundle there were 61 wire-wrapped MARK-II S fuel elements. A cross section of the MARK-II S fuel element with its wire wrap

is included in Figure 4.1.5.3. Table 4.1.1 gives additional details of the MARK-II S fuel element.

There was one fuel slug in each fuel element and the "Top of Core" label in Figure 4.1.5.1 was the top of this fuel slug. The bottom end cap of the fuel element was fitted with a locator tip and the end of the locator tip is indicated in Figure 4.1.5.1 as "Bottom of Pin". The fuel bundle grid plate, which holds these locator tips, is displayed in Figure 4.1.5.1 as a fine horizontal line. Below the fuel bundle grid plate there was the transition region between the top rounded shoulder and the lower cylindrical nozzle parts of the lower adapter. Section D-D is at the top of the rounded shoulder. Section E-E is a simplified hexagonal representation at the bottom of the rounded shoulder, just before the cylindrical nozzle part of the lower adaptor. Section F-F is in the cylindrical nozzle part towards the top, closer to the rounded shoulder.

The lower adapter radial cross-section became an annulus at section G-G. The central part of this section passes through the lower shield, which had a cone-shaped head and is simplified in the elevation drawing with a right cylindrical representation. The lower shield plug sat on a compression spring contained within a tube. Section H-H is a section through that tube but the spring is not shown. The elevation view included in Figure 4.1.5.1 gives the necessary tube dimensions. The flow holes that were drilled into the lower adapter below section H-H for the coolant inlet flow are also shown in the Figure 4.1.5.1.

Also shown on the left hand side of Figure 4.1.5.1 is the elevation view of the guide thimble in which the control subassembly sat. The guide thimble guided the coolant flow into the flow holes. The upper part of the guide thimble was hexagonal and had the same dimensions as the hexagonal tube of the other subassemblies. This is shown by the A-A cross section of the thimble in Figure 4.1.5.2.

Similar to the design of the lower adapter in the subassemblies discussed above, there was a lower guide thimble adapter that locked the thimble in the lower reactor grid plate. Details of this are shown at section D-D below the lower reactor grid plate. The coolant flow slots in the guide thimble lower adapter were above the lower control rod bushing, which is described below, throughout the control rod travel. These flow slots are not shown in Figures 4.1.5.1-4.1.5.3 but they were located above section C-C in the high-pressure inlet plenum. Section B-B is above the rounded shoulder portion of the guide thimble lower adapter.

Although the lower end of the guide thimble is open, sodium flow was restricted by this lower control rod bushing that is designed to limit the sodium leakage through the bottom of the thimble from the high-pressure plenum to the cold pool. The bushings, which are illustrated in Figure 4.1.5.1, were essentially steel rings fitted over the lower control rod adapter to provide bearing-type surfaces between the control rod and the lower bore of the guide tube. There was a second set of upper control rod bushings located higher up on the control rod subassembly above all the flow holes, guide thimble and rod lower adapter that limited the sodium thimble flow leakage in the other direction towards the reactor outlet plenum.

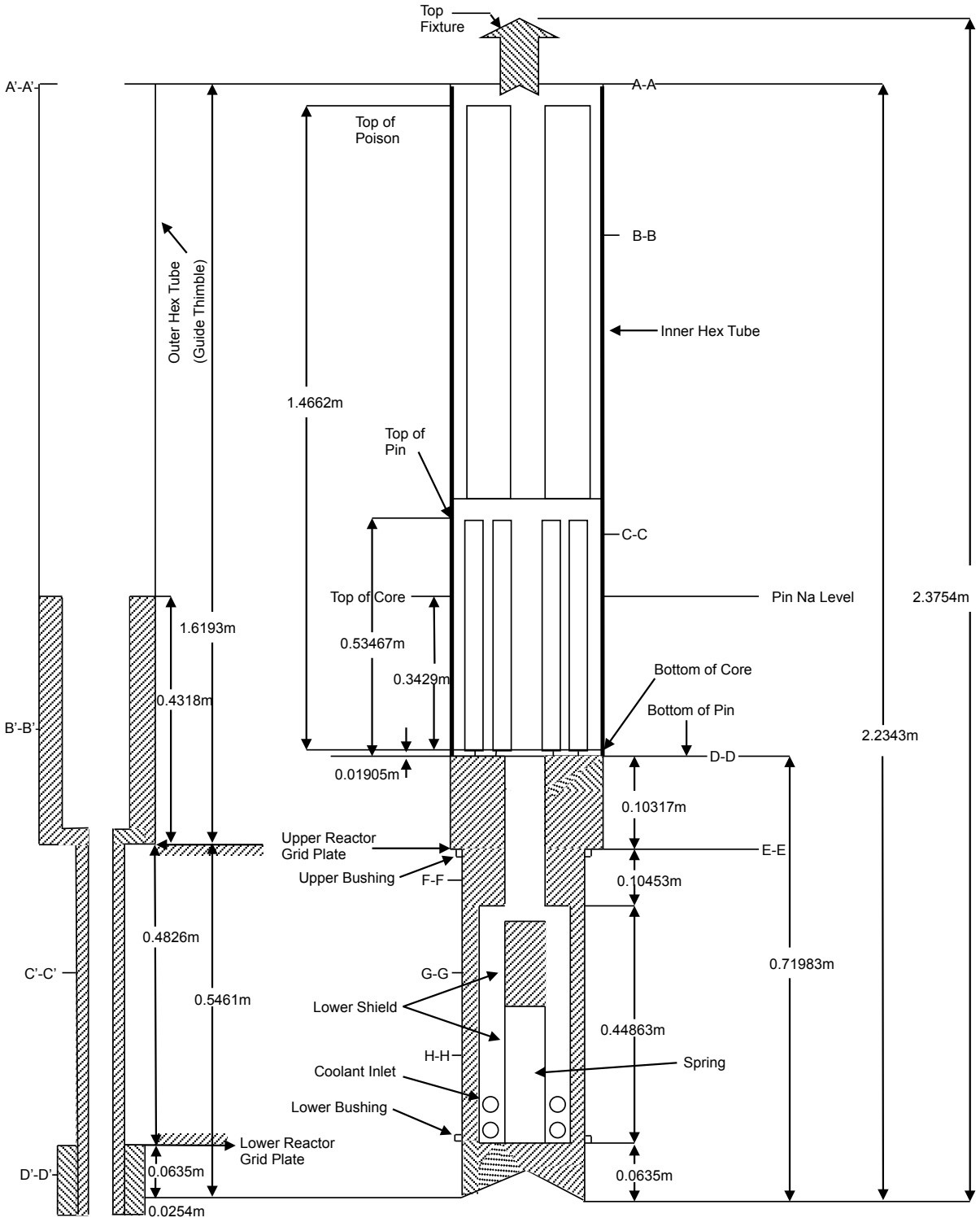

Figure 4.1.5.1. High Worth Control Rod axial section

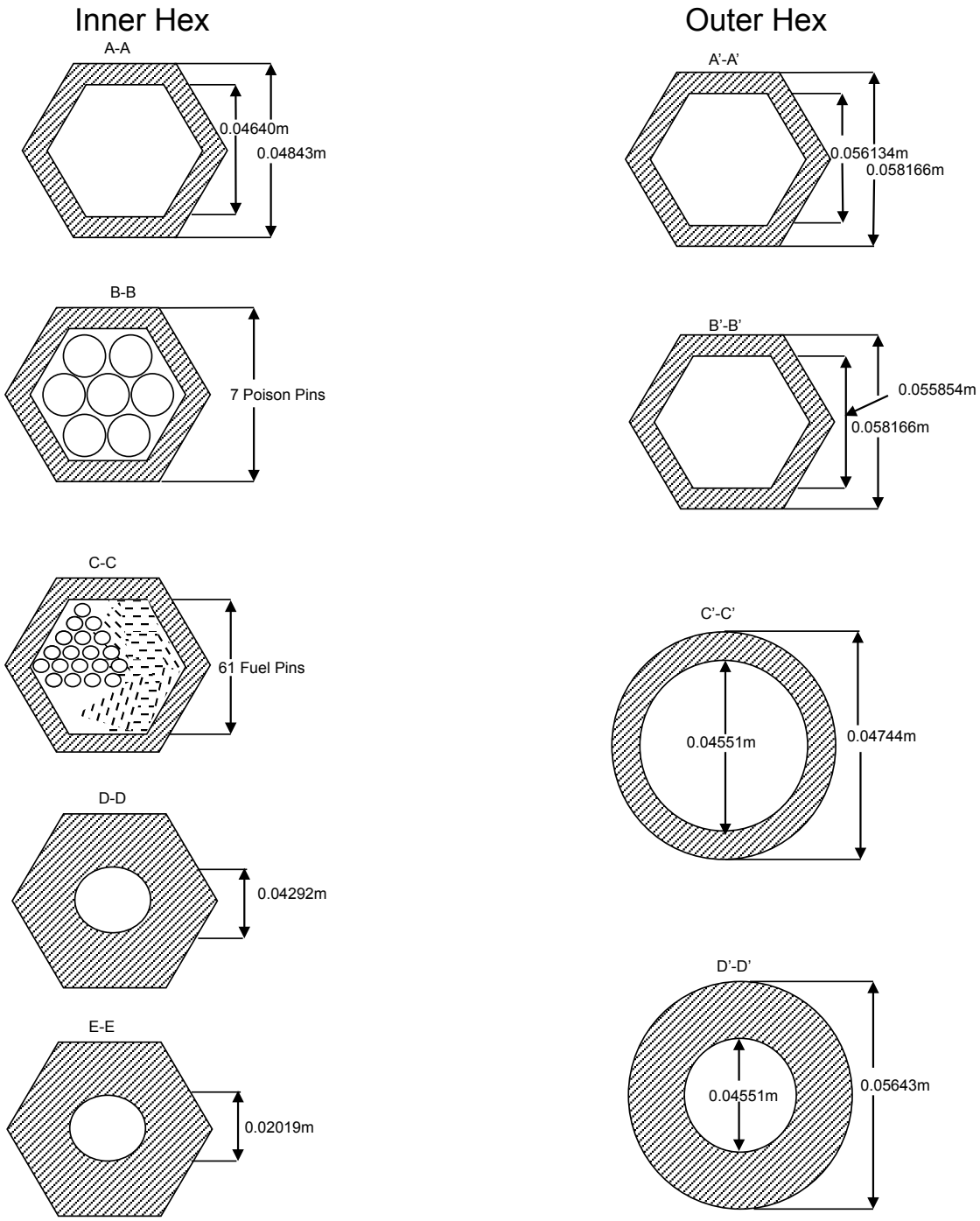

Figure 4.1.5.2. High Worth control Rod plane sections

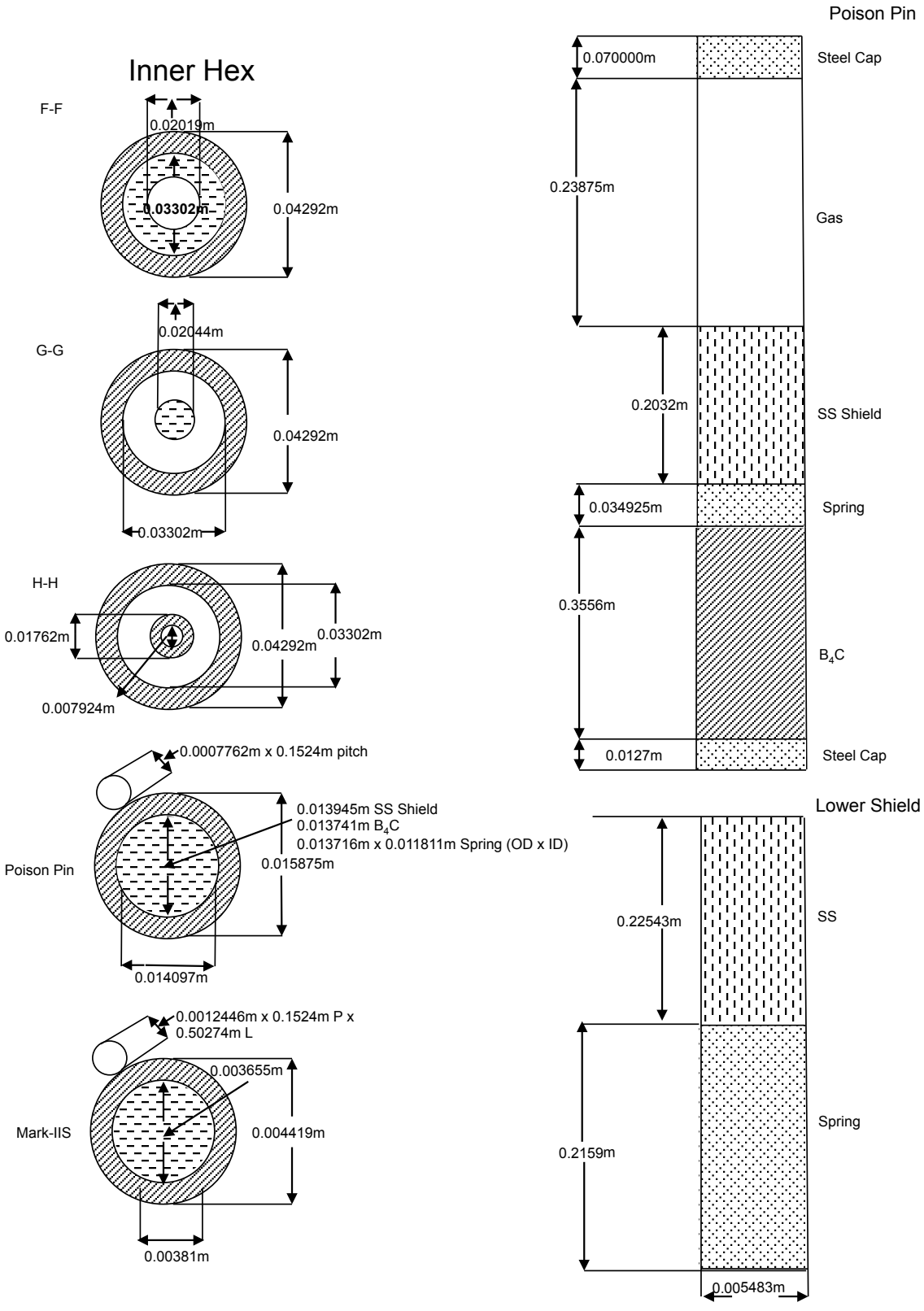

Figure 4.1.5.3. High Worth Control Rod elevation and plane sections

4.1.6 *Safety Rod Subassemblies*

There were two safety subassemblies located in Row 3 of the reactor. Each consisted of a safety rod contained in a hexagonal guide thimble. The guide thimble was similar in outward configuration to the other subassemblies used in the reactor and was semi-permanently installed and secured to an adapter on the reactor lower grid plate. Each safety rod was fitted at the top end with a handling adapter and at the bottom end with a tubular adapter. In between the two ends was a hexagonal tube similar to that of the other subassemblies but with a smaller flat-to-flat dimension so that it could fit within the hexagonal guide thimble. This hexagonal section of the safety rod contained 61 fuel elements located in the approximate center of the rod. The safety rod was positioned in the reactor with the fuel elements at the same elevation as the core region, or it was lowered 35.56 cm (14 inches) to position the fuel element below the core region. For SHRT-45R the safety rod insertion depth at the initiation of the test was such that the bottom of the safety rod fuel bundle was 15.94 cm below that of the fuel bundle of the core driver subassemblies.

Figures 4.1.6.1-4.1.6.3 show axial and plane cross-section views of the subassembly type SAFETY used in the core driver region. The figures show the top and bottom axial shields, pin bundle region and lower adapter (nozzle). The upper adapter with the top handling fixture is also shown. The location of the safety subassembly inner hex tube is indicated in Figure 4.1.6.1 by the thick line. The hex tube extends from the bottom of the pin to section A-A in Figure 4.1.6.1. Portions of the upper and lower shield sections are assumed to extend outward to be flush with the inner surface of the subassembly hex tube. The elevation view of Figure 4.1.6.1 does not show the detailed geometry of the fixture nor the gap between the top fixture and the upper axial shield. The fixture is ignored in the benchmark calculation.

Section A-A at the outlet of the hex tube shows the flow holes and the upper adapter structure. While six flow holes are shown in Figure 4.1.6.2, there were actually twelve flow holes. Six flow holes had a diameter of 7/32 inches and the other six flow holes had a diameter of 11/32 inches. The dimensions of the complex geometry of the upper adapter are not given. Materials that were used are given in Table 4.1.2.

Section B-B is through the gap above the top of the upper shield. Below this, section C-C is through the top part of the upper shield, which was a sextuple fluted section. Approximate dimensions of the fluting are shown in Figure 4.1.6.2. The coolant slots between the flutes had a uniform gap width until the flutes joined at the center core of the shield. Section D-D is a view through the central transition cylindrical piece of the upper shield. The lower part of the upper shield was similar to the upper sextuple fluted part, but these flutes were offset by 60° as shown by cross section E-E.

Details of the gap between the bottom of this upper shield and the top of the MARK-II AI pin bundle are not shown. The dimensions of the wire-wrapped fuel pin in this 61 pin MARK-II AI bundle are given in Figure 4.1.6.3, which corresponds to section F-F.

The top of the core, which is the top of the fuel slug, and the level of the sodium bond in a pin are shown in Figure 4.1.6.1. Consistent with the simplification, the details of the fuel element end cap, the locator tip, the fuel element grid support plate at the bottom of the core and the bottom of the pin are not shown. This section was where the hexagonal tube and the lower adapter were welded. The lower adapter then became cylindrical.

The lower axial shield was located in the top part of this cylindrical tube. The lower shield was a tri-fluted stainless steel shield plug in which the fluting had a rotational pitch designed so there was a 120° twist from the bottom of the lower shield to the top of the lower shield. The tri-fluting is shown by the section G-G in Figure 4.1.6.3.

The reduction in diameter of the lower shield from the bottom of the shield to the top of the shield is ignored in Figure 4.1.6.3. Below the lower axial shield there was a change in the outer diameter of the bottom end safety rod adapter tube with a narrowing of the tube. This transition location was where the upper bushing was located on the outside of the adapter to provide the guide with bearing type surfaces between the safety rod and the lower portion of the guide thimble. The second set of bushings, the lower bushing, was located closer to the bottom of the safety rod below the flow holes around section H-H and just above the bottom tip shown by section I-I. The safety rod was secured to the safety rod drive shaft by a dowel pin located in the bottom tip. There was also a spacer ring welded to the outside of the upper hexagonal tube part of the safety rod to provide additional bearing-type surfaces between the safety rod and the guide thimble.

On the left-hand side of Figure 4.1.6.1 is the elevation view of the guide thimble in which the safety subassembly sits. This guide thimble guided the coolant flow into the flow holes. The upper part of the thimble was hexagonal and the same dimensions as the hexagonal tube of the other subassemblies. This is shown by the A-A cross section of the thimble in Figure 4.1.6.2. Section D-D shows a simplified schematic of the lower guide thimble latching that was used to secure the guide thimble to the lower reactor grid plate. As in the design of the control rod assembly, guide thimble slots permitted entrance of coolant. Sodium entered through these slots in the lower end of the guide thimble and then flowed into the safety rod through the holes around section H-H of the safety rod lower adapter. The coolant flow slots in the guide thimble lower adapter were above the lower safety rod bushing throughout the safety rod travel. These flow slots are not shown in Figure 4.1.6.2 but they were located above section C-C in the high-pressure plenum.

Section B-B is higher up through the rounded shoulder portion of the guide thimble lower adapter. Although the lower end of the guide thimble was open, sodium flow was restricted by this lower safety rod bushing, which therefore limited the sodium leakage from the bottom of the thimble from the high-pressure plenum to the low-pressure plenum. The bushings were essentially steel rings fitted over the lower safety rod adapter to provide bearing type surfaces between the safety rod and the lower bore of the guide thimble tube. There was a second set of upper safety rod bushings located higher up on the safety rod subassembly above all the flow holes, guide thimble and rod lower adapter that limited the sodium thimble flow leakage in the other direction towards the reactor outlet plenum.

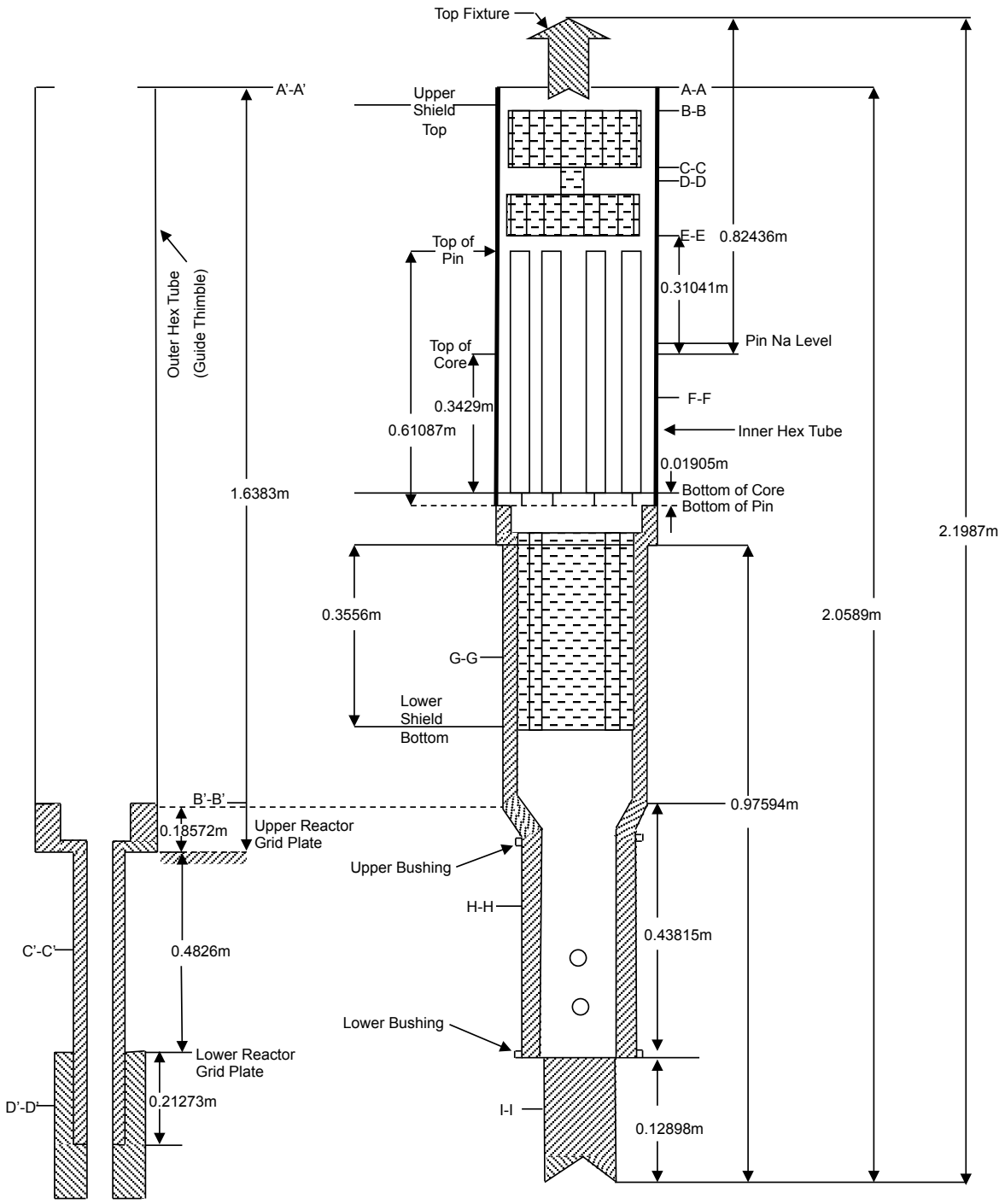

Figure 4.1.6.1. Safety Rod axial section

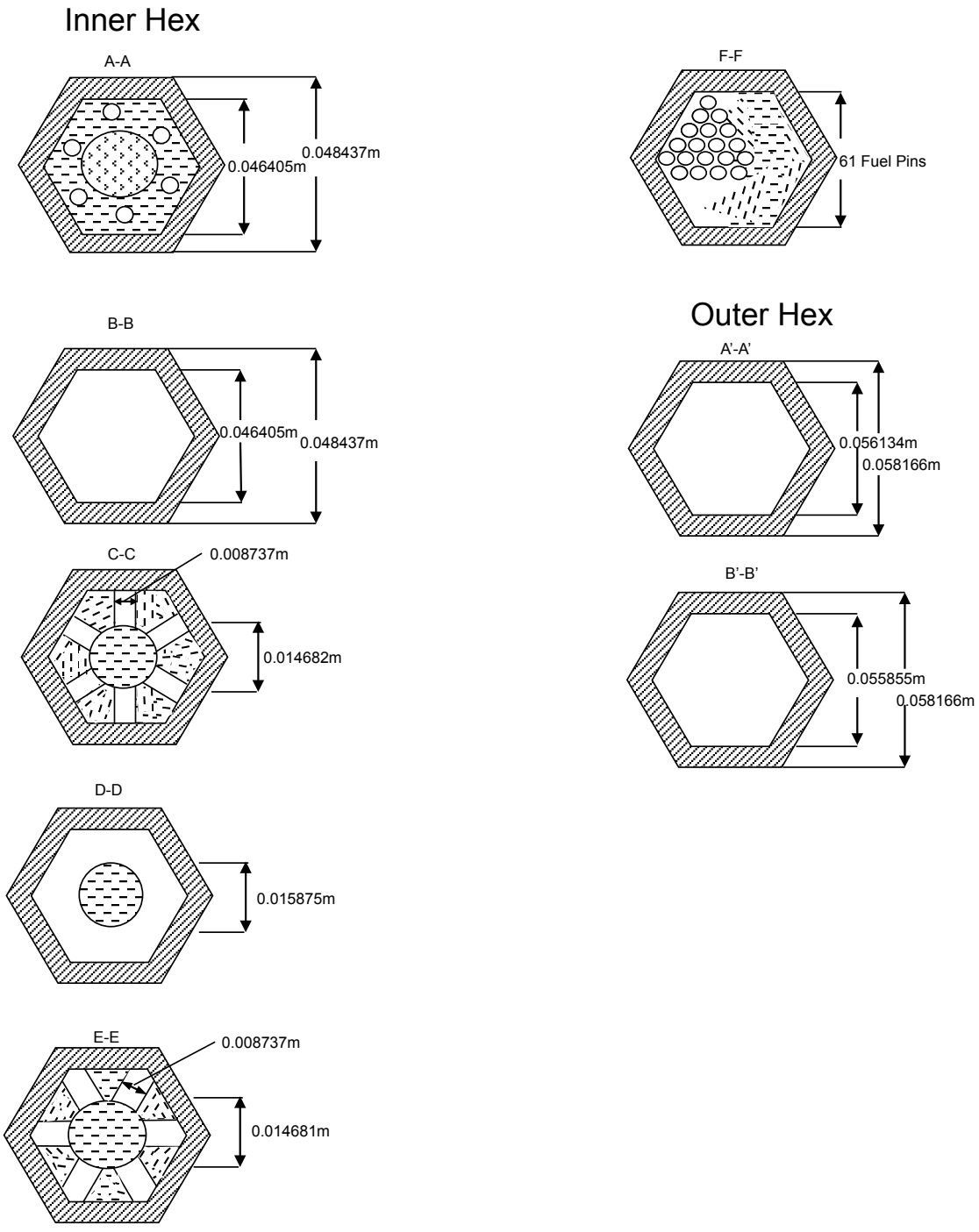

Figure 4.1.6.2. Safety Rod plane sections

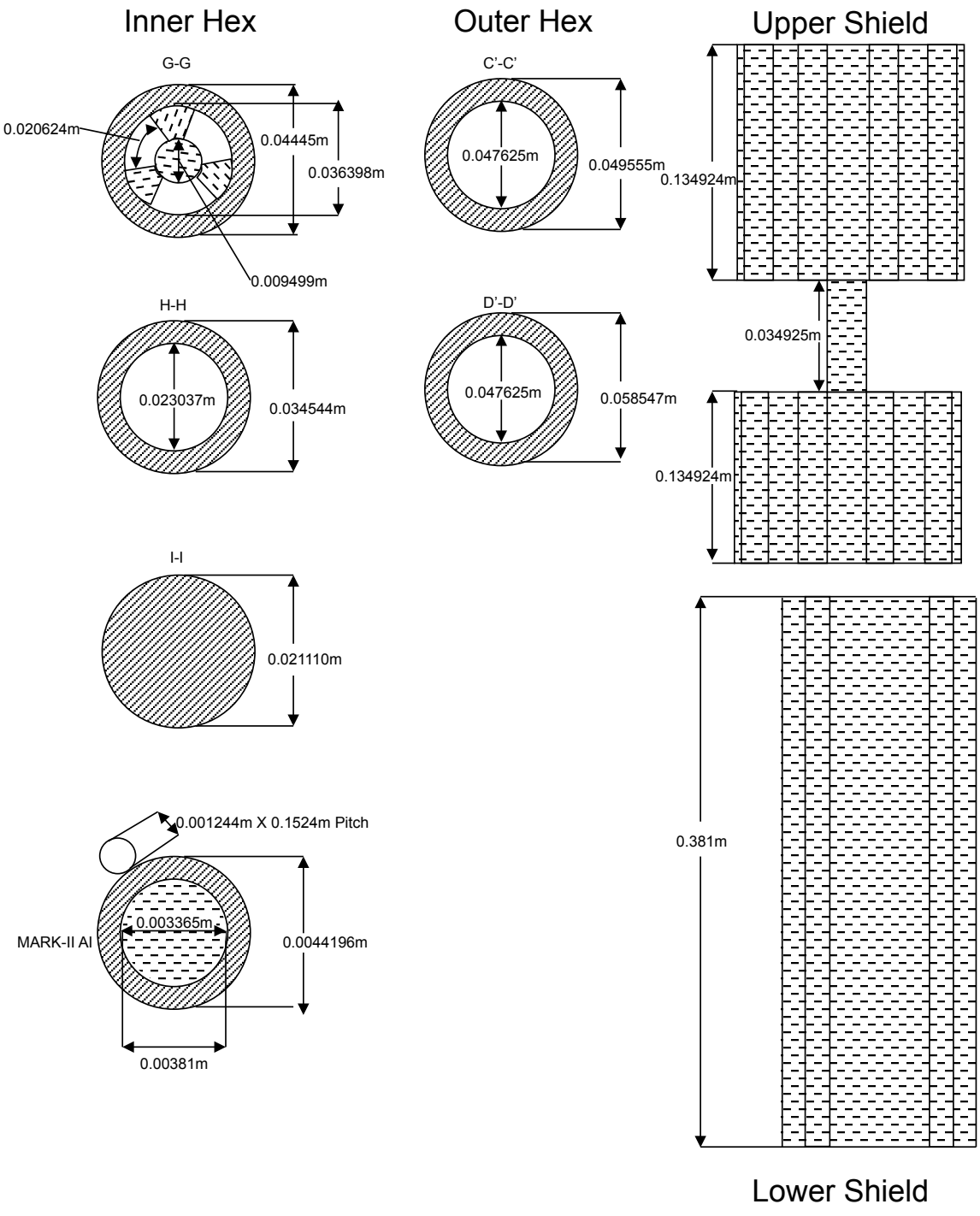

Figure 4.1.6.3. Safety Rod elevation and plane sections

4.1.7 *Instrumented Subassemblies*

Figures 4.1.7.1 and 4.1.7.2 show axial and plane cross-section views of the XX09 instrumented subassembly that was inserted in a core position normally reserved for control rods. XX09 was in the INSAT 2 position depicted in Figure 2.3. XX09 was a fueled subassembly specifically designed with a variety of instrumentation to provide data for benchmark validation purposes. The radial locations of the thermocouples within XX09 are illustrated in Figure 4.1.7.3. Figure 4.1.7.1 shows the upper adapter, center hexagonal tube region and lower adapter (nozzle) and (E) indicates that a dimension is an estimate taken in inches and converted to centimeters. The axial locations of several thermocouple locations are indicated in Figure 4.1.7.1 also.

XX09 was coupled to an extension tube that traversed all the way up to the outside of the primary tank, provided a protected conduit lead for the instrument leads and permitted movement of the subassembly during fuel handling. Details of this extension tube are not provided for the benchmark. Except for some minor modifications, the subassembly outer configuration is the same as a control rod in that XX09 sat within a guide thimble. The upper adapter with the fuel handling fixture is displayed at the top of Figure 4.1.7.1. The elevation view of Figure 4.1.7.1 does not show the detailed geometry of the fixture nor the flow mixer, which sat in the gap between the top fixture and the top of the fuel element bundle (Top of Pin).

The six upper adapter coolant holes and 28 smaller holes for passage and support of instrument leads are also not shown in Figures 4.1.7.1 and 4.1.7.2. The flow mixer provides neutronic shielding equivalent to at least 76.2 mm (3 inches) of stainless steel. The fixture and flow mixer are ignored in the benchmark calculation.

Section A-A at the outlet of the hex tube shows the flow area and the hex tube structure dimensions. Materials that were used are given in Table 4.1.2. Section B-B displays a cross-section through the 61-MARK-II AI element fuel bundle of the subassembly. Fifty-nine of the 61 fuel element positions contained MARK-II AI fuel; the other two positions were hollow tubes used as conduits to permit passage of instrument leads. Details are available in Table 4.1.1 for the bundle element. Details are also shown in Figure 4.1.7.2 for a cross-section through a bundle element. The two element positions reserved for flow meter conduits can be seen in Figure 4.1.7.3.

The MARK-II AI fuel elements had Type 316 stainless steel cladding. Each element contained one metallic uranium slug. The top of this fuel slug was the ‘Top of Core’ location in Figure 4.1.7.1. All of the elements were sodium bonded and contained a tag gas. Wire-wrap was used in this bundle design but twenty-two of the fuel elements were modified by replacing the standard spacer wires with spacer wire thermocouples. These elements were modified by machining the top “crown” weld to accept a sleeve and an extension rod. The rod provided a support surface for brazing the spacer wire coolant thermocouple to the fuel element at a position other than on the element jacket. This was the ‘top instrument adapter’ in the footnote of Tables 4.1.1 and 4.1.2.

The Bottom of Core, which was the bottom of the fuel slug, is taken to be the bottom of the element without regard to the element end cap. The element bottom locator tip, which was part of the end cap, is also shown in Figure 4.1.7.1. The locator tip helped to position the fuel

element on the bottom grid bars. The grid bars, which were welded to the hexagonal liner, were spaced to permit the sodium coolant to flow through the element bundle.

Details are not shown for the locator tips and the bottom grid plate attached to the lower hexagonal liner. This lower hexagonal liner of the center hexagonal tube region starts at section C-C. It formed the subassembly lower axial shield. Two flow meters, one above the other, and a flow diffuser were welded inside this hexagonal liner below the element support grid. This can be seen in the elevation view provided in Figure 4.1.7.1. Section D-D is located just below the lower of the two flow meters. Below section D-D was the top of the lower adapter. The location of the XX09 hex tube is indicated in Figure 4.1.7.1. The hex tube extends from the section C-C to section A-A in Figure 4.1.7.1.

The outer configuration of the lower adapter of this subassembly type and the lower adapter of the control subassembly type were similar (see Figure 4.1.5.1). XX09 sat in the core position normally reserved for control rods. Plane sections E-E to F-F were sections in this lower adapter design. Figure 4.1.7.2 shows the details of the geometry of the lower adapter required for the XX09 subassembly. Section E-E is a plane section through an upper portion of the lower adapter towards the top of the reactor upper grid plate.

The coolant inlet consisted of flow holes drilled into the side of the lower adapter around the nozzle section F-F. Coolant feed from the high-pressure inlet plenum was directed by the guide thimble into this subassembly through these flow holes. Hole dimensions are not provided as pressure drop and subassembly flow information are provided in Sections 3.1.3 and 3.2.3 at steady-state conditions. Details of the solid end of the adaptor beyond section F-F are not given, since these only pertain to the subassembly hold-down on the orientation bars located at the bottom of the lower grid plate.

Also shown on the left side of Figure 4.1.7.1 is the elevation view of the guide thimble in which the XX09 subassembly sat. The guide thimble guided the coolant flow into those flow holes. It was hexagonal and had the same dimensions in the top part of the thimble as the hexagonal tube of the other subassemblies, as shown in A-A cross section in Figure 4.1.7.2.

In the lower part of the guide thimble, as with the other subassemblies types, there was a lower guide thimble adapter that locked the thimble in the lower reactor grid plate through a latch. Details of this are not shown below the lower reactor grid plate. The coolant flow slots in the guide thimble lower adapter were above the lower XX09 adapter bushing, which is described below. These flow slots are not shown in Figure 4.1.7.2 but they were located above section C-C in the high-pressure inlet plenum. Although the lower end of the guide thimble was open, sodium flow was restricted by this lower bushing, which therefore limits the sodium leakage from the high-pressure plenum to the low-pressure plenum through the bottom of the thimble.

The bushings were steel rings fitted over the lower adapter to provide bearing type surfaces between the XX09 lower adapter and the lower bore of the guide tube. There was a second set of upper bushings located higher up on the XX09 subassembly above all the flow holes, guide thimble and rod lower adapter that limited the sodium thimble flow leakage in the other direction towards the reactor outlet plenum. In the case of XX09 sodium flow was required to cool the MARK-II AI fuel elements of the bundle, so the guide thimble flow holes and the XX09 lower adapter flow holes were positioned closely facing each other.

XX09

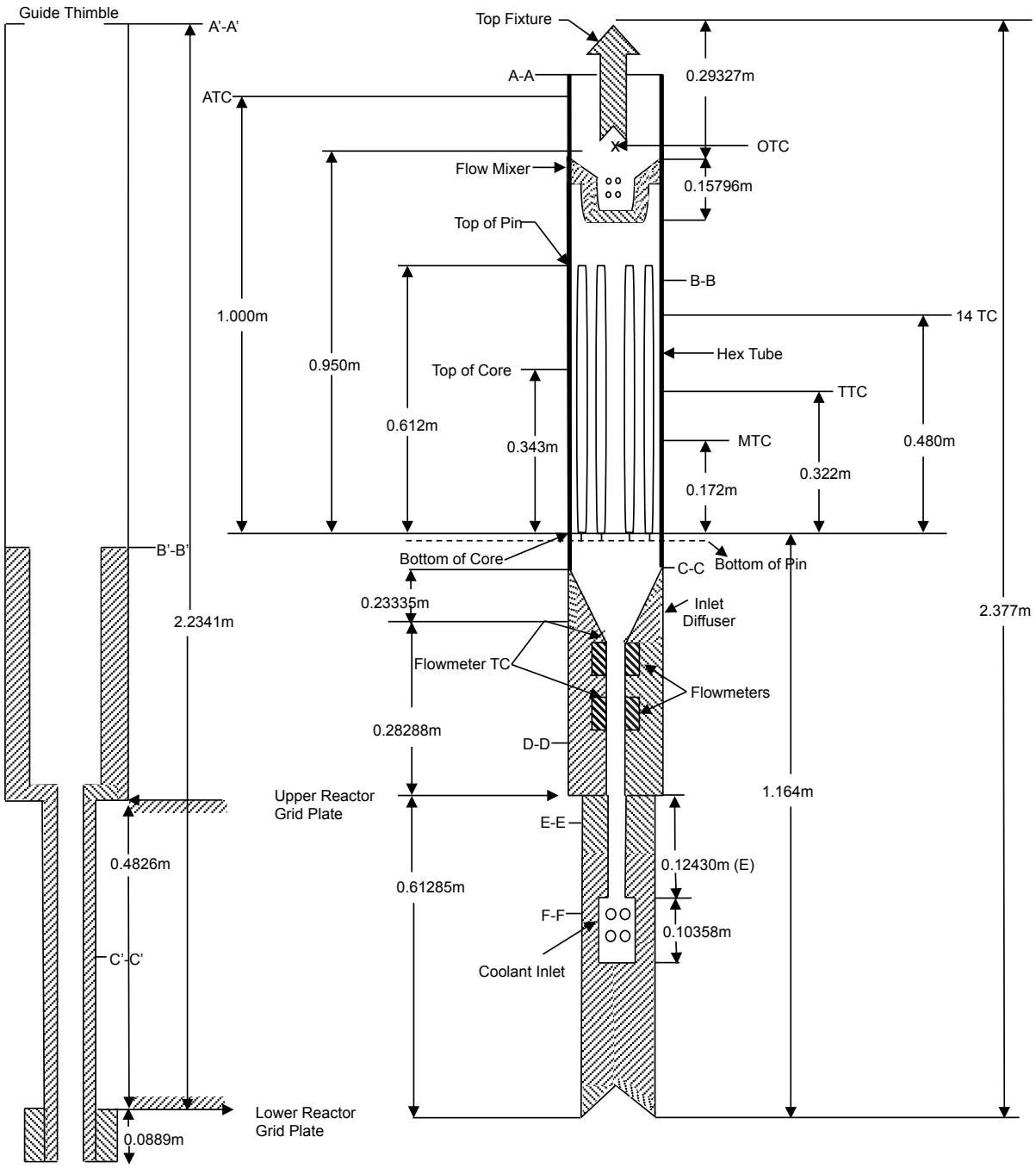

Figure 4.1.7.1. XX09 Instrumented subassembly axial section

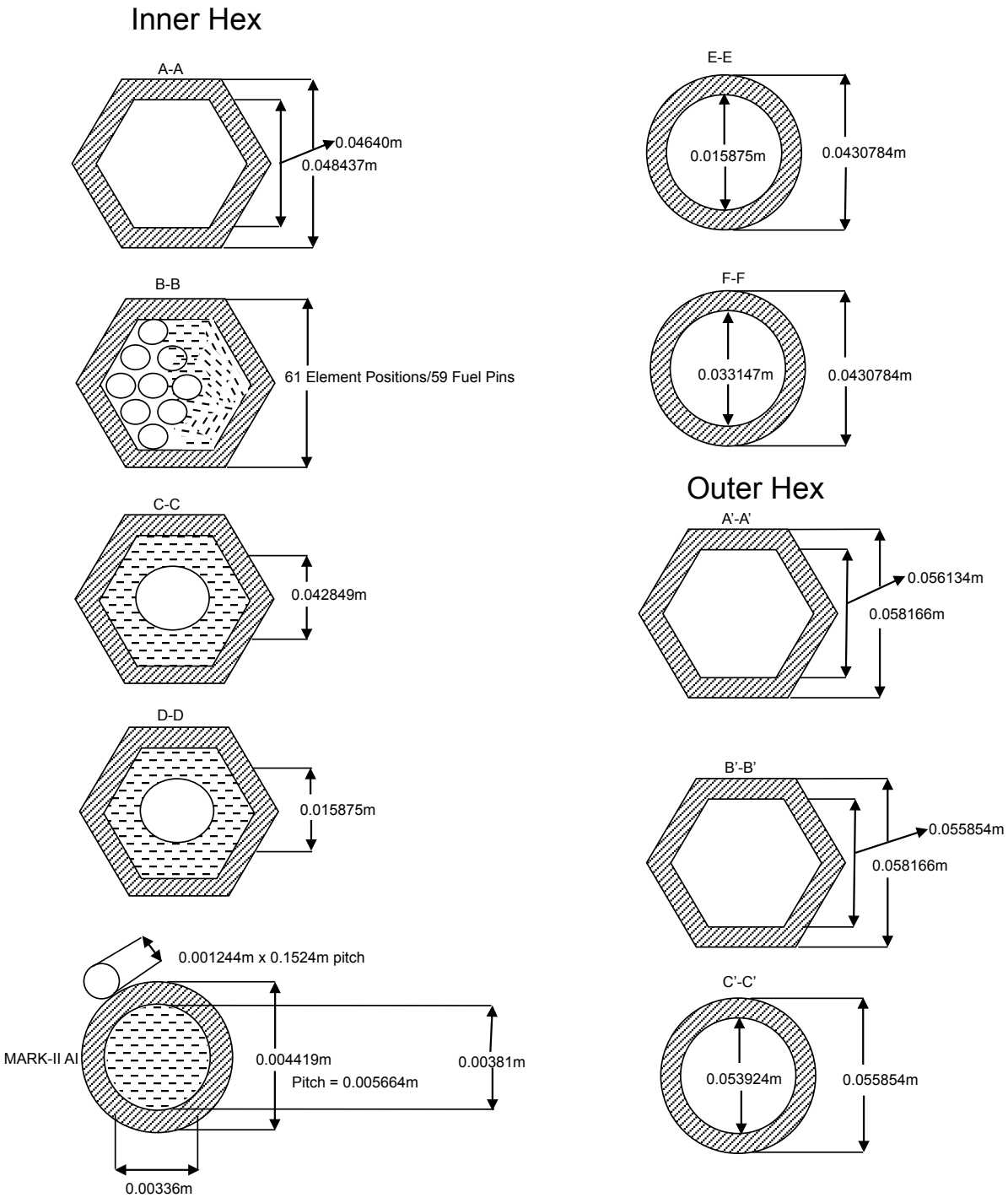

Figure 4.1.7.2. XX09 Instrumented subassembly plane sections

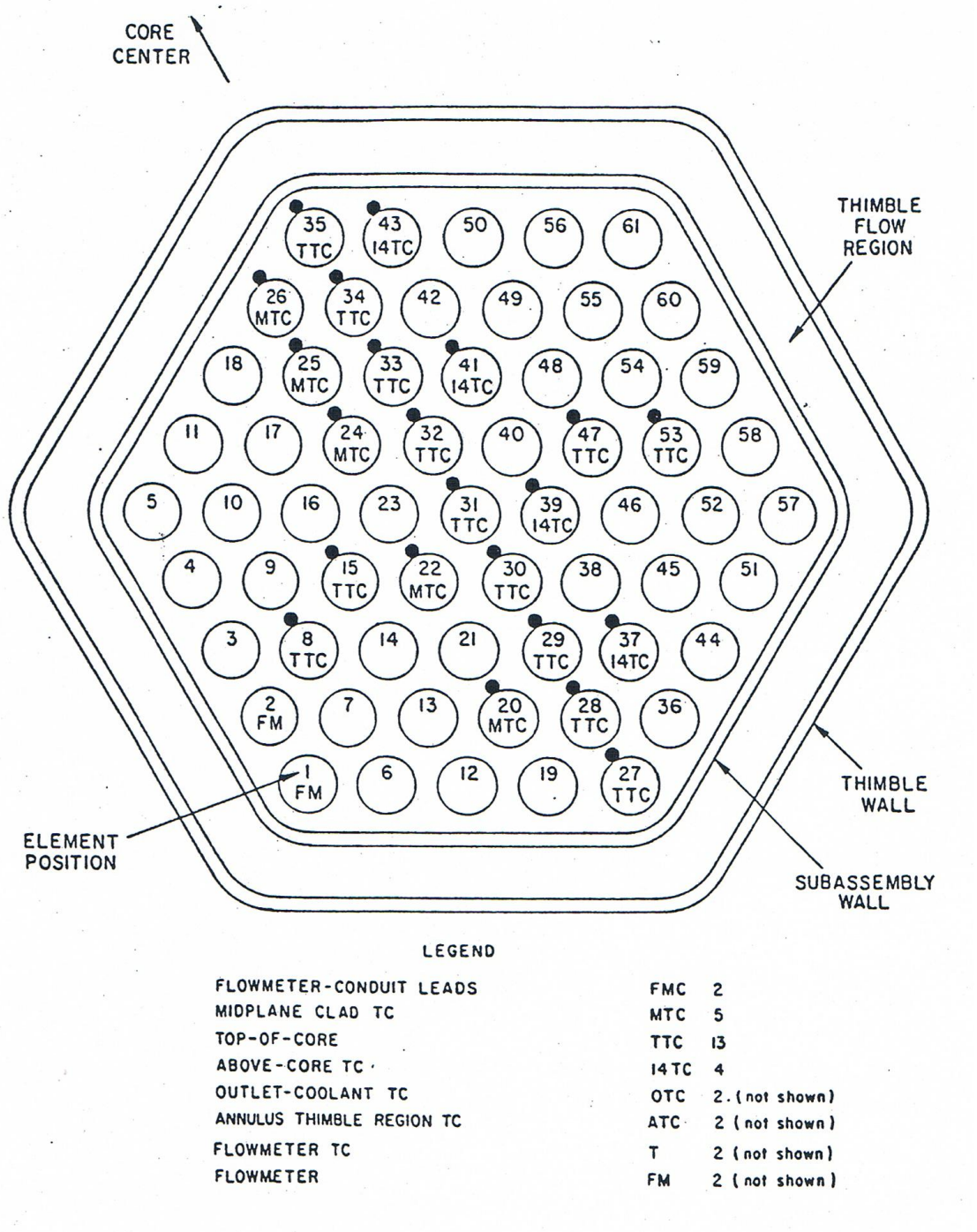

Figure 4.1.7.3. XX09 Instrumented subassembly instrument loading

Figures 4.1.7.4 and 4.1.7.5 show axial and plane cross-section views of the XX10 instrumented subassembly that was inserted in a core position normally reserved for control rods. This position is the INSAT 11 position depicted in Figure 2.3. XX10 was a non-fueled subassembly specifically designed with a variety of instrumentation to provide data for benchmark validation goals. The radial locations of thermocouples with XX10 are illustrated in Figure 4.1.7.6. Figure 4.1.7.4 shows the upper adapter, center hexagonal tube region and lower adapter (nozzle) and (E) indicates a dimension is an estimate taken in inches and converted to centimeters. The axial locations of several thermocouple locations are indicated in Figure 4.1.7.4 also. The subassembly was coupled to an extension tube that traversed all the way up to the outside of the primary tank, provided a protected conduit lead for the instrument leads and permitted movement of the subassembly during fuel handling. Details of this extension tube are not provided for the benchmark.

Except for some minor modifications, the subassembly outer configuration was the same as a control rod, and it sat within a guide thimble. The upper adapter with the fuel handling fixture is displayed at the top of Figure 4.1.7.4. The location of the XX10 hex tube is indicated in Figure 4.1.7.4. The hex tube extends from the section C-C to section A-A in Figure 4.1.7.4. Portions of the upper and lower shield sections are assumed to extend outward to be flush with the inner surface of the subassembly hex tube. with the top of the top fixture, which protruded above the hexagonal tube, and working downward, the elevation view of Figure 4.1.7.4 does not show the detailed geometry of the fixture nor the flow mixer that sat in the gap between the top fixture and the top of the fuel element bundle (Top of Pin). The six upper adapter coolant holes and the 28 smaller holes for passage and support of instrument leads are also not shown in Figure 4.1.7.4. The flow mixer provided neutronic shielding equivalent to at least 76.2 mm (3 inches) of stainless steel. The fixture and flow mixer are ignored in the benchmark calculation.

Section A-A at the outlet of the hex tube shows the flow area and the hex tube structure dimensions. Materials that were used are given in Table 4.1.2. Section B-B displays a cross-section through the 19-element non-fueled blanket type subassembly. Eighteen of the 19 element positions contained solid stainless steel rods; the remaining position was a hollow tube used as a conduit to permit passage of instrument leads. The location of the element position reserved for the flow meter conduit can be seen in Figure 4.1.7.6. Further details are available in Table 4.1.1 for the bundle element. Details are also shown in Figure 4.1.7.5 for a cross-section through a bundle element.

The top of the solid stainless steel rods is the ‘Top of Pin’ location in Figure 4.1.7.4. Wire-wrap was used in this bundle design, but the standard spacer wires were replaced with spacer wire thermocouples. These elements were modified by machining the top to accept a sleeve and an extension rod. The rod provided a support surface for brazing the spacer wire coolant thermocouple to the element at a position other than on the element jacket. This extension rod was the ‘top instrument adapter’ in the footnote of Tables 4.1.1 and 4.1.2. The element bottom locator tip is shown as the Bottom of Pin. The locator tip helped to position the element on the bottom grid bars.

The grid bars, which were welded to the hexagonal liner, were spaced to permit the sodium coolant to flow through the element bundle. The welding of the grid bars and the hexagonal liner formed the element–support-grid assembly. Portions of some grid bars were

cut out to allow the passage of flow meter leads. Details are not shown regarding the locator tips and the bottom grid plate attached to the lower hexagonal liner for this benchmark. This lower hexagonal liner of the center hexagonal tube region began at section C-C. It formed the subassembly lower axial shield.

Two flow meters, one above the other, and a flow diffuser were welded inside this hexagonal liner below the element support grid. This can be seen in the elevation view provided in Figure 4.1.7.4. Section D-D is located just below the lower of the two flow meters. Lower down from section D-D was the top of the lower adapter.

It can be seen that the outer configuration of the lower adapter of this subassembly type and the lower adapter of the control subassembly type were similar (see Figure 4.1.5.1). XX10 sat in a core position normally reserved for control rods. Plane sections E-E to F-F are sections in this lower adapter design. Figure 4.1.7.5 shows the details of the geometry of the lower adapter required for the XX10 subassembly. Section E-E is a plane section through an upper section of the lower adapter towards the top of the reactor upper grid plate. The coolant inlet consisted of the flow holes drilled into the side of the lower adapter around the nozzle section F-F. Coolant feed from the high-pressure inlet plenum was directed by the guide thimble into this instrumented non-fueled subassembly through this flow hole. Hole dimensions are not provided as assembly flows and pressure drops are provided in Sections 3.1.3 and 3.2.3 at steady-state conditions. Details of the solid end of the adaptor beyond section F-F are not given, as these only pertain to the subassembly hold-down on the orientation bars located at the bottom of the lower grid plate.

Also shown on the left-hand side of Figure 4.1.7.4 is the elevation view of the guide thimble in which the XX10 subassembly sat. This guide thimble guided the coolant flow into the flow holes, was hexagonal and had the same dimensions in the top part of the thimble as the hexagonal tube of the other subassemblies. This is illustrated by the A-A section in Figure 4.1.7.5.

In the lower part of the guide thimble, as with the other subassemblies, there was a lower guide thimble adapter that locked the thimble in the lower reactor grid plate through a latch. Details of this are not shown below the lower reactor grid plate. The coolant flow slots in the guide thimble lower adapter were above the lower XX10 adapter bushing. These flow slots are not shown in Figure 4.1.7.5 but they were located above section C-C in the high-pressure inlet plenum. Section B-B was higher up through the rounded shoulder portion of the guide thimble lower adapter. Although the lower end of the guide thimble was open, sodium flow was restricted by this lower bushing, which therefore limited the sodium leakage from the high-pressure plenum to the low-pressure plenum through the bottom of the thimble.

The bushings were steel rings fitted over the lower adapter to provide bearing type surfaces between the XX10 lower adapter and the lower bore of the guide tube. There was a second set of upper bushings located higher up on the XX10 subassembly above all the flow holes, guide thimble and rod lower adapter that limited the sodium thimble flow leakage in the other direction towards the reactor outlet plenum.

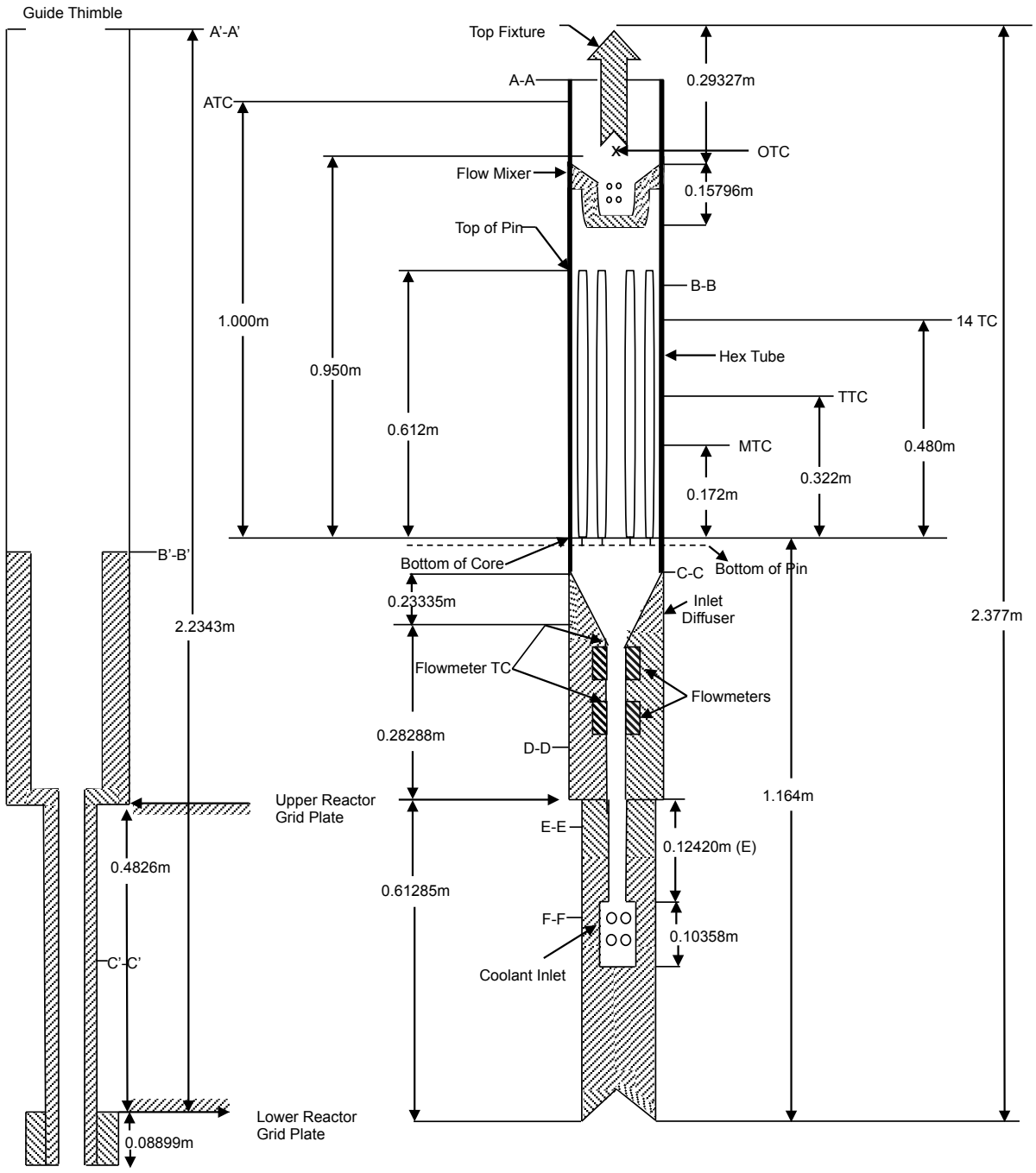

Figure 4.1.7.4. XX10 Instrumented subassembly axial section

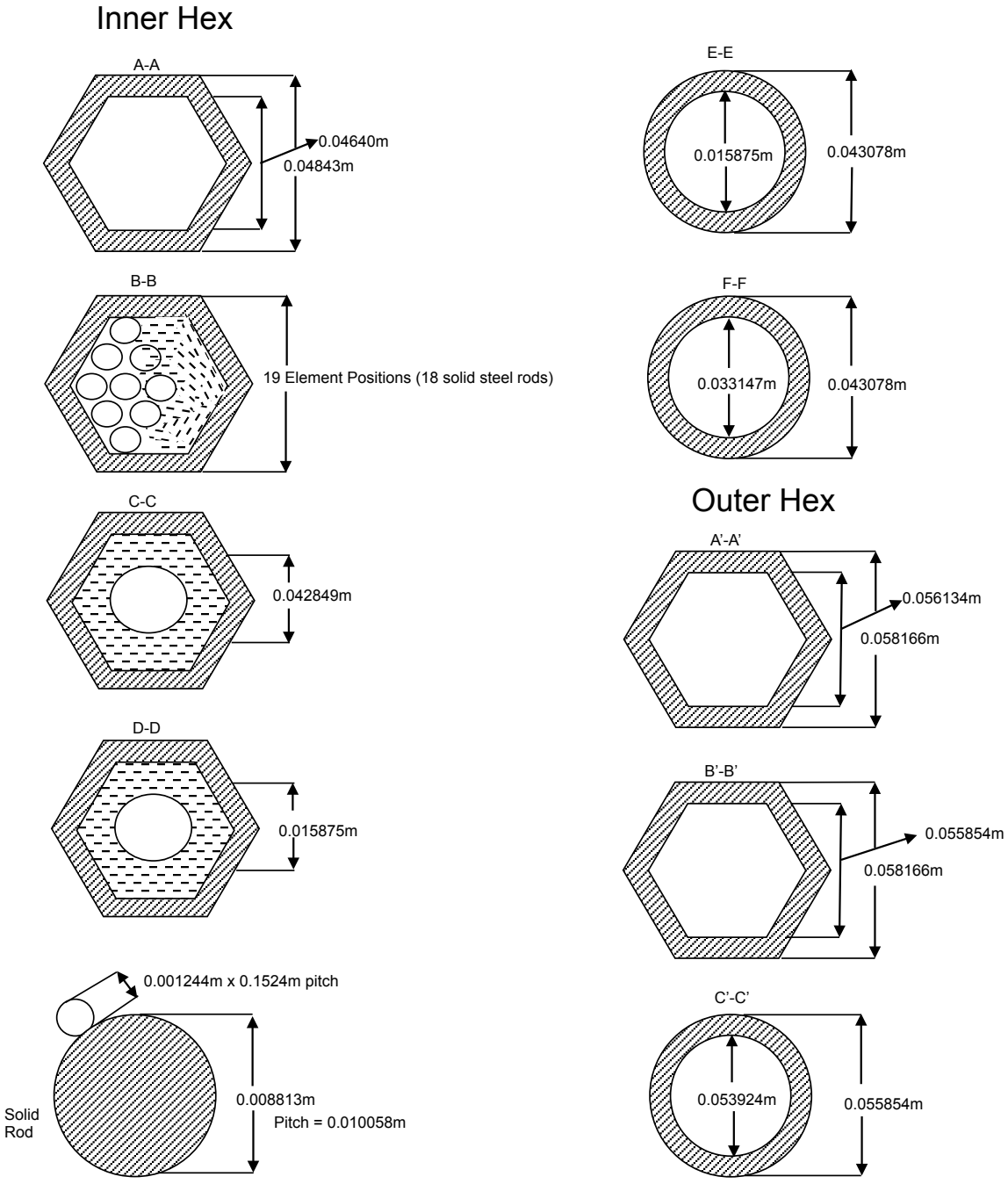

Figure 4.1.7.5. XX10 Instrumented subassembly plane sections

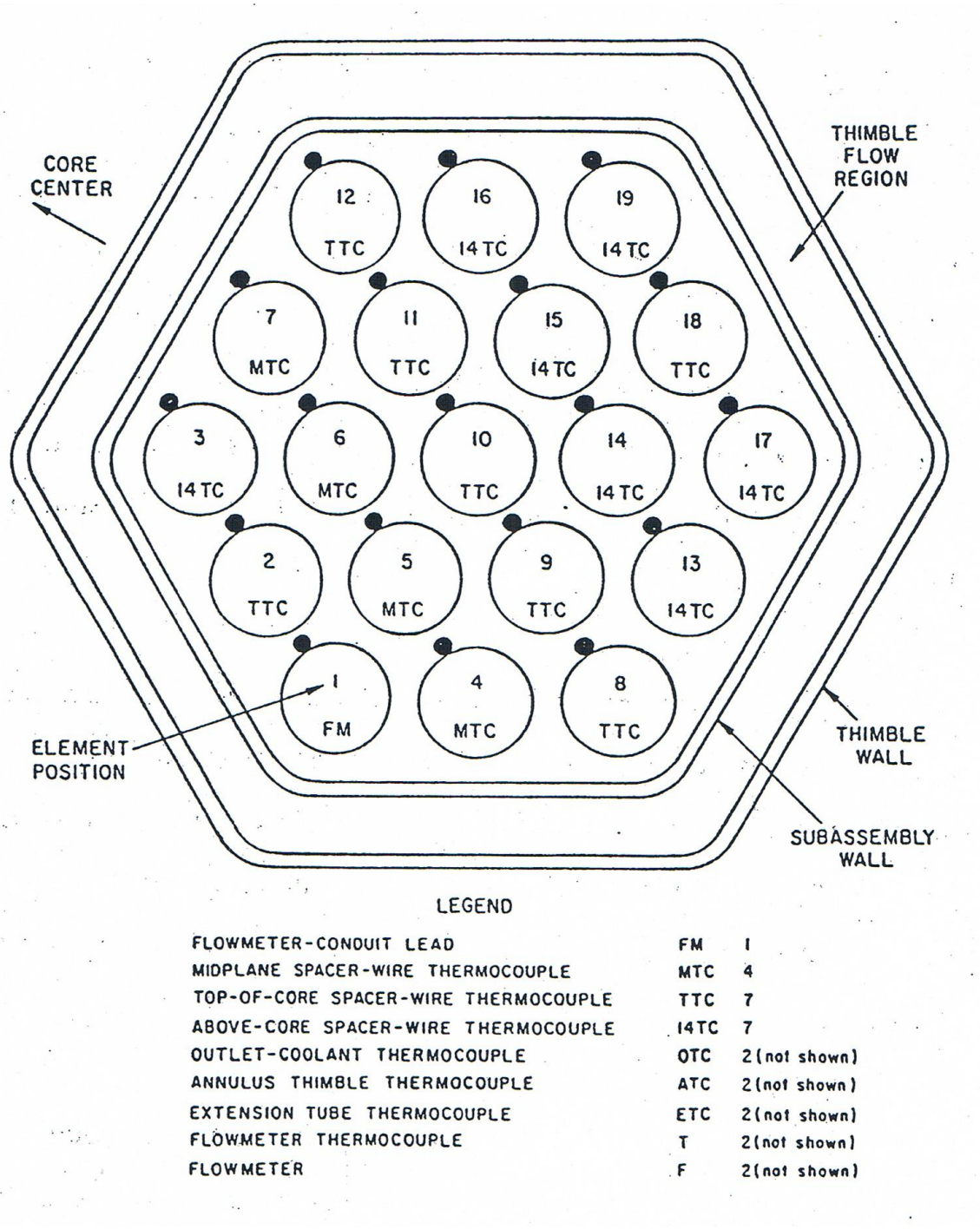

Figure 4.1.7.6. XX10 Instrumented subassembly instrument loading

4.1.8 *SHRT-17 Experimental Subassemblies*

The class of experimental subassemblies for EBR-II was intended to provide a means to insert material and fuel samples in the reactor to expose them to a fast flux radiation environment. Numerous types of subassemblies were designed to accommodate various fuels and fuel elements as well as samples of structural material. Subassemblies were designed for core and blanket insertion to vary flux intensity positions and to provide selectable temperatures and coolant flows. There were many designs for single encapsulation, double encapsulation or even triple encapsulation.

The experimental subassemblies that were loaded into the core for Run 129-C during which the SHRT-17 test was conducted are listed in Table 4.1. Since subassembly XY-16 is one of the four test facilities in row 5 that occupy core positions originally designed for control rod subassemblies, it will be included in this discussion. Experimental subassembly X319 appears to have been related to experimental subassembly X320 as it also used the MARK-M1A subassembly and was a Westinghouse structure irradiation experiment. X320 had a large specimen cage for what appears to have been a Westinghouse design steel fixture with no coolant flow. Similarly, while no information was found about X319, it could be postulated that it was similar to X320. In contrast, information found about X328 shows that it was a MARK-B7A absorber subassembly with seven pins of boron carbide.

X390 was a 91-element MARK-II AI alternate fuel test varying the Fissium composition while X393 was a 91-element MARK-II S fuel test. Experimental subassemblies X399-X402 were 91-element MARK-II A fuel qualification runs. In each of these subassemblies there was one steel element position. X406-X408 were 91-element MARK-II A alternate fuel tests. These subassemblies also had one steel element position. Subassembly X409 was a 91-pin MARK-II A alternate fuel test with no steel positions.

The XY-16 subassembly had 61 solid Type 304 stainless steel wire-wrapped steel MARK-II AI elements. In line with using a control rod position, the steel element bundle was located in the inner hexagon tube within the guide thimble. While not listed in Table 4.1, Figure 4.1 for the core loading (Rows 1-8) shows a subassembly BES (referred to as 1999 in Figure 4.2). This may be a neutron source subassembly that is of yet another subassembly design type. For this benchmark, the BES subassembly is ignored. No information was found on subassembly BETH (referred to as 1929 in Figure 4.2).

4.1.9 *SHRT-45R Experimental Subassemblies*

Experimental subassemblies in EBR-II were intended to provide a means to insert material and fuel samples in the reactor to expose them to a fast flux radiation environment. Numerous types of subassemblies were designed to accommodate various fuels and fuel elements, plus samples of structural materials. Subassemblies were designed for core and blanket insertion to vary flux intensity positions and to provide selectable temperatures and coolant flows. There were many designs for single encapsulation, double encapsulation or even triple encapsulation. The irradiation samples were thus confined in capsules that provided containment function.

In the case of Run 138-B, the experimental subassemblies that were loaded into the core consisted of X320, X402A, X412 and C2776A (XETAGS). As subassembly XY-16 (identified as INCOT6 in Figure 2.3) was one of the four test facilities in Row 5 that occupied

core positions originally designed for control rod subassemblies, it will also be treated as an experimental subassembly.

Experimental subassembly X320 (referred to as X320C in Figure 4.5) was a large specimen structural irradiation subassembly that used the MARK-M1A subassembly. The MARK-M1A subassembly was one of a number of special irradiation-vehicle subassemblies specifically designed to hold irradiation samples. It had a specimen cage for what appears to have been a Westinghouse design steel fixture with no coolant flow. X402A and X412 were both 91-pin MARK-II A fuel element bundle qualification tests. C2776A (XETAGS) was a MARK-II AI subassembly with Xenon tag gas.

The XY-16 subassembly had 61 solid Type 304 stainless steel wire-wrapped steel MARK-II AI elements. In line with using a control rod position, the steel element was located in the inner hexagon tube within the guide thimble. Figure 4.5 shows a subassembly labeled S1951. This was a neutron source subassembly that was of yet another subassembly design type. For this benchmark, S1951 is disregarded as a separate type of subassembly and instead treated as a reflector subassembly.

4.2 Core Data

In addition to the subassembly geometries and the core loading of the different types of subassemblies that have been given in earlier sections, data is provided below regarding (a) the thermal and thermodynamic properties of the fissium fuel slugs unique to EBR-II and (b) various mechanical features of the EBR-II primary tank and reactor structures that could be a factor in the reactivity feedback response of the core during the SHRT-45R test.

4.2.1 *Fuel Properties*

For this benchmark specification, the linear thermal expansion of the U-5 wt % Fs fuel pins pre-irradiated in EBR-II is given as:

$$\frac{\Delta L(T)}{L_2} = \begin{cases} 1.62 \times 10^{-5} (T - 273), & T < 823^{o}K \\ 0.0089 + 5.7 \times 10^{-5} (T - 823) < T < 913^{o}K \\ 0.014 + 2.1 \times 10^{-5} (T - 913), & T > 913^{o}K \end{cases} \quad (4.1)$$

where

$\frac{\Delta L(T)}{L_2}$ = linear thermal expansion from a fixed temperature 273°K to any temperature T, expressed as a fraction of length L_2 at the temperature 273°K.

This correlation is independent of the fission content of the alloy. It was implemented in and tested with the SAS4A code for analysis of EBR-II transient tests.

The reference density which will be used for the U-Fs fuel is 18.2 x 10^3 kg/m^3 at 300°K.

The heat capacity for U-5Fs fuel based on Argonne fuel properties work is

$$c(T) = a + bT + cT^2 \text{ kJ/kg} - {}^{o}\text{K} \begin{cases} 273^{o}\text{K} < T < 833^{o}\text{K} \\ \quad a = 0.13964 \\ \quad b = -1.9785 \times 10^{-5} \\ \quad c = 3.1566 \times 10^{-7} \\ 833^{o}\text{K} < T < 913^{o}\text{K} \\ \quad a = 0.46364 \\ \quad b = -2.615 \times 10^{-4} \\ \quad c = 0.0 \\ 913^{o}\text{K} < T < 1283^{o}\text{K (soldius)} \\ \quad a = 2.40126 \\ \quad b = -3.5126 \times 10^{-3} \\ \quad c = 1.4012 \times 10^{-6} \end{cases} \tag{4.2}$$

At both 833 and 913K there is a solid-to-solid phase transition. The associated enthalpy changes at these temperatures are:

$$T = 833\text{K}, \ \Delta h = 11.715 \ \text{kJ/kg} \tag{4.3}$$

$$T = 913\text{K}, \ \Delta h = 8.368 \ \text{kJ/kg} \tag{4.4}$$

It should be noted that these are very slow phase changes.

The following correlation, which is independent of the fissium content of the alloy, is given for the thermal conductivity of U-5 wt % Fs fuel pins pre-irradiated in EBR-II.

$$k_s(T_c, U-Fs) = \begin{cases} 14.1 + 2.98 \times 10^{-2} T_c + 3.01 \times 10^{-6} T_c^2, & T_c < T_s \\ 56.0, & T_c > T_s \end{cases} \tag{4.5}$$

where

$k_s(T_c, \text{U-5Fs})$ = thermal conductivity at temperature T_c °C of the solid (i.e., nonporous) U-5Fs alloy independent of the Fs content, W/m °C, and

T_s = solidus temperature of the U-5Fs alloy.

The correlations for the thermal conductivity of the fully dense and U-Fs alloy fuels are described in Eq. 4.5. However, the fuel develops fission gas-filled porosities during the steady-state operation of the reactor. The bond sodium used in the fuel-cladding gap of U-Fs

alloy fuel pins can also penetrate the fuel and fill some of the porosities of the fuel during this period. The gas-filled porosities tend to decrease the fuel thermal conductivity whereas the sodium-filled porosities tend to increase it. These effects are considerable in the calculation of fuel temperature distribution. A formula is given below for the evaluation of these two effects using a generalization of the method given in reference for a single type of porosity.

The effective thermal conductivity k of the porous fuel can then be written in terms of the gas-filled volume porosity p_g and the sodium-filled volume porosity p_{Na}

$$\frac{k}{k_s} = 1 - p_g^{2/3} + \frac{p_{Na}^{2/3}}{\left(\frac{k_s}{k_{Na}}\right) p_{Na}^{1/3} + \left(1 - p_{Na}^{1/3}\right)} - p_{Na}^{2/3} \tag{4.6}$$

Equation 4.6 gives the effect of sodium- and gas-filled porosities on fully dense fuel thermal conductivity. It is noted that Equation 4.6 satisfies two limiting conditions: (1) in the absence of any logged sodium in the fuel, the ratio k/k_s equals the known reduction factor of $1 - p_g^{2/3}$ and (2) if k_{Na} is set equal to k_s in Equation 4.6, the last two terms on the right-hand side cancel to make k/k_s again equal to $1 - p_g^{2/3}$ which is expected when the sodium and the fully dense fuel behave alike and the gas-filled porosity is the only nonconductive porosity in the material.

4.2.2 *Core Structural Reactivity Feedbacks*

It is the Argonne experience that core restraint design, core support design and control rod driveline design play a significant role in the reactivity feedback response during unprotected transients. The class of Anticipated Transients without Scram (ATWS) and other similar types of beyond design basis accidents (BDBA) have consequences that are significantly mitigated when inherent reactivity feedback features are part of the design process and are factored into the fission power response. As the system heats up, with the imbalances between fission power production and heat removal induced by the accident initiators, component dimensions and shapes change with thermal expansion. Core fuel slugs start to axially expand. Core fuel and blanket subassemblies start to bow and flower. These dimensional changes all lead to changes in the reactivity balance.

The design of the core restraint system constrains these subassembly dimensional changes and therefore the magnitude of the reactivity feedback induced by these structural reactivity feedback mechanisms. The load pads and dimples of the subassembly hexagonal tube walls, core restraining ring and vessel inner shell are all part of the design of the core restraint system.

Similarly, the core grid plate, which supports the core subassemblies, expands with the thermal heat up. This leads to a radial expansion of the core size that in turns affects the reactivity balance. The movement of the core grid structures can be complicated by whether the core is bottom-supported or top-supported. If the core is supported off the bottom of the primary tank and the primary tank walls elongate downward, there is the possibility that the core fuel assemblies drop away from the control and safety rods and therefore away from the reactivity poisons. This will be affected by the core support design features. Because the control rod drives and drivelines enter from the top of the primary tank, the heat up could

indeed lead to a positive reactivity insertion feedback effect as the core drops away from the control poisons.

There is, however, a counter-balancing effect involving the control rod drivelines. With the heat up the control rod drivelines thermally expand and elongate. The elongation is downward if the control rod insertion is from the top. This would lead to a compensating negative reactivity feedback as the control rod elongation downward would tend to insert additional control poisons into the core. The mechanical design of the control rod driveline would therefore also need to be considered.

The safety rod drive mechanism is more complicated than the control rod drive mechanism. As with the control rod drivelines, the safety rod drivelines enter from the top of the primary tank. However, the safety rods are inserted from the bottom of the core. They are driven in by the safety rod connectors, which sit on top of the safety rod drive beam. The safety rod drive beam is positioned below the reactor vessel and is moved up or down by the movement of the safety rod drivelines from the top of the tank. Details of the EBR-II structural systems that could affect the EBR-II structural reactivity feedbacks during SHRT-45R are presented in Figure 4.2.2.1. Additional information regarding the structural description of the primary tank is given in Section 5.2.1.

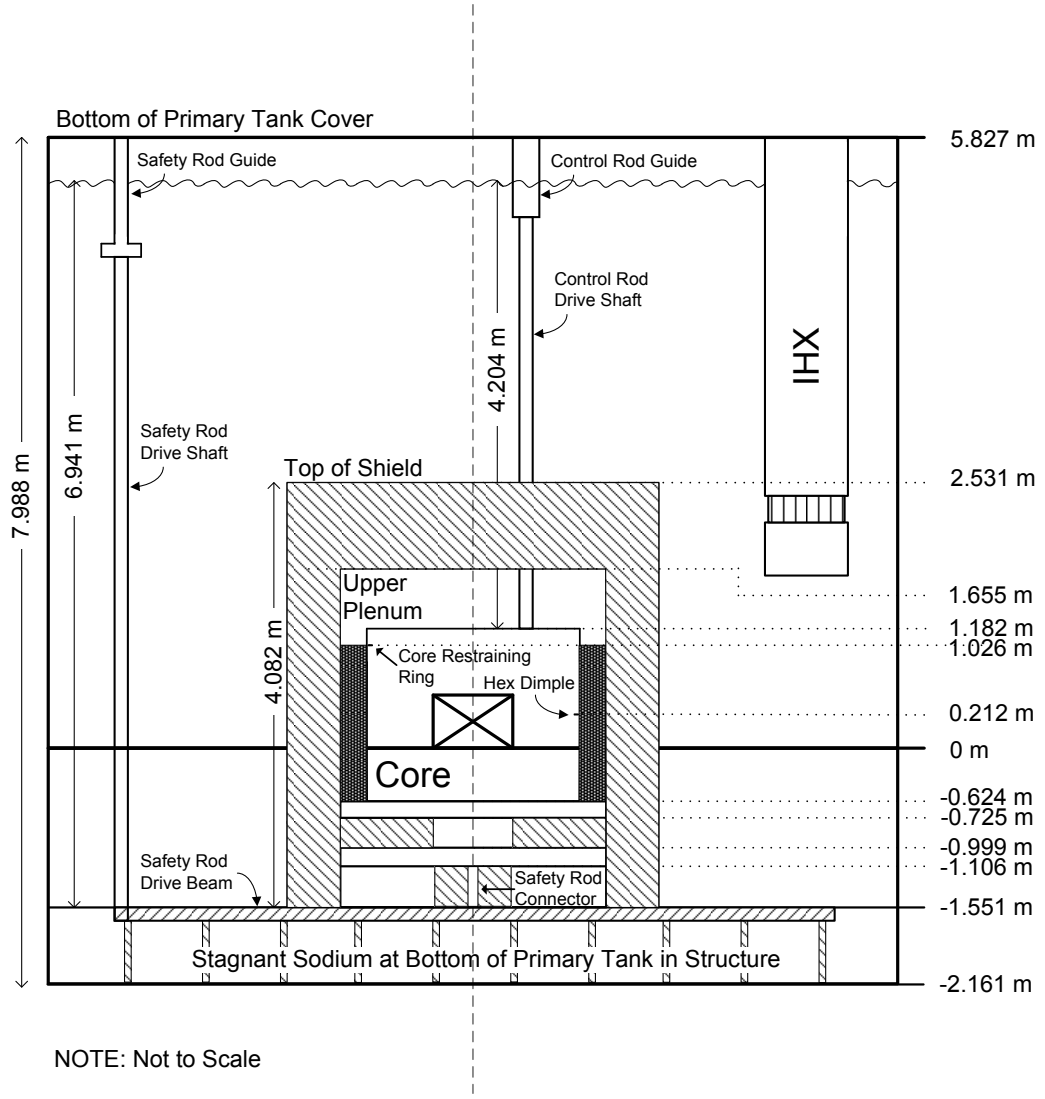

Figure 4.2.2.1. Reactor Structural Features Impacting Core Reactivity Feedback

An additional part of the restraint system was that each tube of every subassembly had a spacer dimple on each of the six faces of the hex tube. This was a spacer button formed by dimpling the tube wall outward. The spacer buttons, 0.9525 cm (3/8 in.) in diameter and 0.03556 cm (0.014 in.) high, were located at the vertical mid-plane of the hex tube along the centerline of each hex face. They served to prevent the subassemblies from touching if bowing were to occur. The subassembly configurations are discussed in Section 4.1.

As discussed in Section 4.1, the lower adapter of each subassembly positioned that subassembly in the grid plenum assembly and was part of the restraint on core motion system. The reactor vessel grid plenum assembly consisted of the upper and lower grid plates and of pressure chambers, in between the two grid plates, with Type 304 stainless steel walls and partitioned by baffle plates. Details of the core grid plate and the grid plenum assembly can be found in Section 5.2.3.

The reactor vessel was mounted on the bottom structure of the tank with the low-pressure plenum bottom plate and grid plenum outer wall supported on the vessel leveling plate as illustrated in Figure 4.2.2.1. The core and the reactor vessel are bottom supported, while the primary tank and the control rod drive mechanism are top supported.

The control rod drives were mounted on top of the primary tank. The main shaft, which was approximately 79.48 cm (26 ft) long, extended from the top adapters of the control rods in the reactor vessel, upward through the reactor vessel cover and then through the primary tank cover. The lower drive shaft had an outer diameter of 6.111 cm. The sodium-washed length of the main shaft is shown in Figure 4.2.2.1 as 4.204 m. While the sodium free surface level could be inferred from this figure, this should not be done. Instead, data given in Chapter 5 on the volume of each major primary system component and of sodium should be used to calculate the sodium free surface level.

The position of the safety rods was controlled by parallel-connected safety rod drive shafts, which were attached to a safety rod beam. This beam was located below the reactor vessel grid plenum assembly. Figure 4.2.2.1 shows the relative location of the safety rod drive mechanism in the primary system. The safety rod drive beam was positioned under the reactor vessel and reactor vessel leveling plate. Two safety rod connectors were mounted to the drive beam and extended through the bottom of the reactor and through the safety rod guide tube adapters, which were secured to the lower grid plate of the reactor. The upper portion of the safety rod connectors was secured to the lower adapters of the safety rods.

The safety rod drive shafts extended up through the primary tank cover. During a scram a spring within the drive unit released to forcefully move the safety drive beam downward thus ejecting the safety rod downwards and out of the core. This was in essence a bottom drive design for the safety rods. The safety rod connectors were 70.80 cm high sitting on top of the safety drive beam. The safety drive shafts had a maximum outer diameter of 11.43 cm. Figure 4.2.2.1 shows the sodium-washed length.

5 EBR-II Coolant System

The EBR-II coolant systems model for the SHRT-17 and SHRT-45R benchmarks includes the major components in the primary sodium circuit and the intermediate side of the intermediate heat exchanger. Beginning at the outlet of the reactor core, the primary sodium circuit includes the upper plenum, reactor outlet piping, auxiliary EM sodium pump, intermediate heat exchanger, primary sodium tank, primary sodium pumps, reactor inlet piping and the high- and low-pressure inlet plena. The inlet and outlet of the intermediate side of the intermediate heat exchanger are boundary conditions for the benchmark model. The necessary measurements of boundary condition data are provided below.

Figures 5.1 and 5.2 below illustrate the major components in the EBR-II primary sodium circuit. Dimensions of the major components are provided in the sections that follow. In Figure 5.1, sodium discharged from the right side of the reactor vessel into the reactor outlet piping, which is known as the 'Z-Pipe.' The shape of the pipe accommodates thermal expansion. The top of the Z-Pipe contained the auxiliary EM pump, which rated to provide up to 0.5% of the nominal pump head.

Sodium exited the Z-Pipe and entered the shell side of the intermediate heat exchanger. Cold sodium was then discharged into the primary sodium tank. The two primary sodium pumps took suction from the primary sodium tank and provided sodium to the reactor inlet piping. Figure 5.1 shows primary sodium pump #1 and its inlet piping, while Figure 5.2 shows primary sodium pump #2 and its inlet piping.

Both sets of inlet piping provided sodium to the high-pressure and low-pressure inlet plena. The high-pressure inlet plenum provided sodium to the subassemblies in the first 7 rows while the low-pressure inlet plenum provided sodium to the remaining subassemblies.

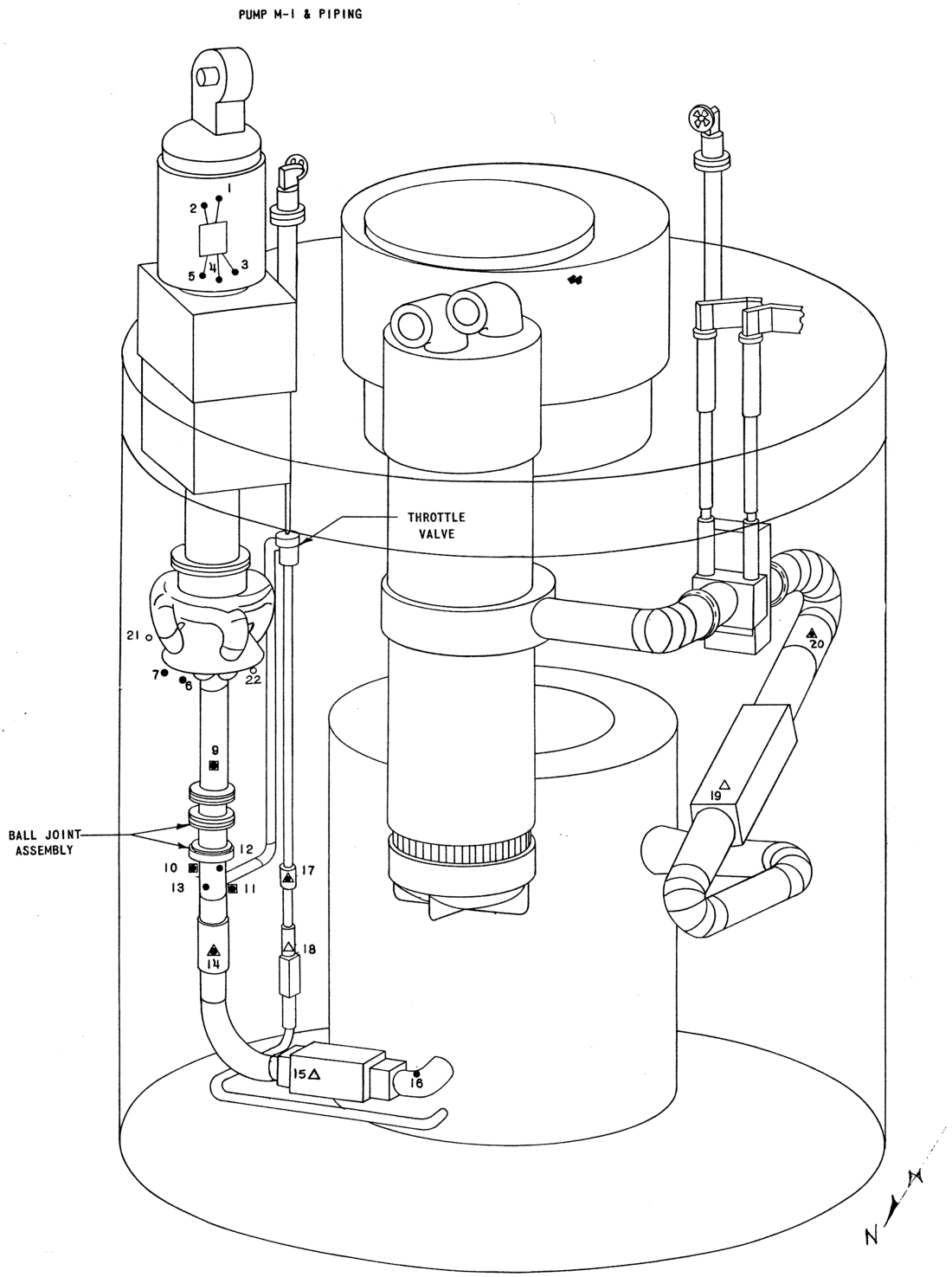

Figure 5.1. EBR-II Primary Tank Layout Including Intermediate Heat Exchanger, Z-Pipe and Primary Sodium Pump #1.

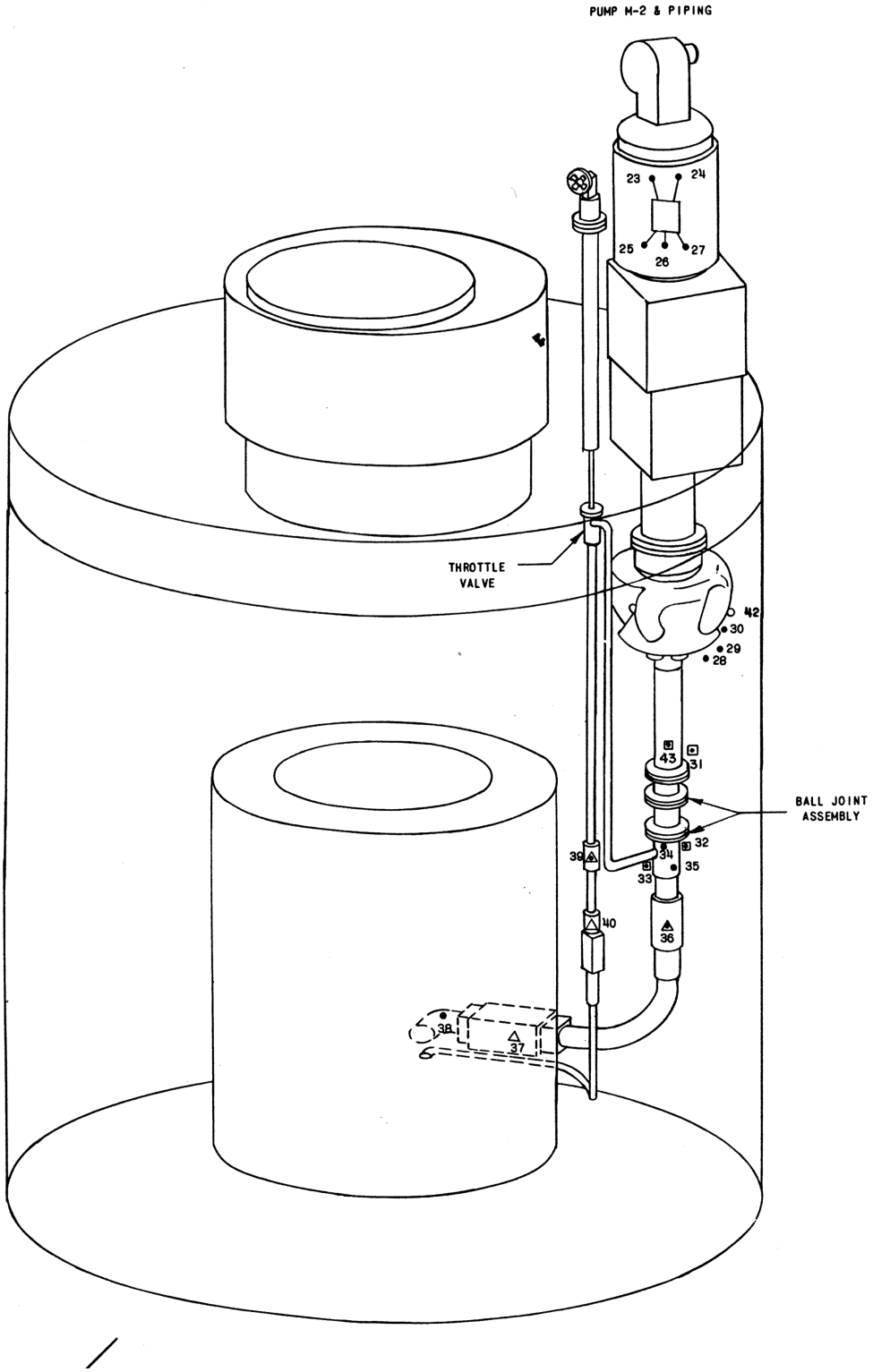

Figure 5.2. EBR-II Primary Tank Layout Including Primary Sodium Pump #2.

5.1 Layout of Components

Figures 5.1.1 and 5.1.2 below illustrate the locations and dimensions of the major components in the benchmark model of the primary sodium circuit. Simplified geometry is given for these components in the benchmark model. Some components in the EBR-II primary tank, such as the structure at the bottom of the primary tank, are assumed to occupy a negligible volume and are therefore not included in the benchmark model.

Figure 5.1.1 provides the elevation view and Figure 5.1.2 provides a view from above looking down on the system. In these two figures, the blue piping represents the reactor outlet pipe, the green piping represents the high-pressure inlet piping and the red piping represents the low-pressure inlet piping. In the discussions that follow, it is assumed that the x-axis is along the direction from the axial centerline of the core to the axial centerline of the IHX and the z-axis is along the axial centerline of the reactor core.

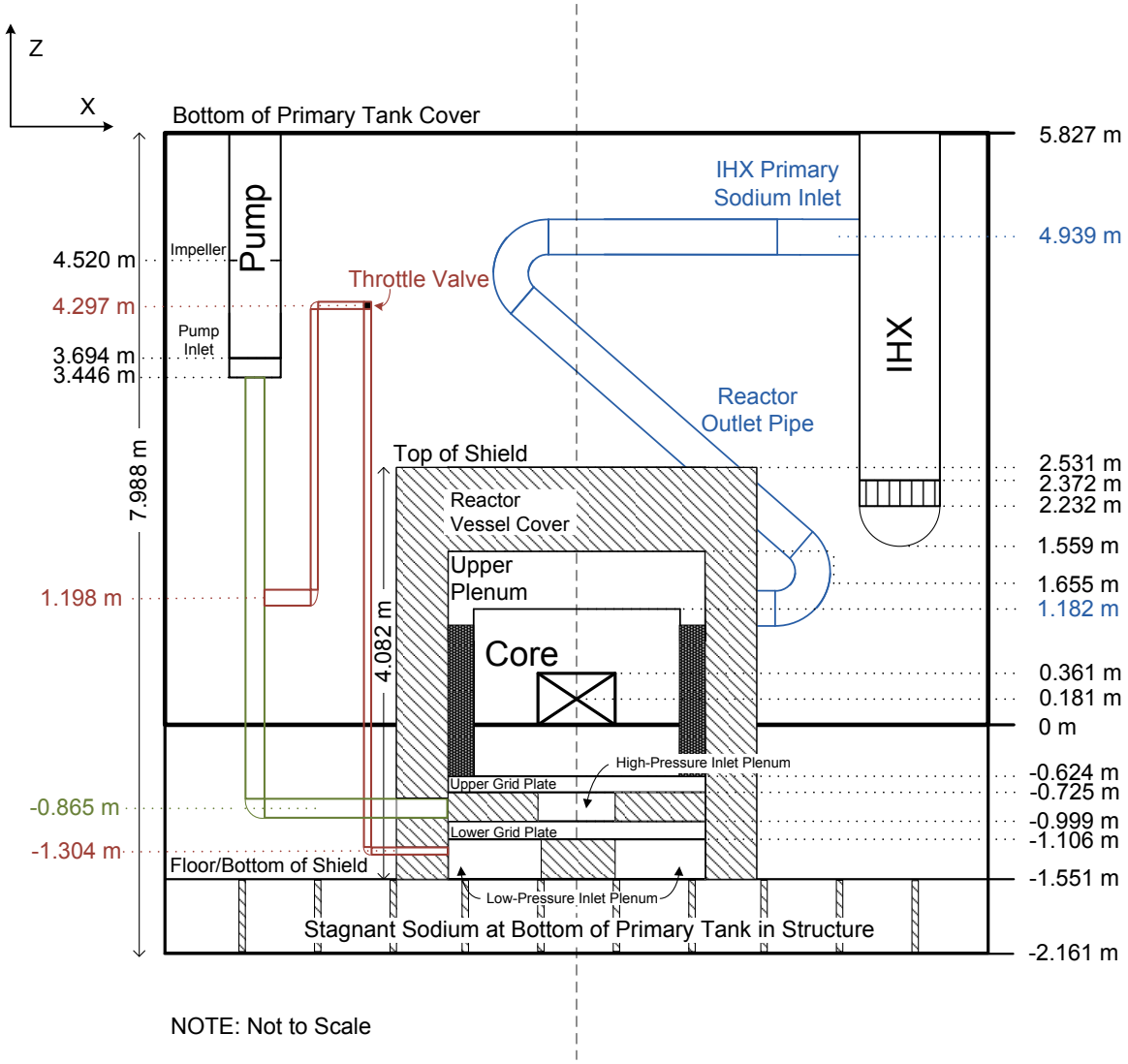

Figure 5.1.1. Benchmark Model of Primary Vessel Components, Elevation View

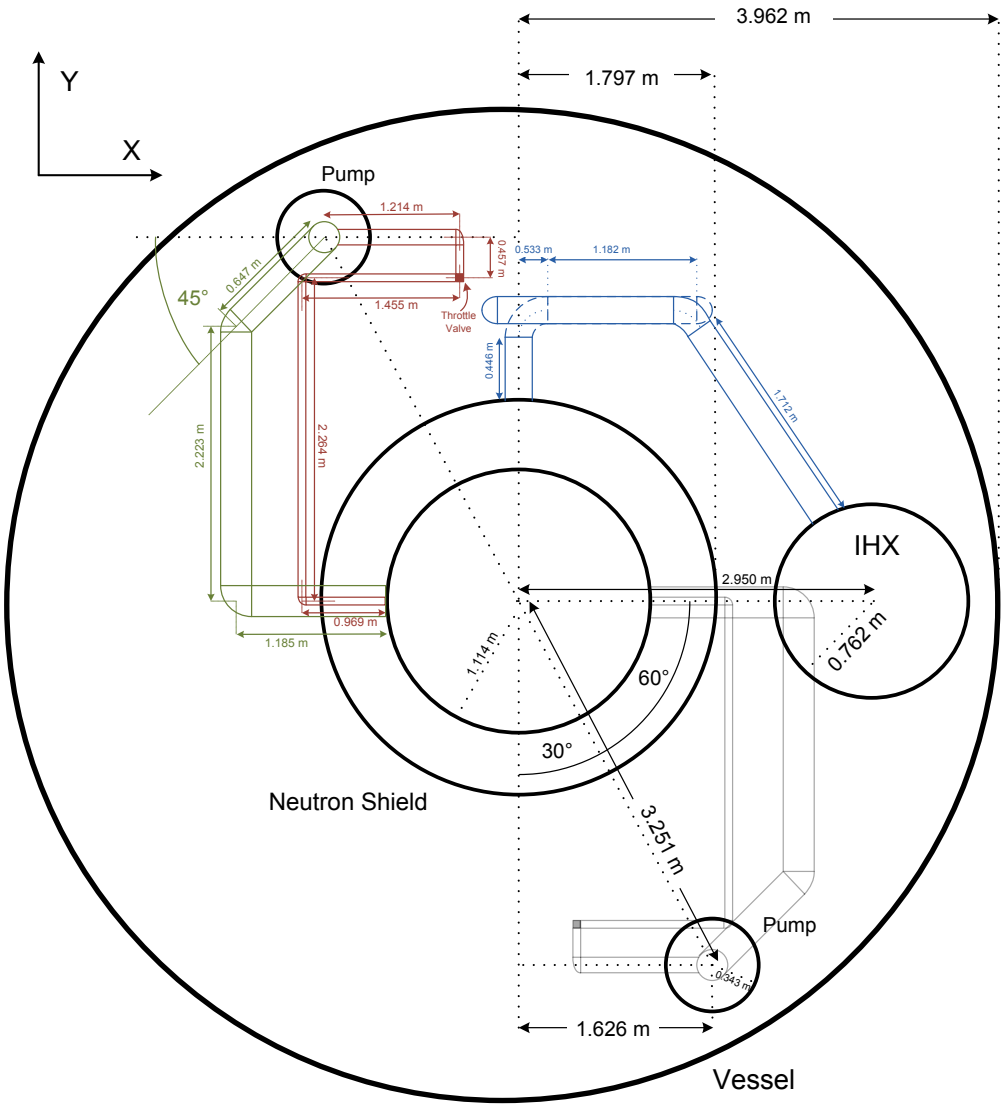

Figure 5.1.2. Benchmark Model of Primary Vessel Components, Plane View

5.2 Component Geometry

The primary tank is the outer boundary of the primary sodium circuit and is modeled as a vertically oriented cylinder. It encompasses all of the major primary sodium components. The reactor vessel, intermediate heat exchanger and two primary sodium pumps are modeled as vertically oriented cylinders. Sodium piping is modeled as a series of straight pipes connected by pipe bends that, unless otherwise stated, have a bend radius equal to the pipe radius. The reactor vessel, IHX, pumps and sodium piping are assumed to be the only components that displace sodium in the primary sodium tank. The dimensions of all components in the benchmark specification are given in the following sections.

5.2.1 *Primary Sodium Tank*

The cylindrical primary sodium tank contains two vessel walls with the space between the inner and outer vessel walls filled with argon gas. The inner surface of the inner vessel wall is a cylinder with a diameter of 7.925 meters and a height of 7.988 meters. This surface extends from 2.161 meters below the bottom of the active core to 5.827 meters above the bottom of the active core. The inner vessel wall has a thickness on all sides of 1.27 cm. Outside of the inner vessel wall is the argon gas layer, which is a 12.7-cm thick cylindrical shell. Outside of the argon gas layer is the outer vessel wall. The inner surface of the outer vessel wall has a diameter of 8.204 meters and extends from 2.301 meters below the bottom of the active core to 5.967 meters above the bottom of the active core. The outer vessel wall has a thickness of 0.635 cm on all sides. Both vessel walls are composed of Type 304 stainless steel.

The total volume of sodium in the primary system is approximately 90,000 gallons at an average nominal temperature of 700°F. This volume of sodium includes all sodium in the major components, piping, reactor subassemblies and primary tank. The remaining volume inside the primary sodium tank above the primary tank sodium is occupied by argon gas. The core support structure below the reactor vessel is assumed to displace a negligible amount of sodium.

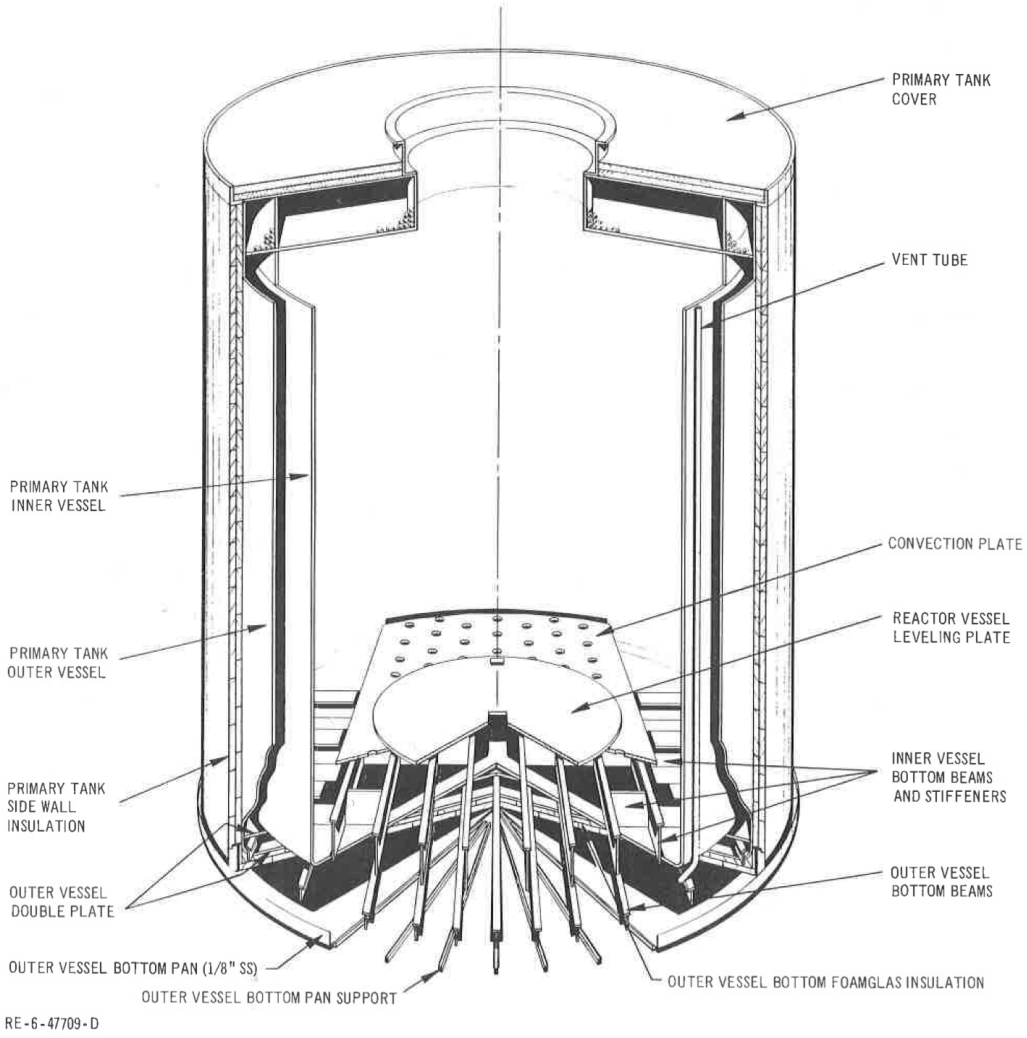

Figure 5.2.1.1. EBR-II Primary Tank Vessel

5.2.2 *Reactor Vessel*

The EBR-II reactor vessel and its internal components are illustrated in Figure 5.2.2.1. Sodium discharged from the primary sodium pumps entered the low-pressure inlet plenum from one of two inlet pipes or the high-pressure inlet plenum from one of two inlet pipes. The high-pressure inlet plenum was situated above the low-pressure inlet plenum. Sodium from these two inlet plena was provided to the reactor subassemblies and then discharged into the common upper, or outlet, plenum. Sodium exited the upper plenum through the Z-Pipe.

The neutron shielding surrounded the reactor, upper plenum and lower plena with sections removed for the inlet and outlet piping. Other than the grid plates that separated the lower plena, there was no significant shielding below the reactor. Above the upper plenum sat the reactor cover, through which control rod drive shafts and instrumentation leads entered the reactor vessel.

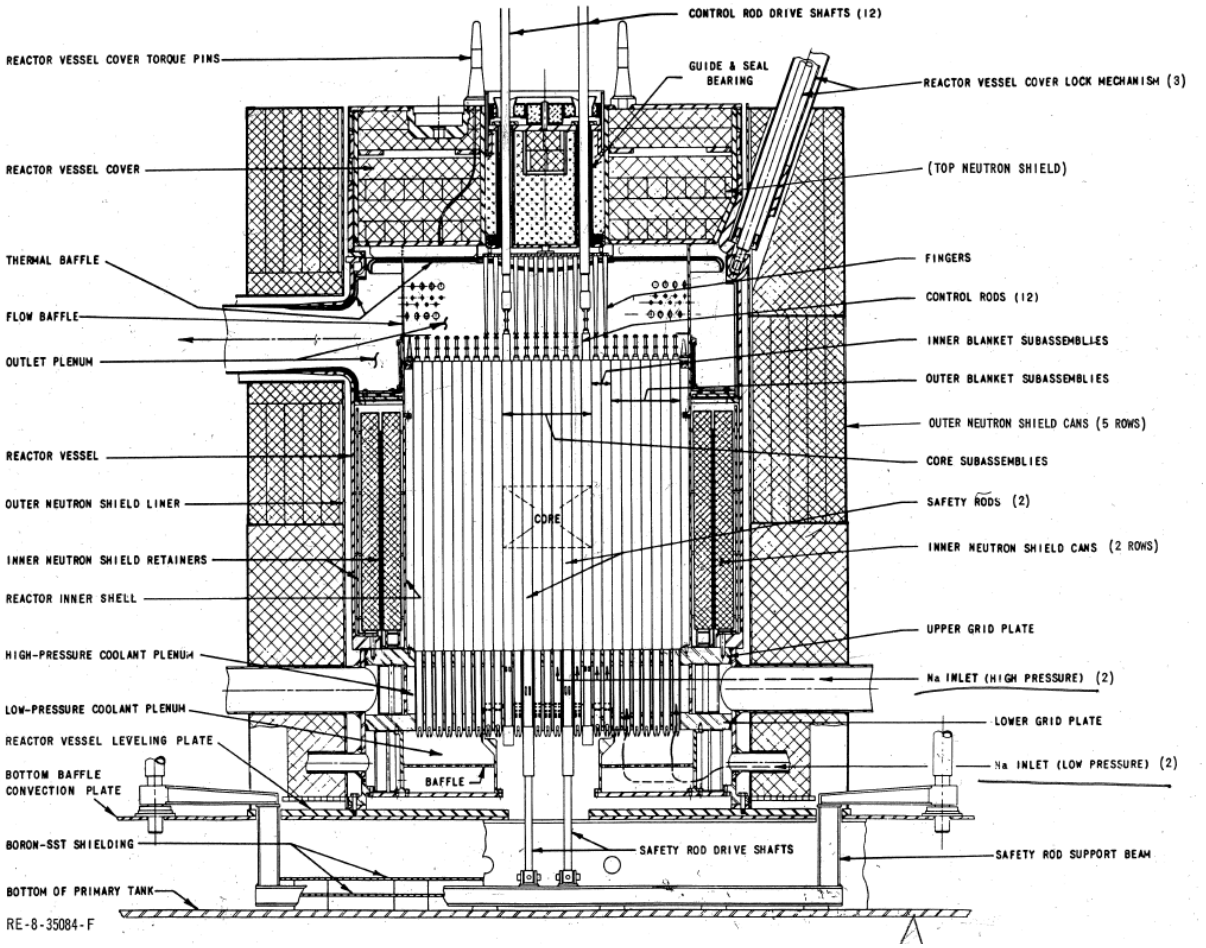

Figure 5.2.2.1. EBR-II Reactor Vessel and Neutron Shield Assembly

The benchmark model of the reactor vessel and neutron shield is a simplified cylindrical representation of the actual EBR-II reactor vessel and neutron shield geometry and is illustrated in Figure 5.2.2.2 below. The shield and reactor cover are assumed to be one component, from here on referred to as the shield, which is composed of graphite.

The cylindrical outer surface of the shield has a radius of 1.797 meters. It extends from 1.551 meters below the bottom of the active core to 2.531 meters above the bottom of the active core. The shield occupies all volume inside this outer surface that is not occupied by the inlet sodium piping, inlet plena, core, upper plenum or outlet sodium piping. The outer dimensions of the upper and lower plena and the core can be seen in Figure 5.2.2.2. The dimensions of the reactor outlet pipe are given in Section 5.2.6.

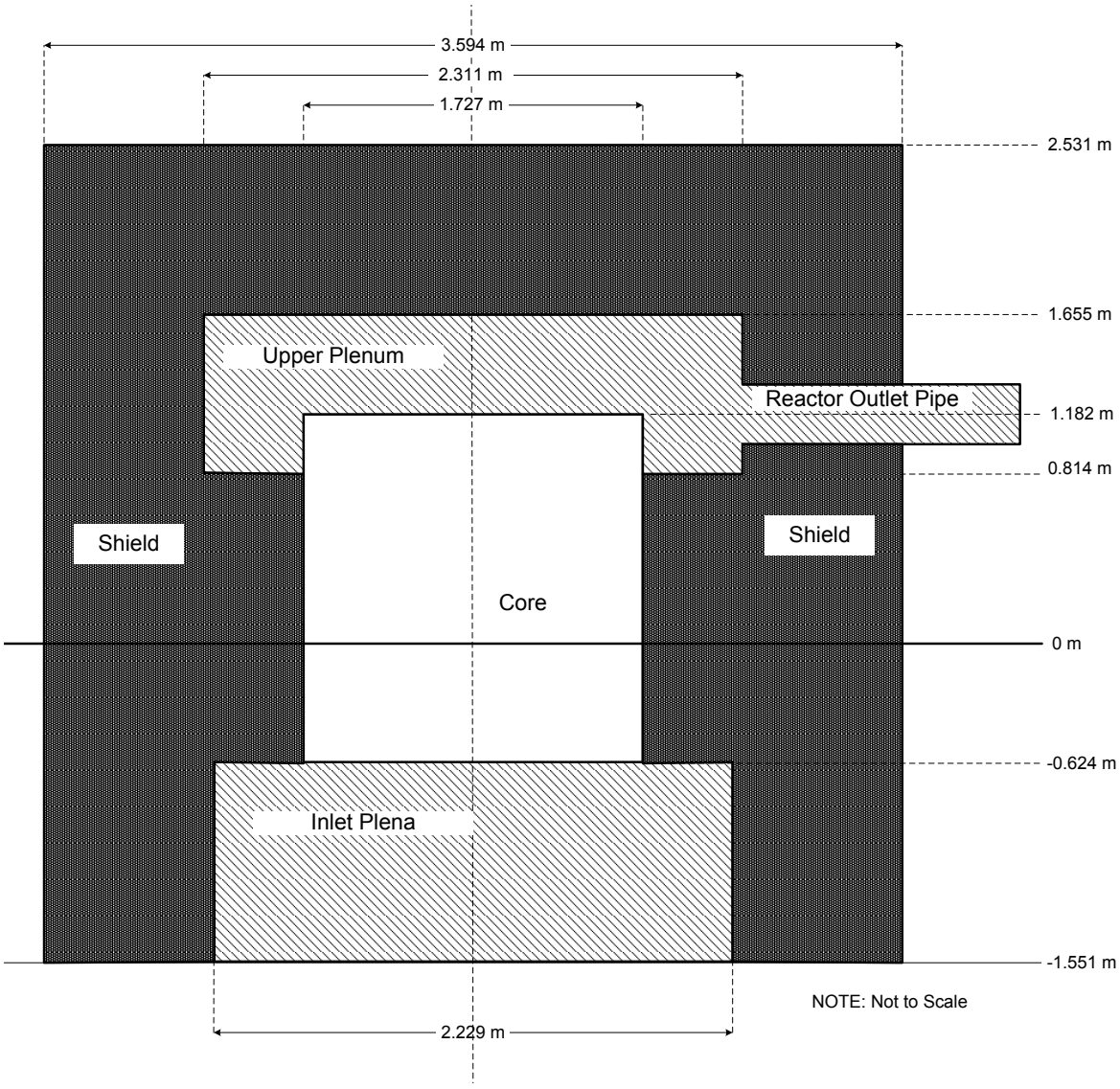

Figure 5.2.2.2. Benchmark Model of Reactor Shield and Cover Geometry

5.2.3 *Inlet Plena*

Figure 5.2.3.1 below illustrates the EBR-II high- and low-pressure inlet plena. The lower plenum received coolant from the two low-pressure inlet pipes. Sodium passed through a vertically oriented baffle plate, then through a horizontally oriented baffle plate and into the low-pressure inlet plenum. Sodium was then provided to the subassemblies in Rows 8-16 through stainless steel grid plate interconnecting vertical tubes, which are identified in Figure 5.2.3.1.

The upper inlet plenum received sodium from the two high-pressure inlet pipes. Sodium then passed through a vertical baffle plate, around the stainless steel tubes connecting the low-pressure plenum with the core, and into the high-pressure inlet plenum. In the high-pressure inlet plenum, sodium was distributed to the subassemblies in Rows 1-7.

The geometry of the benchmark model of the high- and low-pressure inlet plena is presented in Figure 5.2.3.2 below. Except for the high- and low-pressure inlet pipes and the seven concentric hexagonal steps in the high-pressure inlet plenum, this model is symmetric about the axial centerline of the reactor. All structure in the inlet plena is composed of Type 304 stainless steel.

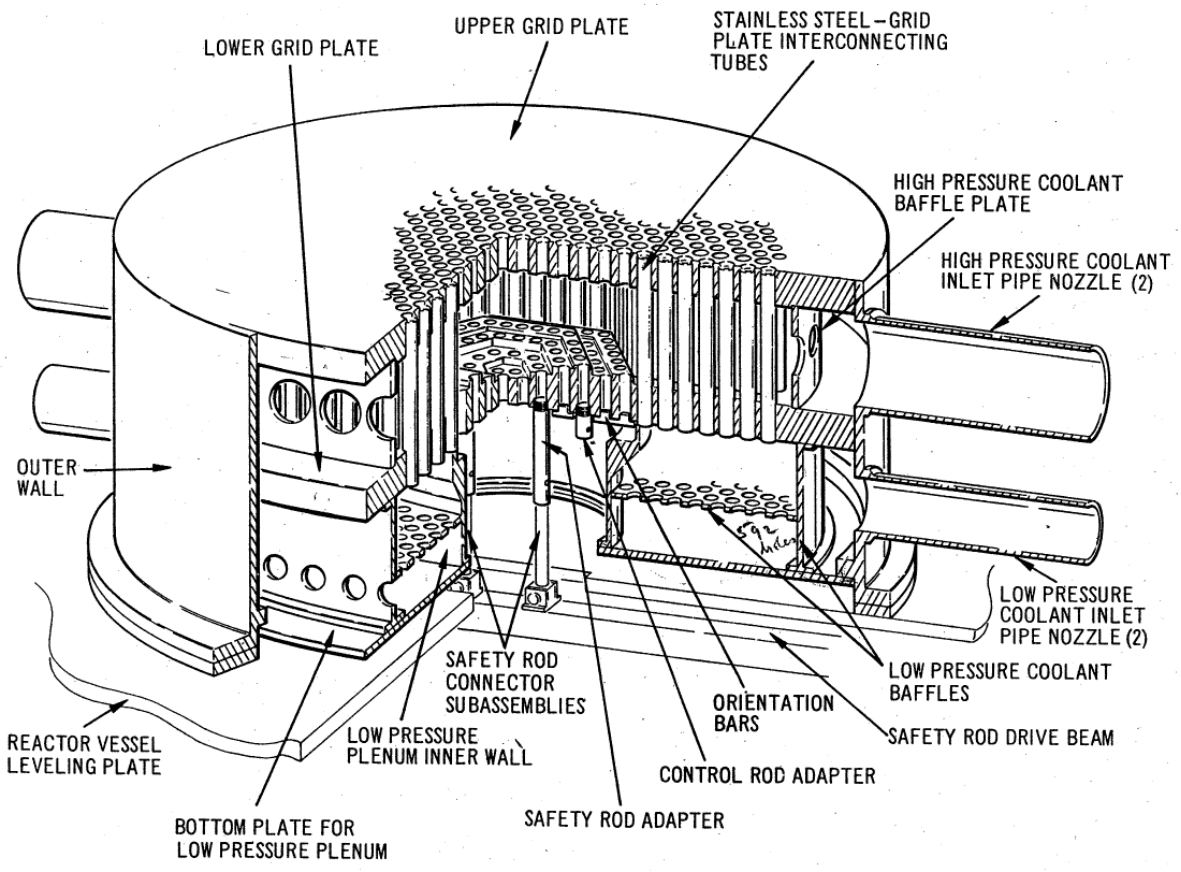

Figure 5.2.3.1. High- and Low-Pressure Inlet Plena

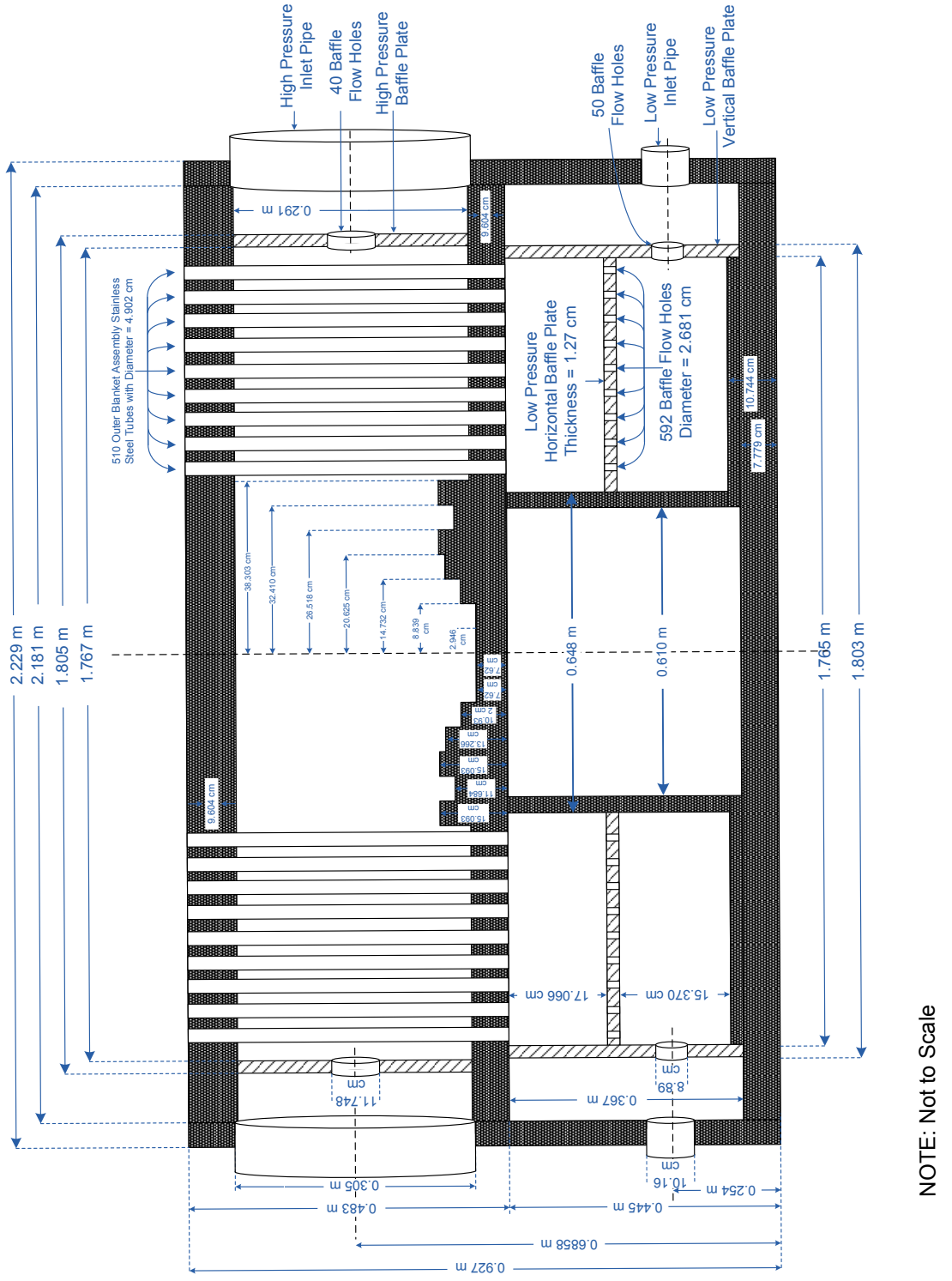

Figure 5.2.3.2. Benchmark Model of High- and Low-Pressure Inlet Plena (Axial View)

Sodium enters the low-pressure inlet plenum through the two 10.16 cm diameter inlet pipes. It passes through a vertically oriented 1.905-cm thick baffle plate with 50 baffle holes, each with a diameter of 8.89 cm. The sodium then passes through a horizontally oriented 1.27-cm thick baffle plate with 592 baffle holes, each with a diameter of 2.681 cm. The sodium then enters one of the 510 outer blanket stainless steel tubes that feed the outer blanket region subassemblies. These tubes have an outer and inner diameter of 4.902 and 3.830 cm, respectively. The 0.610-m diameter central region of the low-pressure inlet plenum is sealed off from the cold pool, sodium is freely exchanged between the two volumes.

Sodium enters the high-pressure inlet plenum through one of two 30.48 diameter pipes. It then passes through a vertically oriented 1.905-cm thick baffle plate with 40 baffle holes, each with a diameter of 11.748 cm. The high-pressure inlet sodium flows around the stainless steel tubes providing sodium to the expanded core subassemblies and into the central region of the high-pressure inlet plenum.

The central region of the high-pressure inlet plenum contains a series of seven concentric hexagonal steps. Each step has an aperture for each subassembly in the row in which the bottom of each subassembly is inserted. As the lower adapter of each subassembly in Rows 1-7 has a series of sodium inlet flow holes, these steps have varying heights to block off certain holes depending on the desired amount of sodium flow through the subassembly. The subassemblies in Row 1-7 are not illustrated in Figure 5.2.3.2. The apertures of the control and safety subassemblies have a diameter of 5.423 cm. The expanded core region subassembly apertures have a diameter of 4.227 cm. The apertures for all other high-pressure subassemblies have a diameter of 4.783 cm.

5.2.4 *Upper Plenum*

The benchmark geometry of the upper plenum is illustrated in Figure 5.2.4.1. The actual EBR-II upper plenum contained a baffle plate to mix the outlet sodium flow. Not enough detail is available for the upper plenum baffle plate, so the baffle plate is not included in the benchmark model, and it is assumed that the sodium leaving the upper plenum is fully mixed when it enters the reactor outlet pipe.

The upper plenum consists of two regions: a cylindrical region directly above the reactor subassemblies and an annular region surrounding the cylindrical region. The upper surface of both regions is 1.655 meters above the bottom of the active core. The cylindrical region is a 0.473-meter tall cylinder with a diameter of 86.36 cm. The annular region of the upper plenum directly surrounds the cylindrical region. The annular region of the upper plenum has an inner diameter of 86.36 cm and an outer diameter of 115.57 cm. Sodium leaves the upper plenum through the reactor outlet pipe and into the Z-Pipe.

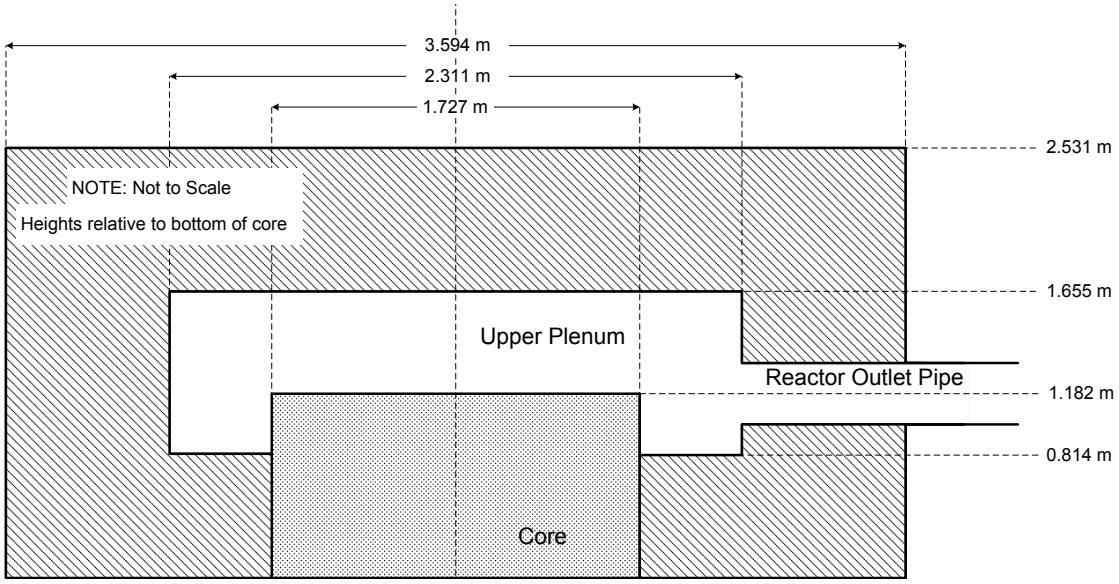

Figure 5.2.4.1. Benchmark Model of Upper Plenum (Axial View)

5.2.5 *Pumps*

The primary sodium circuit has three pumps: two main and one electromagnetic pump. The two main primary sodium pumps lay opposite each other at a radius of 3.251 meters from the center of the core. Primary sodium pump #1 was located 120° counter-clockwise from the IHX, while primary sodium pump #2 was located 60° clockwise from the IHX. The electromagnetic pump was located around part of the Z-Pipe. Both types of pumps are assumed to be constructed of Type 304 stainless steel.

In this benchmark, both main primary sodium pumps are modeled as a vertically oriented cylinder suspended from the primary tank cover with a lower surface 3.446 meters above the bottom of the active core and a radius of 0.343 meters. The pumps extend 2.381 meters upwards to the bottom of the primary tank cover. Sodium enters the primary sodium pumps at an elevation of 3.694 meters, continues upward to the pump impeller at an elevation of 4.520 meters and is discharged into the high-pressure inlet piping at an elevation of 3.446 meters. Refer to Section 3.4.1 for a discussion on the EBR-II pump model that should be used for benchmark simulations.

The auxiliary EM pump was attached to the outside of the 1.572-meter long segment of the Z-Pipe, which is discussed below. As the auxiliary EM pump was situated around the reactor outlet pipe, the pipe dimensions at the location of the auxiliary EM pump should remain unchanged. Suggestions have been made in Section 3.4.1 for the modeling of the auxiliary EM pump during the transients.

5.2.6 *Piping*

Two sets of sodium piping were installed in the primary sodium circuit: the reactor outlet piping and the reactor inlet piping. The reactor outlet pipe, or Z-Pipe, began at the reactor outlet plenum and ended at the intermediate heat exchanger. It was constructed in a Z-shape to account for thermal expansion during periods of elevated outlet and cold pool sodium

temperatures. The reactor inlet piping was two identical sets of piping from both of the primary sodium pumps to the inlet plena. Both sets of piping were constructed of Type 304 stainless steel. In the following piping descriptions, the x-axis is assumed to be on the line between the axial centerlines of the reactor core and IHX. The y-axis is assumed to be in the up direction in Figures 5.2.6.2 and 5.2.6.3.

The Z-Pipe is illustrated from the side and from above in Figures 5.2.6.1 and 5.2.6.2. Because the sodium in the reactor outlet pipe is at a higher temperature than the bulk sodium surrounding it, the Z-Pipe is a double-walled structure. The inner pipe is a 14-inch schedule 10 pipe and the outer pipe is an 18-inch schedule 10 pipe. The annular region between the two pipe walls is filled with static sodium. In the upper section of the Z-Pipe resides the auxiliary EM pump, which is assumed to have the same pipe thickness and flow area as the rest of the Z-Pipe.

The Z-Pipe consists of five straight segments and four bend segments. The bend segments have an assumed bend radius of 53.3 cm and approximate bend angles of 90, 135, 135, and 69 degrees. Including the bend segments, the total length of the Z-Pipe is 11.652 meters and the elevation change from the inlet to the outlet is 3.726 meters. The first segment of the Z-Pipe has an elevation of 1.182 meters above the bottom of the active core.

The Z-Pipe begins 1.797 meters from the center of the core at the outer edge of the neutron shield. It travels 0.446 meters in the positive y-direction, then makes a 90° turn to the positive x-direction. The Z-Pipe continues in the positive x-direction for 1.182 meters before making a 135° bend to the direction that bisects the negative x-direction and positive z-direction. The Z-Pipe travels 2.737 meters in this direction and makes another 135° bend back to the positive x-direction before a 1.572 meter-long straight segment. At the end of this segment, the Z-Pipe makes another bend to begin traveling 69° below the positive x-direction. The final segment of the Z-Pipe is a 1.712-meter straight segment that ends at the outer surface of the Z-Pipe, 4.908 meters above the bottom of the active core.

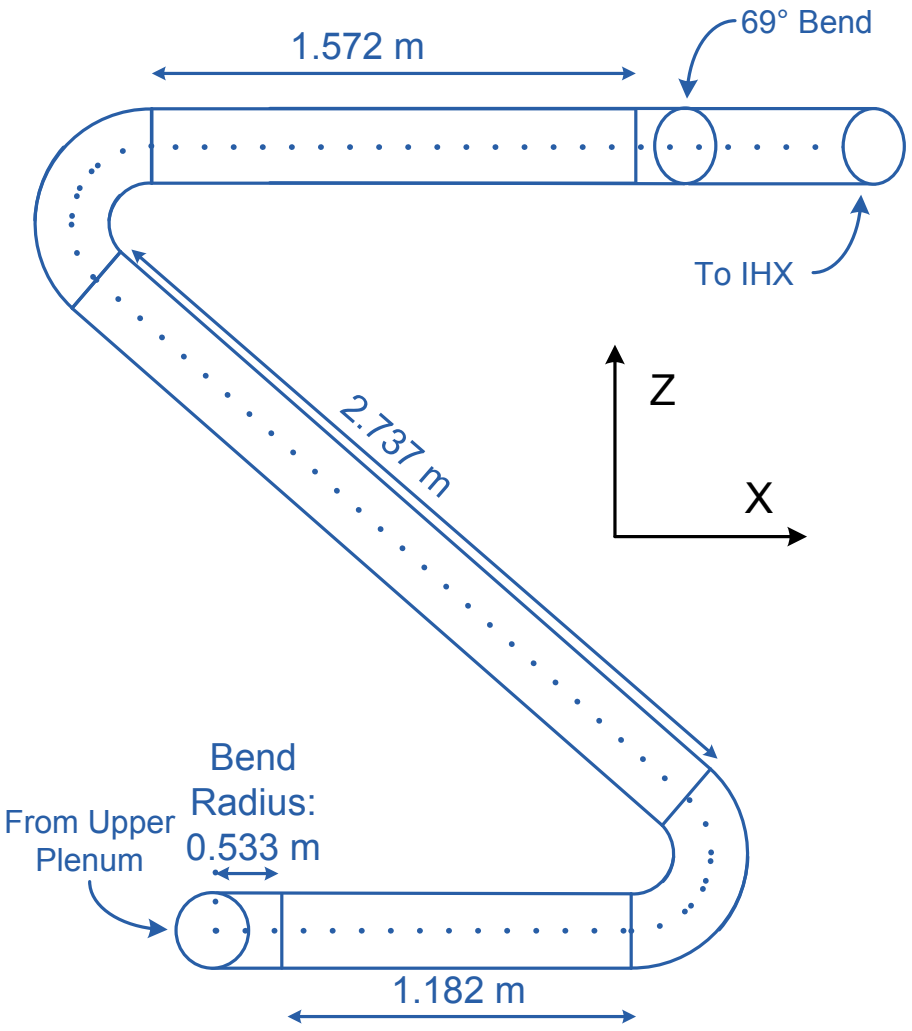

Figure 5.2.6.1. Benchmark Model of Reactor Outlet Piping (Axial View)

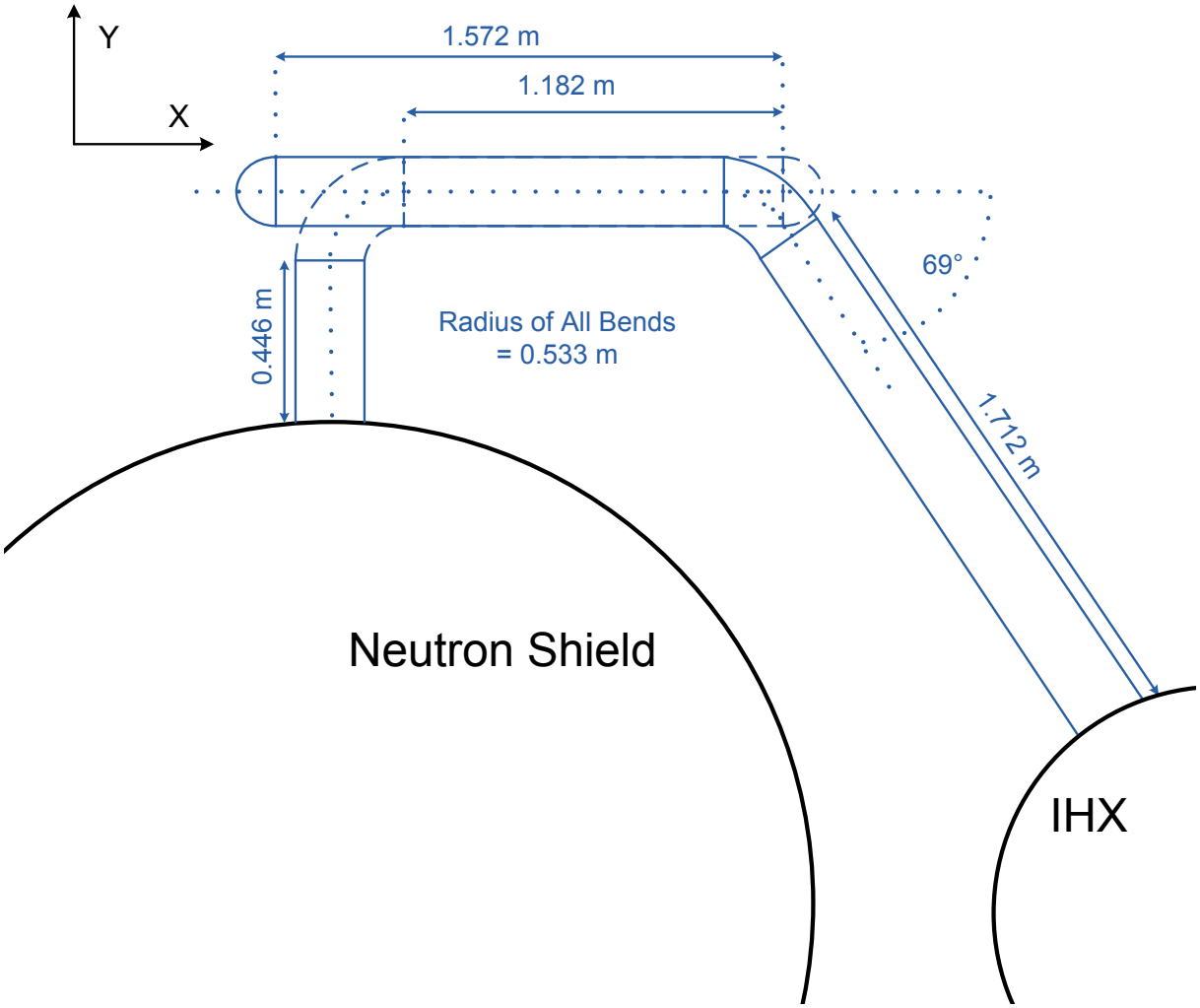

Figure 5.2.6.2. Benchmark Model of Reactor Outlet Piping (Radial View)

The reactor inlet piping leading from the primary sodium pumps to the inlet plena is illustrated in Figure 5.1.1 from the side and in Figure 5.1.2 from above. Figure 5.2.6.3 provides a closer view from above of the inlet piping from pump #1. The green piping in these figures represents the high-pressure inlet piping and the red piping represents the low-pressure inlet piping. The two sets of inlet piping are identical so the second set of piping is grayed out in Figure 5.1.2 to allow for greater detail for the pump. The description of the inlet piping below applies to both sets of pipes. Unless otherwise stated, all bends in the inlet piping are assumed to have a bend radius equal to the pipe radius.

The two primary sodium pumps take suction from the bulk sodium cold pool and output sodium to the high-pressure coolant system. Sodium exits the pump at an elevation of 3.446 meters above the bottom of the core. The sodium then travels straight down for 4.311 meters through the high-pressure piping, which is 12-inch schedule 40 piping. 0.865 meters below the bottom of the core, the high-pressure piping makes a 90° turn and begins traveling in the direction that bisects the negative x-direction and negative y-direction. The high-pressure piping continues for 0.647 meters before making a 45° turn to the negative y-direction. The high-pressure piping continues in the negative y-direction for 2.223 meters before turning 90° to the positive x-direction. The final leg of the high-pressure piping has a length of 1.185 meters and outputs sodium to the inlet plena. All high-pressure piping bends have a bend radius of 6 inches.

At an elevation of 1.198 meters above the bottom of the core, 2.248 meters below the bottom of the pump, a 6-inch schedule 40 pipe is welded onto the side of the high-pressure piping. This pipe feeds the low-pressure inlet piping. The 6-inch schedule 40 pipe continues for 1.214 meters before turning 90° upward. This 90° turn is a reducing bend that connects the 6-inch piping to 4-inch schedule 40 piping. This leg travels 3.099 meters upward and then makes another 90° turn to the negative y-direction. After 0.457 meters in this direction, the sodium reaches a throttle valve, which is used to distribute flow appropriately between the high- and low-pressure pipes.

At the exit of the throttle valve, the low-pressure piping continues for 5.601 meters straight down before turning to the negative x-direction. This pipe segment continues for 1.455 meters before turning to the negative y-direction for 2.264 meters. Finally, the low-pressure piping travels 0.969 meters in the positive x-direction, ending at the inlet plena. Except for the 90° reducing bend, the low-pressure piping bends have a bend radius of 2 inches.

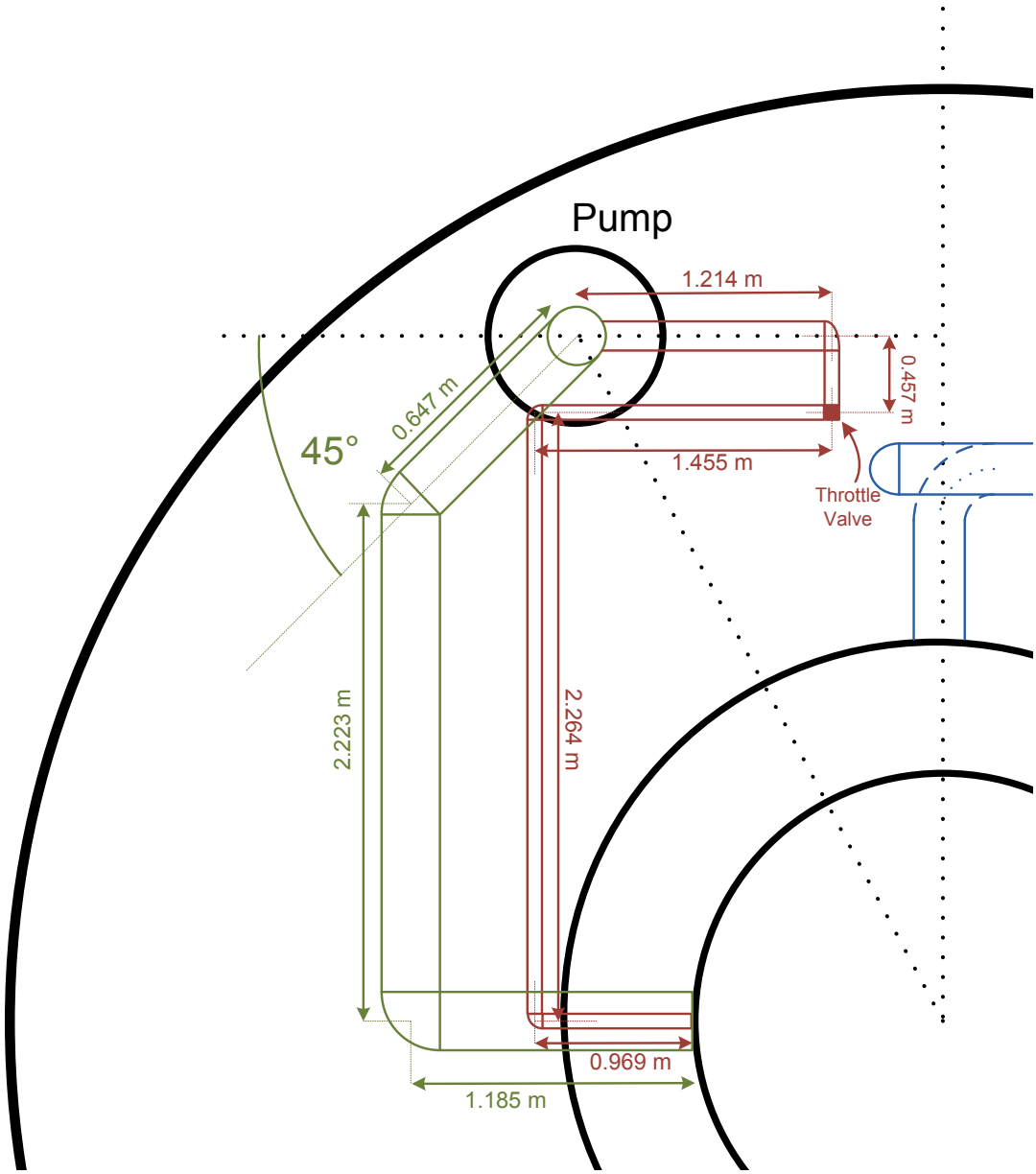

Figure 5.2.6.3. Benchmark Model of Reactor Inlet Piping

5.2.7 *Intermediate Heat Exchanger*

The intermediate heat exchanger transfers heat from the radioactive primary system to the intermediate system and isolates the primary system from the water inventory in the steam plant. The heat exchanger is a tube-and-shell design with single-wall straight tubes and is operated in the counter flow mode. The intermediate heat exchanger is illustrated in Figures 5.2.7.1 and 5.2.7.2. The benchmark model of the heat exchanger is illustrated in Figure 5.2.7.3. Primary and intermediate sodium flow paths are illustrated in blue and red, respectively, in Figure 5.2.7.3.

The heat exchanger consists of three modules or components, all composed of Type 304 stainless steel. The well casing is a cylindrical annulus with its major axis oriented vertically and it hangs from the primary tank cover from a lip at the upper end of the well casing and continues downward to an elevation of 1.559 meters above the bottom of the active core. It consists of four concentric steel cylinders with stagnant sodium between each layer. The lower end of the casing is terminated by a hemispherical head. The tube bundle is inserted into the well casing through the opening at the upper end. Welded to the top of the tube bundle is the shield plug. Once the tube bundle and shield plug are lowered as a unit into the well casing, a cover is placed over the open end of the well casing and welded shut.

Heat transfer from primary to intermediate sodium takes place in the lower half of the intermediate heat exchanger where the tube bundle is located. The primary coolant is admitted on the shell side through a horizontal inlet pipe (i.e. the outlet of the Z-Pipe) that penetrates the well casing wall 4.939 meters above the bottom of the active core. The fluid exits the inlet pipe and enters the upper region of the tube bundle, where it is distributed horizontally by baffles. The upper end of the tube bundle (above the inlet pipe) is terminated by the upper tube sheet, resulting in the primary sodium being directed downward parallel to the tubes. The primary sodium travels down the length of the tubes and exits the well casing horizontally just above the lower tube sheet through an annular opening in the well casing.

The intermediate sodium enters the intermediate heat exchanger through a vertical pipe that penetrates the well casing cover. This pipe extends down the length of the well casing to the hemispherical region defined by the lower tube sheet and the well casing lower head. A set of hemispherical baffles redirect the fluid 180° so that it flows upward. The fluid then enters the bottom of the tubes at the lower tube sheet. The fluid flows up the length of the tubes and then exits the tubes into another hemispherical-shaped region defined on its bottom by the upper tube sheet and on its upper side by a hemispherical-shaped cap spun from metal. An exit pipe is welded to the upper hemispherical cap. The exit pipe travels the length of the upper-half of the well casing up to the well casing cover, where it exits the intermediate heat exchanger through a penetration in the well casing cover. Boundary conditions for the intermediate inlet sodium temperature and flow have been given above in Section 3.4.2.

The collection of internals in the upper half of the well casing is known as the shield plug. The shield plug contains the inlet and outlet intermediate side pipes, while the remaining space is occupied by various thermal and radiation shields. The shield plug represents a large thermal mass but its thermal connections to both the primary and intermediate flow paths are rather weak, with time scales on the order of seconds or minutes. The areas available for heat transfer and the radius of the shield plug are such that heat transfer rates are small compared

to the energy storage capability of the shield material. Table 5.2.7.1 lists important dimensions for the IHX components.

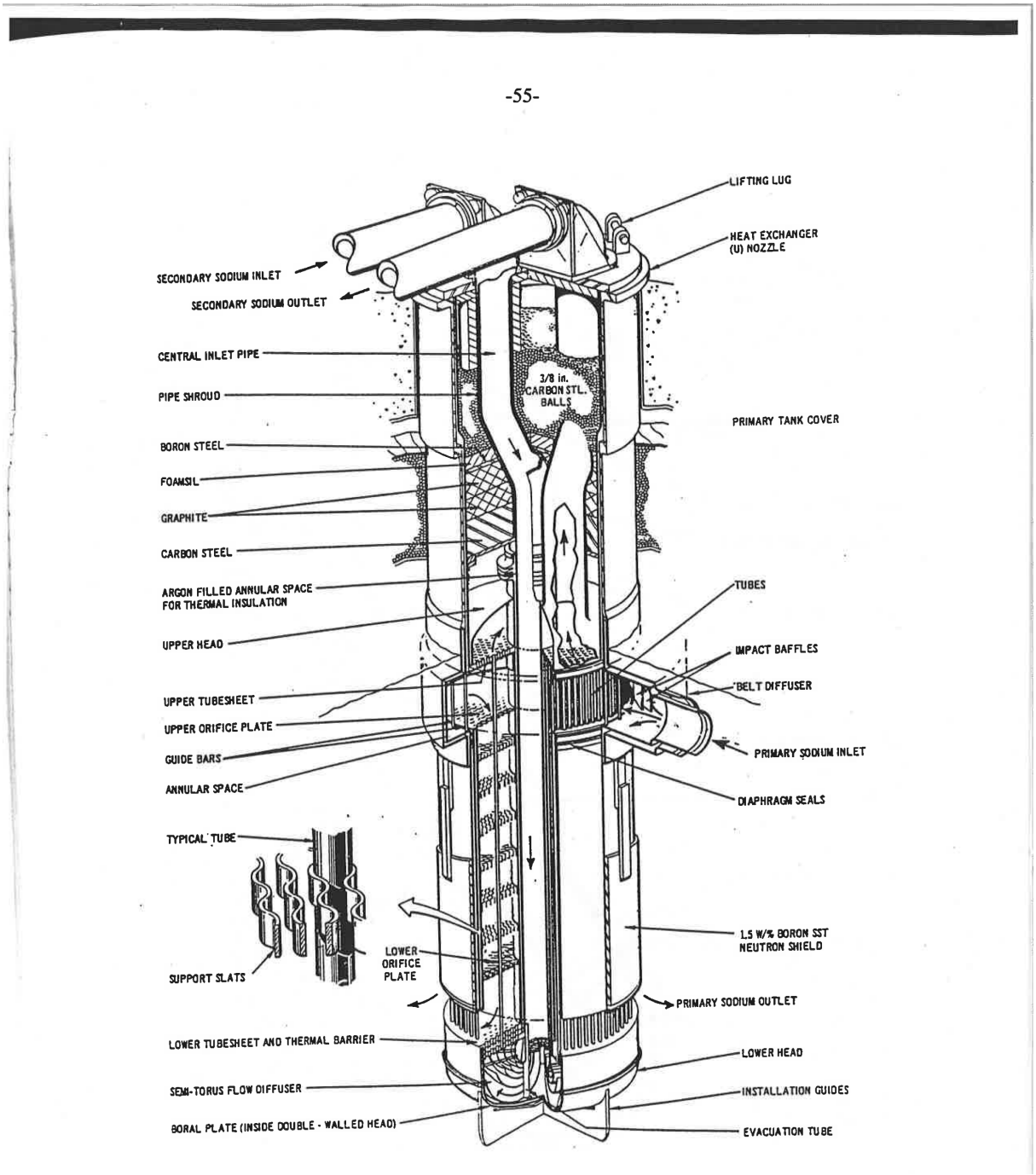

Figure 5.2.7.1. Intermediate Heat Exchanger

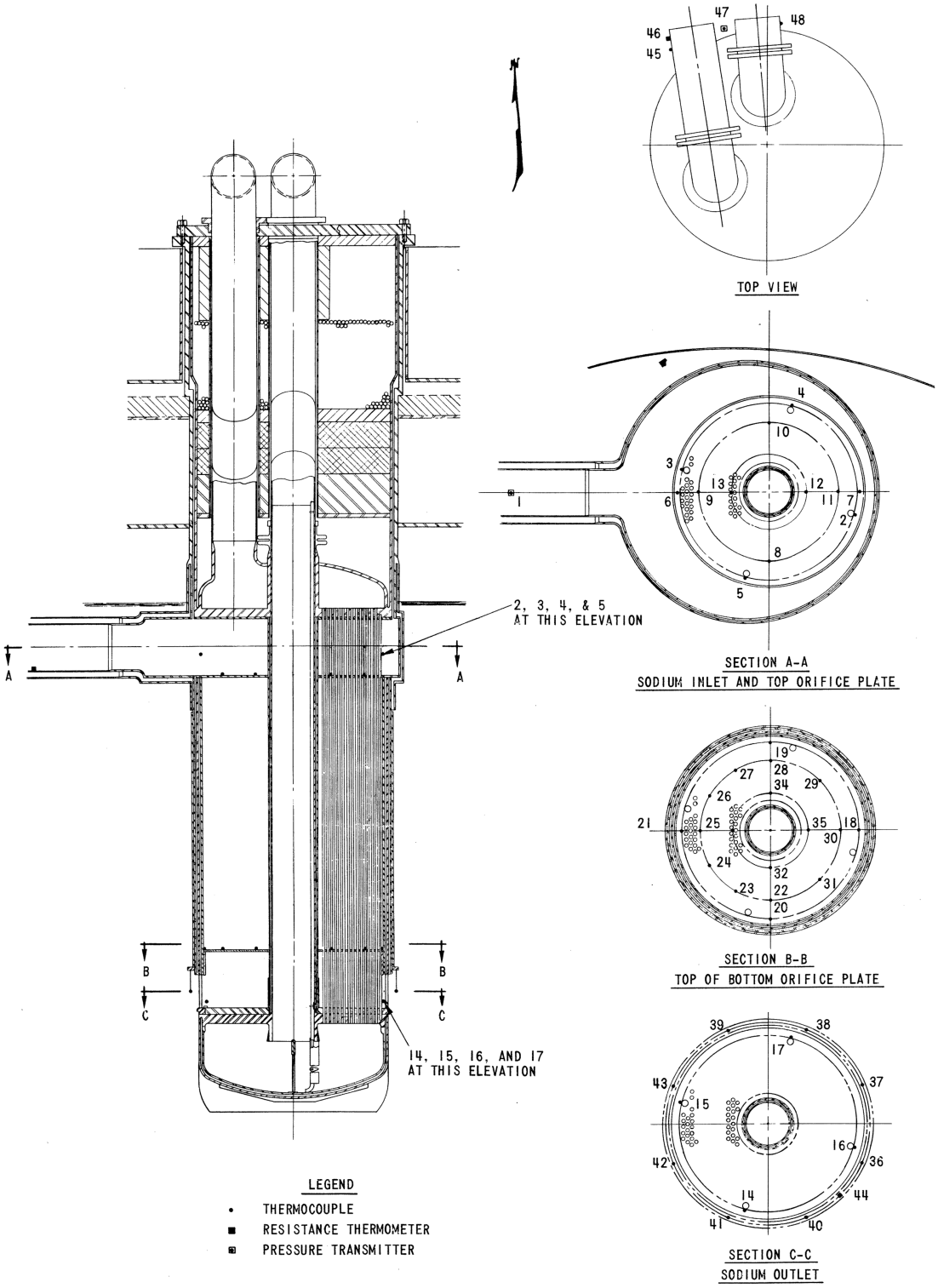

Figure 5.2.7.2. Intermediate Heat Exchanger Plane Sections

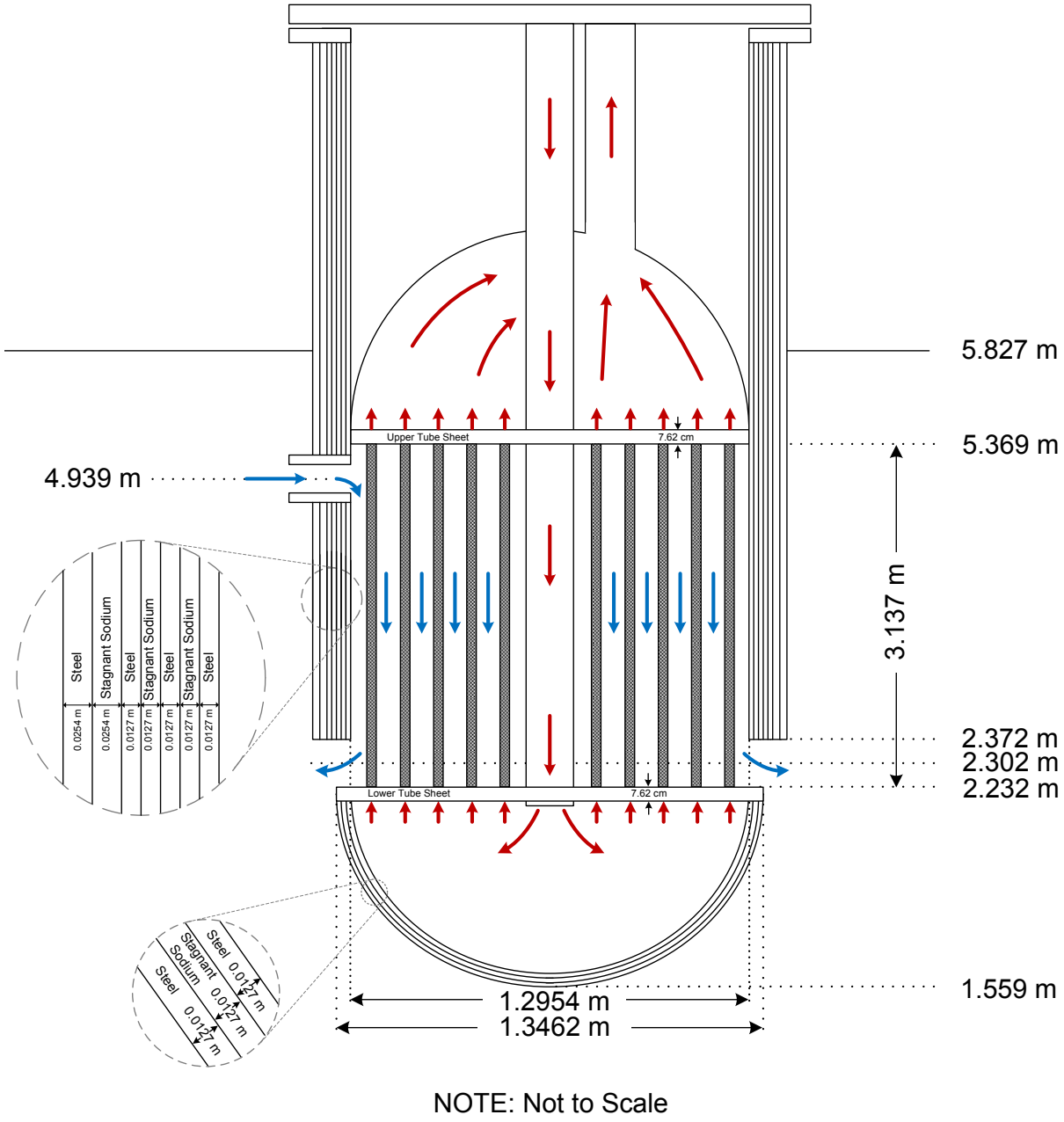

Figure 5.2.7.3. Benchmark Model of Intermediate Heat Exchanger

Table 5.2.7.1. IHX Dimensions

Number of Tubes	3026
Tube Outer Diameter (cm)	1.588
Tube Wall Thickness (cm)	0.124
Tube Pitch (cm)	2.064
Tube Length (m)	3.137
Well Casing Length (m)	5.639
Well Casing Inner Diameter (m)	1.295
Intermediate Inlet Pipe Outer Diameter (m)	0.324
Intermediate Inlet Pipe Wall Thickness (cm)	0.635
Intermediate Outlet Pipe Outer Diameter (m)	0.324
Intermediate Outlet Pipe Wall Thickness (cm)	0.635
Inlet Plenum Volume (Intermediate Side, m^3)	0.774
Outlet Plenum Volume (Intermediate Side, m^3)	0.774
Upper Tube Sheet Thickness (cm)	7.620
Lower Tube Sheet Thickness (cm)	7.620

5.3 Flow Paths

Predicted leakage flow rates at various locations throughout the primary sodium flow path are given in the EBR-II system design descriptions. These leakage rates have been scaled such that the combined flow rates at the outlet of the two primary sodium pumps and the flow rate at the inlet of the Z-Pipe match the measurements for each test.

5.3.1 *SHRT-17 Sodium Flow*

Sodium mass flow rate measurements for SHRT-17 were limited. The flow rate at the outlet of the core was 8500 gpm, which was similar to the value for SHRT-45R of 8766.6 gpm. Because the two core flow rates were very close and the flow rates for SHRT-45R were better defined, the sodium mass flow rates for SHRT-17 are assumed to be those from SHRT-45R scaled to match the total core outlet flow rate of 8500 gpm. The following are the leakage flow rates throughout the primary sodium circuit.

- Start of each of two sets of high-pressure piping: 2.9 gpm,
- Each of two throttle valves: 7.3 gpm,
- Core subassembly adapters: 43.9 gpm,
- Control and Safety subassembly adapters: 73.2 gpm,
- Expanded Core subassembly adapters: 61.5 gpm
- Reactor cover: 61.5 gpm, and
- Heat exchanger inlet: 17.6 gpm.

The resulting sodium mass flow rates in gpm and percent at various locations in the primary sodium circuit are given in Table 5.3.1.1.

Table 5.3.1.1. Initial SHRT-17 Primary Sodium Mass Flow Rates at Various Locations

Location	%	Gallons per minute
Sodium Pumps	100.00	8699.1 (4352.6 + 4346.5)
Lower Plena Inlet	99.76	8678.6
Reactor Core Outlet	97.71	8500.0
Heat Exchanger Inlet	97.01	8438.5
Heat Exchanger Outlet	96.80	8421.0

The total flow rate of 8500.0 gpm at the outlet of the reactor core includes the sodium flow through all subassemblies and three clearance flow paths through the following locations:

- Clearances between the subassemblies: 17.6 gpm,
- Control and safety subassembly thimble clearances: 43.9 gpm, and
- Grid structure, vent holes and neutron shield: 8.8 gpm.

Therefore, 8429.7 gpm remains for sodium flow through the subassemblies themselves. Figure 3.1.3.2 gives the predicted flow rates for each subassembly for Run 129-C. Note that primary and intermediate sodium flow rates were measured in gallons per minute and calibrated at 800°F and 582°F, respectively.

5.3.2 *SHRT-45R Sodium Flow*

At the beginning of SHRT-45R, primary sodium pump #1 provided 4489.1 gpm of sodium flow and primary sodium pump #2 provided 4482.8 gpm of sodium flow for a total mass flow rate of 8971.9 gpm. At the inlet of the Z-Pipe, the nominal mass flow rate was measured as 8703.2 gpm, resulting in a loss of 268.7 gpm between the pumps and the Z-Pipe. The following are the scaled leakage flow rates throughout the primary sodium circuit. Note that the leakage at the heat exchanger inlet takes places after the Z-Pipe inlet and is therefore not included in the 268.7 gpm leakage measurement. The leakage flow paths listed below with flow rates of 45.3, 75.5 and 63.4 gpm are assumed to be from the high-pressure inlet plenum to the cold pool.

- Start of each of two sets of high-pressure piping: 3.0 gpm,
- Each of two throttle valves: 7.5 gpm,
- Core subassembly adapters: 45.3 gpm,
- Control and Safety subassembly adapters: 75.5 gpm,
- Expanded Core subassembly adapters: 63.4 gpm
- Reactor cover: 63.4 gpm, and
- Heat exchanger inlet: 18.1 gpm.

The resulting sodium mass flow rates in gpm and percent at various locations in the primary sodium circuit are given in Table 5.3.1.

Table 5.3.2.1. Initial SHRT-45R Primary Sodium Mass Flow Rates at Various Locations

Location	%	Gallons per minute
Sodium Pumps	100.00	8971.9 (4489.1 + 4482.8)
Lower Plena Inlet	99.76	8950.8
Reactor Core Outlet	97.71	8766.6
Heat Exchanger Inlet	97.01	8703.2
Heat Exchanger Outlet	96.80	8685.1

The total flow rate of 8766.6 gpm at the outlet of the reactor core includes the sodium flow through all subassemblies and three clearance flow paths through the following locations:

- Clearances between the subassemblies: 18.1 gpm,
- Control and safety subassembly thimble clearances: 45.3 gpm, and
- Grid structure, vent holes and neutron shield: 9.1 gpm.

Therefore, 8694.1 gpm remains for sodium flow through the subassemblies themselves. Figure 3.2.3.2 gives the predicted flow rates for each subassembly for Run 138-B but note that the total flow rate given in this figure is higher than the 8694.1 gpm flow rate that SHRT-45R actually experienced. Note that primary and intermediate sodium flow rates were measured in gallons per minute and calibrated at 800°F and 582°F, respectively.

6 Benchmark Values to Calculate

Many measurements were recorded during the SHRT tests. The measurements best suited for comparison with the benchmark calculations are listed below. Benchmark participants should calculate these values during their benchmark simulations. Several other calculated values are included in this list that were not measured during the SHRT tests but would be ideal for direct code-to-code comparisons amongst benchmark participants. Those values that benchmark participants should calculate during the transients are:

- High-pressure and low-pressure inlet plena temperatures,
- Z-Pipe inlet temperature,
- IHX primary side inlet temperature,
- Sodium mass flow rate at the primary sodium pumps,
- IHX intermediate side outlet temperature,
- XX09 and XX10 temperatures at the thermocouples locations described in Section 4.1.7,
- XX09 and XX10 sodium mass flow rate,
- Peak cladding temperature,
- Peak fuel temperature,
- Peak in-core coolant temperature,
- Minimum margin to coolant boiling,
- For SHRT-45R only: net reactivity, and fission power, and total power.

Additionally, two thermocouple trees were installed prior to the SHRT-45R test. As an option for those participants who wish to calculate more detailed cold pool temperature profiles, measurements from these thermocouple trees are available for comparison with benchmark calculations. The two trees, labeled F-Probe and G-Probe, each had 32 thermocouples, spaced nine inches apart axially. Measurements were taken every 30 seconds during the test. No thermocouple trees were installed in the cold pool for the SHRT-17 test.

Table 6.1 lists the approximate distance of each thermocouple from the bottom of the primary tank. Note that the top most thermocouple was in the cover gas region. The radial location of each thermocouple relative to the IHX and pumps is illustrated in Figure 6.1. Please note that the radial and axial locations of the thermocouples are best guess approximations.

Table 6.1. Axial location of thermocouples in F-Probe and G-Probe trees

Thermocouple	Distance From Bottom of Primary Tank (m)
32	7.61
31	7.38
30	7.15
29	6.92
28	6.69
27	6.46
26	6.24
25	6.01
24	5.78
23	5.55
22	5.32
21	5.09
20	4.86
19	4.64
18	4.41
17	4.18
16	3.95
15	3.72
14	3.49
13	3.26
12	3.04
11	2.81
10	2.58
9	2.35
8	2.12
7	1.89
6	1.66
5	1.44
4	1.21
3	0.98
2	0.75
1	0.52

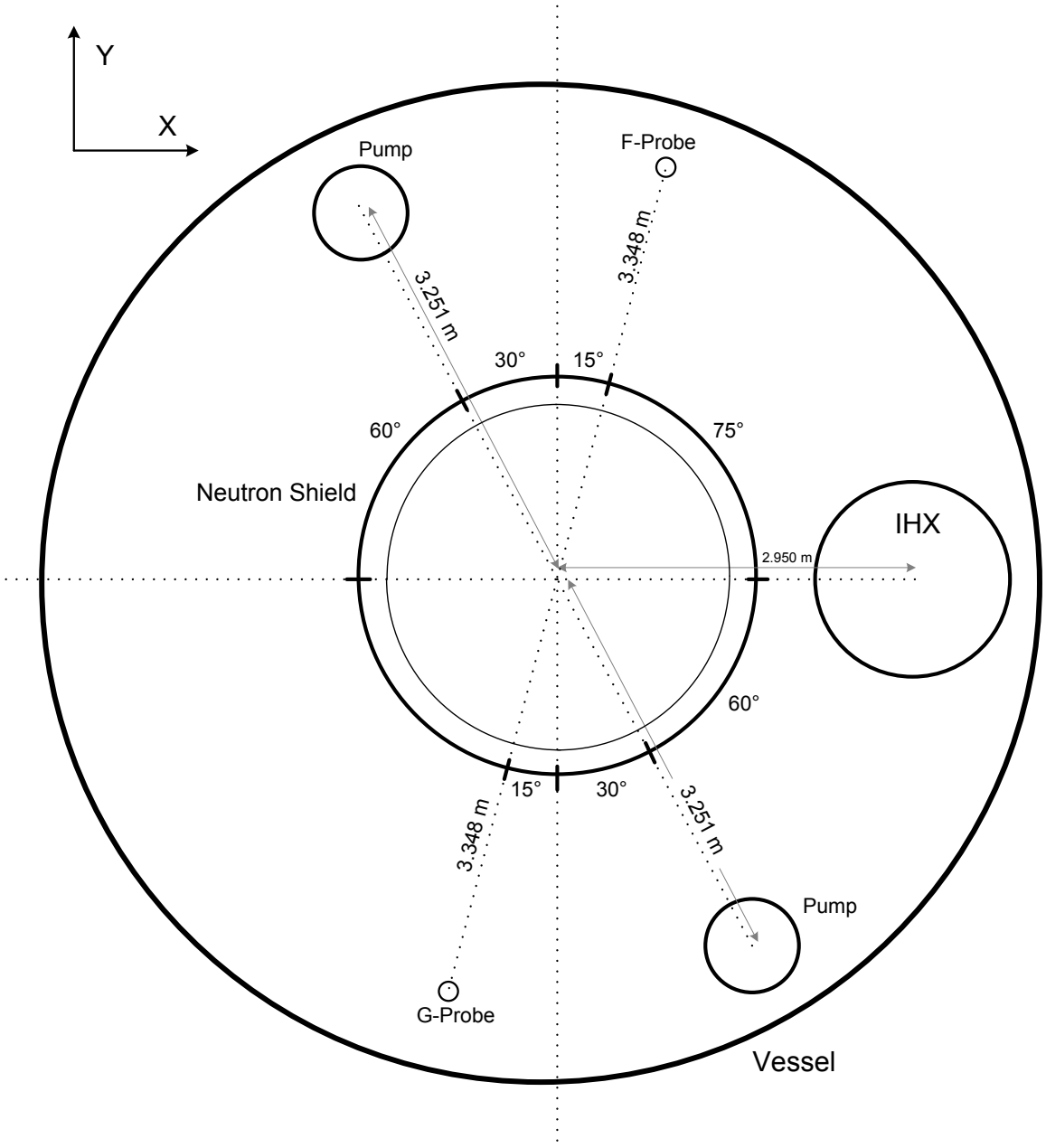

Figure 6.1. Radial Location of F-Probe and G-Probe Thermocouple Trees

Nuclear Engineering Division
Argonne National Laboratory
9700 South Cass Avenue, Bldg. 208
Argonne, IL 60439

www.anl.gov

Argonne National Laboratory is a U.S. Department of Energy
laboratory managed by UChicago Argonne, LLC